SEVERITY OF CLINICAL DISEASE AND PATHOLOGY IN FERRETS EXPERIMENTALLY INFECTED WITH INFLUENZA VIRUSES IS INFLUENCED BY AGE AND INOCULUM VOLUME

By

Ian Nyerere Moore

A DISSERTATION

Submitted to
Michigan State University
in partial fulfillment of the requirements
for the degree of

Pathobiology- Doctor of Philosophy

2014

ABSTRACT

SEVERITY OF CLINICAL DISEASE AND PATHOLOGY IN FERRETS EXPERIMENTALLY INFECTED WITH INFLUENZA VIRUSES IS INFLUENCED BY AGE AND INOCULUM VOLUME

By

Ian Nyerere Moore

Ferrets are a valuable model for influenza pathogenesis, virus transmission and antiviral therapy studies. In our analysis of the current literature related to the use of the ferret model shortly after the emergence of the 2009 H1N1 pandemic (H1N1pdm) influenza virus, we noted substantial variation in clinical disease outcomes for ferrets that were administered similar H1N1pdm viruses intranasally at a dose of 10^6 $TCID_{50}$. Interestingly, comparison of these ferret studies revealed that, of the animals in the studies, both volume of inoculum administered and animal age at the time of infection. We therefore began to assess the role of inoculum volume and animal age on the severity of clinical disease ferrets experimentally infected with influenza virus. We administered the H1N1pdm (A/California/07/2009) and the H3N2-variant (H3N2v) (A/Minnesota/11/2010) influenza viruses to young (8 week old) and old (6 month old) ferrets intranasally in a range of inoculum volumes (0.2, 0.5, or 1.0 ml), and followed viral replication, clinical disease and pathology over 6 days. In addition to clinical disease we examined the ferret's immune response following infection and we evaluated the anatomy of the ferret's respiratory tract and their contributions to disease severity.

We found that clinical illness and respiratory tract pathology were most severe and most consistent in older (6 month old) ferrets and when the viruses were administered in a volume of 1.0 ml. Previous studies in our lab showed similar clinical disease outcomes in young and old ferrets infected with highly pathogenic avian influenza (HPAI) virus (A/Vietnam/1203/2004;

H5N1). Using a modified micro-CT imaging method, we found that the right main stem bronchus was consistently larger in diameter than the left main stem bronchus though the latter was longer and straighter. Based on our findings, these anatomic features likely influence the distribution of inoculum in the lower respiratory tract. A 1.0 ml volume of inoculum is optimal for delivery of virus to the lower respiratory tract of ferrets, particularly when evaluation of clinical disease is desired. Furthermore, we highlight important anatomical features of the ferret lung that influence the kinetics of viral replication, clinical disease severity and lung pathology.

I dedicate my dissertation work to my loving wife Rashida whose love, patience, and support are unrivalled and are forever cherished. To my children Rian and Drew, you represent the best of me and the best "projects" I have ever completed. You boys provide me with a purpose in life and give me the drive to better myself on a daily basis. I would like to thank my mom and dad for sacrificing greatly in order to give me a fair shot at success. This work would not have been possible without the support, sacrifice, prayers, and timely humor provided by others.

I also dedicate this dissertation work to Dr. Daniel Myers who has been a constant source of encouragement and support throughout my many years of school. I will always appreciate you for giving me sound advice and for making me believe that the sky is truly the limit ("Rocket Man"). I love you all and hope that the course of my life and career will be testament to the positive effects of love, support, and sacrifice.

ACKNOWLEDGEMENTS

I would like to express my sincere thanks to my two supervisors, Drs. Kanta Subbarao and Mark Simpson for their support and guidance.

I would like to thank the members of the Subbarao lab past and present for their thoughtful advice and discussions.

I would like to thank my committee members (Drs. Kurt Williams, Steve Bolin, Norbert Kaminski and James Wagner) for their patience, wisdom, and guidance throughout the doctoral process.

I would like to thank Michigan State University, the Graduate Partnerships Program, and the National Institutes of Health for funding and facilitating my education and this research.

TABLE OF CONTENTS

LIST OF TABLES

LIST OF FIGURES

KEY TO SYMBOLS AND ABBREVIATIONS

H1N1pdm	pandemic H1N1
H3N2v	H3N2-variant
$TCID_{50}$	tissue culture infectious dose 50%
HA	hemagglutinin
NA	neuraminidase
SA	sialic acid
SAt	sialyltransferase
IFNγ	interferon-gamma
IL-6	interleukin-6
TNFα	tumor necrosis factor-alpha
IP-10 (CXCL10)	interferon-induced protein-10
RNA	ribonucleic acid
vRNA	viral ribonucleic acid
cRNA	complementary ribonucleic acid
mRNA	messenger ribonucleic acid
ssRNA	single-stranded ribonucleic acid
TLR	toll-like receptor
FFPE	formalin-fixed paraffin-embedded
IHC	immunohistochemistry

CHAPTER 1: Introduction

Influenza epidemiology

Influenza is a viral pathogen that is classically associated with the respiratory disease of the same name in humans that ranges in severity from mild to severe and in some cases, can result in death (CDC, 2014; Cox & Subbarao, 2000). Influenza A virus infections are associated with substantial morbidity and mortality in humans and have been estimated to cause more than 36,000 deaths and over 200,000 hospitalizations annually (Rosenthal et al., 1998; Thompson et al., 2003). In the Northern hemisphere, seasonal influenza virus infections are most commonly observed during the winter months in the, with the highest influenza activity noted in February (CDC, 2013).

In addition to seasonal influenza epidemics, which are common and follow predictable seasonal patterns, the emergence of new influenza A virus subtypes can result in global outbreaks (pandemics) of infection and disease for which there is little to no preexisting immunity (Taubenberger & Morens, 2010). Influenza pandemics, though rare, have been associated with severe disease (Taubenberger & Kash, 2011) and have occurred multiple times in a century (Morens & Fauci, 2007). In April of 2009, a newly-emerged pandemic H1N1 (H1N1pdm) influenza virus that was a triple reassortant composed of gene segments derived from swine, avian and human influenza viruses (Garten et al., 2009; G. J. Smith et al., 2009). This H1N1pdm influenza virus had not been previously identified in humans or animals and was closely related to North American swine H1N1 and Eurasian lineage swine H1N1 influenza viruses (Garten et al., 2009). This virus caused the greatest morbidity and mortality in infants

and young adults (Jhung et al., 2011) and the lowest incidence of disease occurred in the older segment of the population (>60 years old) (Jhung et al., 2011), presumably due to cross-reactive antibodies from previous exposure to older antigenically related seasonal H1N1 viruses (Heldt, Frensing, & Reichl, 2012; Jegaskanda et al., 2013; Toennessen, Lauscher, & Rimstad, 2009).

The H1N1pdm virus spread to over 200 countries worldwide and resulted in over 1 million deaths during the first year of its circulation (Dawood et al., 2012). In typical seasonal influenza virus epidemics, the elderly, individuals with other co-morbidities (chronic diseases), and young children are often the most vulnerable targets for infection (Dorrington & Bowdish, 2013). In models, vaccination with some previously circulating seasonal H1N1 influenza A viruses confers protection from infection with the H1N1pdm virus (Dubois, Terrier, & Rosa-Calatrava, 2014). Decreased disease severity in older individuals is likely the result of previous exposure or infection with such viruses (Jegaskanda et al., 2013; Toennessen et al., 2009). Influenza viruses are ever changing and evolving and H1N1pdm influenza viruses provided many insights into the critical aspects of pandemic preparedness and response.

Influenza A, B and C viruses

These enveloped viruses are in the family *Orthomyxoviridae* and are composed of a single-stranded, segmented genome that encodes for at least 11 structural and nonstructural proteins (Dorrington & Bowdish, 2013; Shaw, 2007). The viral messenger RNAs are transcribed from the viral RNA segments and are therefore considered negative-sense (Dorrington & Bowdish, 2013; Shaw, 2007). In addition to influenza A, B and C viruses, *Orthomyxoviridae* contains two other genera of influenza viruses which are Thogotovirus and

Isavirus (Toennessen et al., 2009). The separation of influenza viruses into types, A, B and C is based on the antigenicity of two of their internal proteins, the nucleoprotein (NP) and matrix (M) protein (Reading, Miller, & Anders, 2000).

Influenza A virions are composed of a host-derived lipid envelope which harbors the hemagglutinin (HA), neuraminidase (NA) and the M2 proteins which project from the viral surface (Terajima, Babon, Co, & Ennis, 2013). These surface proteins are embedded in the Matrix (M_1) protein layer located just beneath the lipid bilayer of the viral envelope (Neverov, Lezhnina, Kondrashov, & Bazykin, 2014). The ribonucleoprotein core of the viral particle contains 8 viral RNA segments (PB2, PB1, PA, HA, NP, NA, M1/M2 and NS1/NS2); segmentation of the viral genome allows influenza viruses to undergo genetic reassortment, and thus readily exchange genetic information (Peiris, de Jong, & Guan, 2007). Genetic reassortment is a common phenomenon among influenza viruses but, reassortment between viruses of different genera has not been reported (Neverov et al., 2014).

Influenza B viruses are structurally similar to influenza A, however, influenza B viruses have 4 envelope proteins HA, NA, NB, and BM_2 (Imai, Watanabe, Ninomiya, Obuchi, & Odagiri, 2004). Like the M_2 protein of influenza A, the BM_2 protein is a proton channel that is responsible for the uncoating process (Imai et al., 2004). The role of the NB protein is less defined but has been shown to not be necessary for viral replication in vitro (Hatta & Kawaoka, 2003).

Influenza C viruses are less commonly associated with epidemic disease and are even more divergent from the two previously described virus types (Taubenberger & Kash, 2010). Influenza C viruses are structurally different from both A and B viruses (Imai, Kawasaki, & Odagiri, 2008). Influenza C viruses contain 7 gene segments (PB1, PB2, P3, HEF, NP, M

(CM_2, CM_1), NS1) that encode 9 proteins and are enveloped, similar to both A and B viruses (Dorrington & Bowdish, 2013; Shaw, 2007). The polymerase complex of the influenza C virus is composed of PB1 and PB2 proteins that are homologous to the corresponding influenza A and B virus proteins (Compans, Bishop, & Meier-Ewert, 1977). The third polymerase component is named P3 because it does not exhibit an acidic charge at neutral pH, as do the PA proteins for both influenza A and B viruses (Wang et al., 2012). The surface of the influenza C virus is covered by hexagonal structures arranged in cords that project from the surface of the viral envelope (Compans et al., 1977). In contrast to influenza A and B viruses, the viral core contains 7 genome segments, and CM_2 ion channel envelope protein and a envelope glycoprotein called the Hemagglutinin-esterase-fusion (HEF) protein which serves the same function as the HA and NA of influenza A and B viruses (Rosenthal et al., 1998).

Influenza viruses attach to the host cell by multiple mechanisms including pinocytosis, clathrin-coated pits and by binding to glycosylated oligosaccharides that terminate in a sialic acid (SA) (Reading et al., 2000). The latter form of attachment has recently been at the forefront of influenza transmission research and has been investigated in multiple avian (Kimble, Nieto, & Perez, 2010) and mammalian (Trebbien, Larsen, & Viuff, 2011) species for the similarity of viral receptor distribution, compared to viral receptors present throughout the human respiratory tract (Shinya et al., 2006; van Riel et al., 2006). These SA residues are bound to glycans through α2,3 or α2,6 linkage by sialyltransferases that are expressed in a cell and species-specific manner (Ibricevic et al., 2006). Epithelial cells within the respiratory tract are the primary targets of influenza virus infection, this targeting is facilitated by the presence of α2,3 or α2,6 receptors (van Riel et al., 2007). The location of these receptors differs by species and may contribute significantly to level of infection (Garcia-Sastre, 2010; Weis et al., 1988). Mammalian influenza

viruses preferentially bind SA with an α2,6 linkage while avian viruses preferentially bind SA with α2,3 linkages (Suzuki et al., 2000; Wang et al., 2012). In humans, the epithelial cell targets of the upper airways express a predominance of α2,6 SA receptors and are therefore the target of many mammalian influenza viruses (Baum & Paulson, 1990; Matrosovich, Matrosovich, Gray, Roberts, & Klenk, 2004). In the lower respiratory tract, cells predominantly express α2,3 SA and are therefore targeted by avian-type influenza viruses (Franca, Stallknecht, & Howerth, 2013; Yao, Korteweg, Hsueh, & Gu, 2008).

Influenza disease in humans

Infectious viral particles are most commonly spread via respiratory droplets (Bridges, Kuehnert, & Hall, 2003; Mubareka et al., 2009) and in some cases spread to the respiratory tract has been shown to occur following inoculation of the conjunctiva with certain H7 virus subtypes in animal models (Belser et al., 2012). Of the three influenza virus types, influenza A viruses have been associated with the most severe clinical disease which can include cough, fever, sore throat, nasal discharge, myalgia and less often vomiting and diarrhea (Douglas, 1990). In addition, influenza A viruses demonstrate a very broad host range that comprises both avian and mammalian species, including birds, humans, pigs, sea mammals and horses (Reading et al., 2000). Of the 18 HA and 11NA virus subtypes known, aquatic waterfowl serve as a reservoir for 16 HA and 9 NA influenza A viruses (Reading et al., 2000) while molecular evidence of H17N10 and H18N11 viruses have been identified in bats (Tong et al., 2012; Tong et al., 2013). The virus' wide host range contributes to the ability of divergent influenza A viruses to reassort and give rise to novel, potentially more virulent viruses in a phenomenon known as "antigenic

shift" (Fleischmann, 1996). In contrast to such sporadic events, in a more continuous process, point mutations can occur in the HA and NA genes altering the virus' antigenicity enough to allow the virus to evade the host's immune response; this more gradual change is termed "antigenic drift" (Fleischmann, 1996; Shaw, 2007).

Influenza B viruses are only known to infect humans and seals (Bodewes et al., 2013). Because a reservoir of non-human influenza B viruses does not exist, influenza B-associated pandemics do not occur. Antigenic drift also occurs in influenza B viruses, albeit at rates 2-3 times slower than in influenza A viruses (Webster & Berton, 1981). Influenza C viruses are associated with infections in humans and pigs (Kimura et al., 1997) although severe disease and local epidemics have been reported (Matsuzaki et al., 2007), the course of clinical disease is most often mild and self-limiting.

Influenza viruses have been implicated in some of the largest recorded incidences of mass human morbidity and mortality known to mankind. One of the earliest documented pandemics was the "Russian flu" pandemic, which was one of the last influenza pandemics of the 19th century and was speculated to be the result of the emergence of an H3N8 influenza A virus (Valleron et al., 2010). The 20th century was host to 3 major pandemics, of which, the 1918 "Spanish flu" pandemic was the most severe (Taubenberger & Kash, 2011). The 21st century has recently served as host for another influenza pandemic which was the result of a newly-emerged triple reassortant swine origin H1N1 influenza A virus. This virus was first detected in the U.S. in April of 2009 (Garten et al., 2009). The virus was composed of a unique constellation of influenza virus genes never before identified in animal or humans; specifically, the gene constellations were a combination of North American swine lineage H1N1 and Eurasian lineage swine H1N1 influenza viruses (Garten et al., 2009). The virus was initially referred to as

a “swine flu” virus, however subsequent investigations showed that the virus was circulating and transmitting from person to person and was not the result of exposure to swine herds.

Lung development

In the developing fetus, the lungs first appear as an out-pouching of the ventral wall of the foregut (K. A. Moore et al., 2005). The internal lining of the lungs, larynx, trachea, and bronchi are of endodermal origin (T. W. Sadler, 2011). In the earliest stages of development, the lungs share a communication with the foregut but further development results in the formation of the esophagotracheal septum, which further divides the foregut into dorsal and ventral portions, namely the esophagus and trachea (Pepicelli, Lewis, & McMahon, 1998), respectively. The lower portions of the respiratory tract develop into the trachea, bronchi, and lungs. The lung buds give rise to the trachea and two lateral outgrowths, the bronchial buds. The buds enlarge to form the right and left main bronchi. The right forms three secondary bronchi while the left forms two secondary bronchi which expand in both caudal and lateral directions (Carlson, 2014). Further, the secondary bronchi divide repeatedly and in a dichotomous fashion forming tertiary, segmental, bronchi in both the right and left lung, forming the bronchopulmonary segments of the adult lung (T. W. Sadler, 2011).

The development from fetal to adult lung involves specific phases of prenatal and postnatal development that include the embryonic stage and the fetal period; the latter is subdivided into pseudoglandular, canalicular, and saccular stages. The pseudoglandular stage (~5-17 weeks) is stimulated by the presence of surrounding mesenchyme and the conducting airways are formed from the continuous dichotomous branching of thick epithelial-lined tubules

(pseudoglandular appearance) (Kotecha, 2000). In the canalicular stage (~16-28 weeks) the basic structures of the gas-exchanging portions of the lung and blood vessels are formed (Colin, McEvoy, & Castile, 2010). Differentiation of the airways starts with widening of the lumina and gradual thinning of the cuboidal epithelium (Carlson, 2014). In addition to vessels, respiratory bronchioles begin to form, delineating the acinus. This process of lung branching is regulated by epithelial-mesenchymal interactions between the endoderm of the lung buds and the splanchnic mesoderm that surrounds them (Pepicelli, Lewis, & McMahon, 1998). Branching signals arise from the mesoderm and involve members of the Fibroblast Growth Factor (FGF) family (Bellusci, Grindley, Emoto, Itoh, & Hogan, 1997). In the saccular stage (~36 weeks to birth), the airways begin to terminate in large smooth-walled cylindrical structures that are subdivided by ridges called crests. The crests protrude into the saccule, pulling a capillary network along with them, creating subsaccules, which go on to become the alveolus (T. W. Sadler, 2011). The alveolar stage that begins in utero (~36 weeks) extends in the 2nd year of postnatal life (Burri, 2006). These developmental changes result in the formation of a structurally mature and physiologically competent lung that further continues to remodel and change, both grossly and microscopically until the 2nd decade of life (Sharma & Goodwin, 2006).

Immune response to influenza

In human influenza virus infections, hemagglutinin (HA) and neuraminidase (NA) are the major glycoproteins detected by the host's immune system (Johansson, Bucher, & Kilbourne, 1989; Subbarao, Murphy, & Fauci, 2006). Professional antigen-presenting cells (macrophages and dendritic cells) in the respiratory tract are exposed to the virus and produce inflammatory mediators which send signals to other dendritic cells which then upregulate chemokine receptors that allow them to migrate to lymph nodes where they activate T cells (Woodland & Scott, 2005). The newly alerted T cells and Natural Killer (NK) cells secrete IFN-γ, which induces an anti-viral state or results in the production of perforin and granzyme B- mediates lysis of virus infected-cells (Edwards, Davis, Browne, Sutton, & Trapani, 1999).

The recognition of viral proteins begins the cascade of events that leads to an innate immune response and ultimately the development of adaptive immunity. Typically, infection is initiated when virus enters the respiratory tract and interacts with host cells by attaching to the target cell (respiratory epithelium) via the viral hemagglutinin that binds to sialic acid (SA) receptors along the surface of the host cell (Garcia-Sastre, 2010). In addition to respiratory epithelium, macrophages and dendritic cells can also support virus infection (Short, Brooks, Reading, & Londrigan, 2012). After attachment, the virus is endocytosed where, a decrease in endosomal pH results in a conformational change in the viral HA leading to subsequent fusion of the host and viral cell membranes (Stegmann, Morselt, Scholma, & Wilschut, 1987). The M2 protein forms an ion channel that allows the entry of protons into the core of the viral particle where a lower pH also facilitates the disassembly and release of viral RNA (vRNA) into the cytoplasm of the host cell (Lamb, Zebedee, & Richardson, 1985; McCown & Pekosz, 2006). The negative-

sense vRNA are then transported to the nucleus where the virally-encoded RNA-dependent RNA polymerase uses vRNA as a template to transcribe the positive-sense complementary (cRNA) and messenger RNA (mRNA) (Dorrington & Bowdish, 2013; Shaw, 2007). The newly transcribed mRNAs are exported to the cytoplasm for translation, while cRNA remains in the nucleus and serves as a template for progeny vRNA (Dorrington & Bowdish, 2013; Shaw, 2007). Nascent viral proteins are either secreted through the Golgi apparatus and to the cell surface or transported back to the nucleus where they bind viral RNA (Doyle, Roth, Sambrook, & Gething, 1985; Katze et al., 1988). Hemagglutinin and neuraminidase localize in protrusions along the surface of the host cell where they are joined by the newly synthesized viral RNAs to form mature virions which then bud from the surface of the host cell by forming a sphere of host-derived phospholipid, now covered by both HA and NA molecules (Rossman & Lamb, 2011). At the final stage, the host cell sialic acids are cleaved by the enzymatic activity of the NA and the viral particle is released and as able to infect another host cell (Rossman & Lamb, 2011).

In order to limit and ultimately eliminate the virus from the host's system, the innate immune response is mediated by identification of the virus' specific pathogen-associated molecular patterns (PAMPs) that are recognized by pattern recognition receptors (PRRs), resulting in the induction of type 1 interferons (IFNα and IFNβ) and other pro-inflammatory cytokines and chemokines (Iwasaki & Medzhitov, 2010). Influenza viruses are recognized by a number of PRRs including retinoic acid-inducible gene 1 (RIG-I) (Pichlmair & Reis e Sousa, 2007), NOD-like receptor family member NOD-LRR and pyrin domain-containing 3 (NLRP3) (Ichinohe, Iwasaki, & Hasegawa, 2008), and Toll-like receptors (TLR 3, 7, and 8) (Iwasaki & Pillai, 2014; Rock, Hardiman, Timans, Kastelein, & Bazan, 1998). Within this method of pathogen detection, two pathways have been identified; cell-intrinsic and cell-extrinsic. RIG-I

and NLRP3 detect viruses that are present in the cytoplasm of host cells (cell-intrinsic) and TLR 3 detects double-stranded RNA (dsRNA), while TLRs 7 and 8 both detect single-stranded RNA (ssRNA). Further, the mechanism of TLR recognition in influenza virus is based on the detection of virus that has been taken into cellular endosomes and is therefore considered to be the cell-extrinsic pattern of pathogen recognition (Iwasaki & Medzhitov, 2010). RIG-I, as a cytoplasmic sensor, detects influenza virus by the recognition of 5'triphosphates (5'PPP), which are present on ssRNA and are produced after viral fusion and replication have occurred (Uzri & Gehrke, 2009). The recognition of 5'PPP causes RIG-I to interact with the adaptor protein, interferon-β promoter stimulator-1 (IPS-1; also known as MAVS), which results in the translocation of RIG-I to the mitochondrial membrane leading to the activation of multiple transcription factors including interferon regulatory factors (IRF) 3, IRF7, and nuclear factor kappa-light-chain-enhancer of activated B cells (NF-κB) (Goulet et al., 2013). IRF3 and IRF7 translocate to the nucleus and activate the transcription of alpha and beta interferons, while NF-κB translocates to the nucleus where it acts as a transcription factor for the induction of proinflammatory cytokines including IL-6, TNF-α, the pro-form of IL-1β and IL-18 (inflammasome complex) (Iwasaki & Medzhitov, 2010; Matrosovich et al., 2004).

Similarly, NLRP3's role in anti-influenza immunity also begins following the detection of virus in the cellular cytoplasm. However, upon detection, NLRP3 recruits the adaptor protein apoptosis-associated speck-like protein containing a caspase recruitment domain (ASC), which activates pro-caspase-1. Active casapse-1 cleaves the pro-forms of IL-1β and IL-18, resulting in activation of the inflammasome and secretion of proinflammatory cytokines (Martinon, Burns, & Tschopp, 2002).

Within the endosome of macrophages, TLR 3 detects dsRNA from dead or dying cells that have been phagocytosed. In the phagosome, dsRNA interacts with the TLR3 receptor, which in turn recruits the adapter protein TIR-domain-containing adapter-inducing interferon-β (TRIF) and further downstream leads to the transcription of type 1 interferons and pro-inflammatory cytokines via production of IRF3 and NF-κB, respectively (Iwasaki & Pillai, 2014). In plasmacytoid dendritic cells (pDC), ssRNA is detected within endosomes via TLR7 which then recruits the adaptor protein Myeloid differentiation primary response gene-88 (MYD88) that induces transcription of proinflammatory cytokines and type 1 interferons via signaling through NF-κB or IRF7, respectively (Iwasaki & Pillai, 2014). The secretion of type 1 interferons (α and β) promotes an anti-viral state in which infected cells send chemical signals to neighboring uninfected cells that cause them to shutdown the cellular machinery that would normally be commandeered by the invading influenza virus in order to facilitate transcription and translation. Upon binding of the type 1 interferon receptor (IFNAR), the tyrosine kinases (Jak1 and Tyk1) phosphorylate the signal transducers and activators of transcription (STATs) (Pauli et al., 2008). After dimerization (STAT1 and STAT2) and association with IRF9, these components form the signaling complex ISG factor 3 (ISGF3) that translocates to the nucleus where it initiates the transcription of ISGs (Pauli et al., 2008). One of the more well-characterized (interferon stimulated genes) IFN-induced antiviral effectors is protein kinase R (PKR) which is a member of the eukaryotic initiation factor 2α (eIF2α) kinase family (Bergmann et al., 2000). PKR binds viral dsRNA and inhibits translation, which results in a decrease in total cellular and viral protein synthesis and, therefore reducing viral replication (Min, Li, Sen, & Krug, 2007). Activation of the PKR pathway in infected cells results in the initiation of apoptosis, cell growth arrest and

autophagy, all decreasing the ability of the virus to spread and replicate in host cells (Iwasaki & Pillai, 2014).

The adaptive arm of the immune response is directed by the interactions of the host and the virus in the course of innate immunity. Innate immunity is geared towards slowing viral spread and replication within host cells while adaptive immunity is focused on viral clearance and the host's recovery from infection. Professional antigen presenting cells, such as dendritic cells (DCs), play a key role in bridging the innate and adaptive immune responses following influenza A virus infection. The APCs migrate, via afferent lymphatics, to the draining lymph node (LN) where they present peptide antigen to naive T cells via MHC molecules (Masson, Mount, Wilson, & Belz, 2008). This interaction between DCs and T cells within the LN result in the production and activation of antigen-specific CD8+ (cytotoxic) T cells and the production of CD4+ Helper (T_h) T cells. Helper T cells (CD4+) present virus antigen to B cells which then proliferate and further differentiate into plasma cells that secrete antibodies (Iwasaki & Pillai, 2014). Antibodies bind directly to the virus particle to prevent attachment or antibody can bind to infected cells and result in cell destruction by antibody-dependent complement-mediated lysis or by antibody-dependent cell-mediated cytotoxicity (ADCC) (McMichael, Gotch, Noble, & Beare, 1983). In influenza infections, the most commonly described method of eliminating virally infected cells is via the actions of Cytotoxic T cells (CD8+) (Doherty et al., 1997). Effector CD8 cells cause target cells to undergo lysis and apoptosis, via the action of perforin and granzyme, respectively (Doherty et al., 1997). In both the humoral (B cell) and cell-mediated (T cell; CD4 and CD8) responses, a subset of each cell-type persists as memory cells which can thereafter recognize the virus at a later time and mount a strong and abbreviated immune response (Thomas, Keating, Hulse-Post, & Doherty, 2006).

Animal Models for influenza

The sporadic emergence of novel influenza viruses in humans led to the need for the development and use of animal models in order to investigate the pathogenicity of these viruses and new strategies to alleviate or abrogate virus infections. Moreover, there are major limitations associated with assessing the behavior and pathogenesis of influenza viruses in the respiratory tract of humans, in particular, within the lower respiratory tract. Therefore, a major challenge for investigators in influenza research is the selection of an appropriate animal model that accurately recapitulates influenza disease and subsequent immune response observed in humans (O'Donnell & Subbarao, 2011) As a result, a number of animal models have been employed to investigate this pathogen. Some of the more commonly used animal species used to study different aspects of influenza virus pathogenesis are mice (Boon et al., 2009; Lu et al., 1999; Simeckova-Rosenberg, Yun, Wyde, & Atassi, 1995; Tumpey et al., 2007), rats (Eichelberger, Prince, & Ottolini, 2004; Straight, Ottolini, Prince, & Eichelberger, 2008), guinea pigs (Lowen et al., 2009; Mubareka et al., 2009), hamsters (Ali, Teh, Jennings, & Potter, 1982; Round & Stebbing, 1981), ferrets (Fan et al., 2004; Maines et al., 2009; O'Donnell et al., 2014), chickens (Faulkner, Estevez, Yu, & Suarez, 2013), and non-human primates (Fan et al., 2004; Maines et al., 2009; Matsuoka et al., 2014; Saslaw, Wilson, & et al., 1946).

Mice have been used extensively in influenza research to assess the pathogenesis of influenza disease, immunological responses and for the assessment of drug or vaccine efficacy (Furuya, 2012). Mice have proven to be a popular model due to their size, cost-effectiveness, minimal husbandry requirements, and the availability of species-specific immunological reagents. Although the mouse is a popular model for influenza studies, mice are not uniformly

susceptible to experimental influenza infection; susceptibility to different influenza viruses is dependent upon the individual virus strain and the strain of mouse infected (Bouvier & Lowen, 2010). As a result, many strains of influenza must be mouse-adapted in order to cause infection (Ilyushina et al., 2010). Adaptation of influenza viruses in mice requires multiple passages until disease is achieved (Brown, Liu, Kit, Baird, & Nesrallah, 2001). Although the ability to infect mouse lungs with influenza has proven to be an invaluable tool for studying the mechanisms of viral virulence, the adaptation of influenza viruses in mice can cause significant changes including mutations in the HA and other genes, which alter the virus and can result in increased virulence (Brown et al., 2001; Jackson, Hossain, Hickman, Perez, & Lamb, 2008). Xu and others showed that a strain of seasonal H1N1, almost avirulent in mice, became extremely virulent after multiple passages in mouse lungs, compared to mice infected with the wild-type (WT) strain of the virus. They found that the increase in virulence was related to three mutations that occurred in the HA protein over the span of passages (Xu et al., 2011). Moreover, a majority of inbred mice are highly susceptible to disease and death following intranasal infection with certain influenza viruses (Boon et al., 2011). In contrast, wild mice are typically resistant to experimental infection with viruses that have been associated with disease in laboratory strains, even at very high doses (Baker, 1998; Bouvier & Lowen, 2010). This resistance of wild mice to infection is controlled by alleles at the Mx1 locus on chromosome 16 (Staeheli, Grob, Meier, Sutcliffe, & Haller, 1988). The mouse Mx1 gene encodes an interferon (IFN)-inducible nuclear protein and confers resistance to influenza A and B virus infection (Jin, Yamashita, Ochiai, Haller, & Watanabe, 1998). Many standard laboratory mouse strains carry $Mx1^{-/-}$ alleles and are susceptible to influenza virus infection. Staeheli et al (Staeheli & Sutcliffe, 1988) were the first to show that the susceptible genotype was the result of either deletions or a nonsense mutation.

Mice carrying the $Mx1^{+/+}$ alleles synthesize the Mx protein which is localized in the nucleus and is synthesized in response to IFN (IFN-α and IFN-β) production (Haller, Kochs, & Weber, 2006).

Ferrets (*mustela putorious furo*) are another common model and among one of the most popular for influenza research. In general, ferrets are also easy to handle and maintain in a research setting. Since the 1930's (Smith, 1936), ferrets have been used to assess the pathogenicity of human influenza isolates and to propagate and maintain certain strains of influenza viruses that were isolated from the throat washings of human patients (WSN/33; H1N1). Ferrets are outbred animals that are naturally permissive to influenza virus infection with both mammalian and avian influenza viruses (Matsuoka, Lamirande, & Subbarao, 2009), they have similarities in lung anatomy and physiology to that of humans (Johnson-Delaney & Orosz, 2011). Avian and mammalian influenza viruses show a similar pattern of attachment in the respiratory tract of ferrets and humans, largely based on similarities in the distribution of sialic acid (SA) receptors between ferrets and humans (van Riel et al., 2006). Following infection, ferrets exhibit clinical signs of influenza disease that are similar those observed in humans including, fever, weight loss, ocular and nasal discharge and sneezing (Bouvier & Lowen, 2010; Matsuoka et al., 2009). The course of clinical disease in ferrets has been used to extrapolate the severity of disease expected with various influenza virus strains in humans. One of the most notable disadvantages of the model is the lack of species-specific antibodies to investigate many aspects of the ferret immune response (Ichinohe et al., 2008; Matsuoka et al., 2009). However, a number of investigators have employed a number of methods to circumvent this obstacle (Cheng et al., 2013; Music et al., 2014; Rutigliano et al., 2008); humoral and

cellular immune response of ferrets were studied by using a combination of monoclonal antibodies that were produced by immunization of mice (CD5 and CD8) and others that were produced from hybridoma cells that were generated from the splenocytes of immunized mice (Ravi, Sundar, Kumar, Parvathi, & Paul, 2007). Svitek (Svitek & von Messling, 2007) and others (Maines et al., 2012) evaluated the local innate immune response in ferrets following infection with H5N1, H1N1, and H3N2 influenza viruses by evaluating messenger RNA (mRNA) expression of a number of cytokines and chemokines in the upper and lower respiratory tract.

Non-human primates (NHP) have also been used for influenza studies because of the close phylogenic relationship between NHP and humans and because of the relative abundance of reagents available to investigate the immunological mechanisms associated with experimental infection and vaccination strategies (Baskin et al., 2004; Murphy, Sly, Hosier, London, & Chanock, 1980). In traditional influenza studies using NHPs Old World primates (OWP) (Rhesus and Pig Tail Macaques) are among the most commonly used model (Jegaskanda et al., 2013; Polacino et al., 2008). Although NHP are of interest due to their similarities to humans, regulation and cost of maintenance are in some cases prohibitive. In addition, OWP are carriers of blood-borne pathogens that can be lethal if contracted by their human caretakers and other research staff. Recently, for the first time, New World monkeys (NWM) were shown to be productively infected and transmit virus between animals (Moncla et al., 2013); prior to this, ferrets and guinea pigs were among the most commonly used models for transmission studies.

Aims of Thesis

As discussed above, there are a number of animal models available for influenza virus pathogenesis studies. However, many of the more commonly used models have advantages and disadvantages that must be taken into consideration prior to designing a study. Of the animal models mentioned, the ferret has been considered the most practical choice due to its relatively small size, general ease of husbandry, comparable respiratory tract anatomy (to humans), demonstration of clinical disease (similar to humans), and natural susceptibility to a wide variety of influenza virus subtypes.

The onset of the 2009 pandemic prompted many influenza investigators to begin studies aimed at mapping clinical disease outcomes, kinetics of virus replication, and the pathogenesis of this newly-emerged influenza virus strain. Many investigators sought to evaluate these parameters using the ferret model. We reviewed a number of publications that utilized the ferret model during the initial stages of the 2009 influenza pandemic and found that despite the use of similar viruses at a similar dose, the clinical disease outcomes in ferrets were highly variable and ranged from asymptomatic to lethal. Further analysis revealed that in the various studies, animals could be separated into groups, along the spectrum of clinical disease severity, by age, and the volume of inoculum administered during experimental infection.

Based on the wide range of clinical outcomes reported in ferrets, we hypothesized that, the severity of disease and efficiency of viral replication in the upper and lower respiratory tract during experimental influenza A virus infection in ferrets is influenced by inoculum volume, age of animal at time of infection, and the virus subtype. In order to address this hypothesis, we identified three specific aims that will be addressed in the coming chapters. (1) We sought to

determine the significance of animal age and inoculum volume on clinical and virologic outcomes following experimental infection of ferrets with the 2009 pandemic H1N1 (H1N1pdm) influenza virus. (2) We evaluated the pathology and immunology of the H1N1pdm influenza virus in the upper and lower respiratory tract of experimentally infected ferrets. (3) We assessed whether the clinical, virologic, and pathologic outcomes observed in ferrets following experimental infection with the H1N1pdm influenza virus, were also seen following infection with another influenza A virus- the H3N2-variant virus (H3N2v).

CHAPTER 2: Clinical disease outcomes in influenza virus-infected ferrets based on volume of inoculum administered

INTRODUCTION

Animal experimentation is an important tool for the study of pathogenesis of infectious diseases and test novel drugs and vaccines. Over the past century, animal models have vastly added to knowledge of mechanisms of infection and general disease pathogenesis. The choice of appropriate animal models for in vivo studies is a key element for improved understanding of infectious diseases. The goal of an animal model of infectious human disease is to, recapitulate disease in humans as closely as possible. In some cases, an animal's response to a human pathogen may be divergent from what is expected in humans. Although this may indicate that the model is not optimal for the study of a particular pathogen, differential outcomes in outbred animal may identify unique perspectives and provide new insights into host-pathogen interactions or may be more reflective of differential disease outcomes in heterogeneous populations. This chapter focuses on the differential disease outcomes observed in ferrets experimentally infected with influenza A viruses, based on the volume of inoculum administered.

ABSTRACT

Ferrets are a valuable model for influenza pathogenesis, virus transmission and antiviral therapy studies. However, the contributions of volume of inoculum administered and the ferret's respiratory tract anatomy to disease outcome have not been explored. We noted variation in clinical disease outcomes and the volume of inoculum administered and investigated these differences by administering two influenza viruses (A/California/07/2009 (H1N1pdm) and A/Minnesota/11/2010 (H3N2v) to ferrets intranasally at a dose of 10^6 $TCID_{50}$ in a range of inoculum volumes (0.2, 0.5, or 1.0 ml), and followed viral replication, clinical disease and pathology over 6 days. Clinical illness and respiratory tract pathology were most severe and most consistent when the viruses were administered in a volume of 1.0 ml. Using a modified micro-CT imaging method and examining gross specimens, we found that the right main stem bronchus was consistently larger in diameter than the left main stem bronchus though the latter was longer and straighter. These anatomic features likely influence the distribution of inoculum in the lower respiratory tract. A 1.0 ml volume of inoculum is optimal for delivery of virus to the lower respiratory tract of ferrets, particularly when evaluation of clinical disease is desired. Furthermore, we highlight important anatomical features of the ferret lung that influence the kinetics of viral replication, clinical disease severity and lung pathology.

MATERIALS AND METHODS

Viruses. Viruses were propagated in the allantoic cavity of 9 to 11 day old specific-pathogen-free embryonated hen's eggs (Charles River Laboratories, Franklin, CT) at 37°C. Virus titers were determined in Madin-Darby canine kidney (MDCK) cells (ATCC, Manassas, VA) and calculated using the Reed and Muench method (Reed, 1938).

Animals. Six month old male and female ferrets (Triple F Farms, Sayre, PA) were used. All of the ferrets in each of the cohorts infected with the H1N1pdm and H3N2v viruses were born on the same day. All ferrets were seronegative for hemagglutination inhibition (HAI) antibodies against currently circulating human H1N1 and H3N2 viruses. All ferret experiments were performed at the NIH with approval of and in compliance with the guidelines of the NIAID/NIH institutional animal care and use committee.

Experimental influenza virus infection. Ferrets (n=12) were lightly anesthetized via inhalation of isoflurane and held in an upright position and inoculated intranasally (i.n.) with 0.2, 0.5, or 1.0 ml containing 10^6 $TCID_{50}$ of the H1N1pdm or H3N2v influenza virus; a total of 36 ferrets were infected with either virus subtype. The total volume of each inoculum was administered in roughly equal portions into the two nares. The ferrets were held upright for 10-15 seconds after virus administration, to allow a few normal breaths before they were placed prone in their cage. The ferrets were sedated deeply enough to suppress sneezing and they regained consciousness within 5 minutes of intranasal administration of the inoculum.

Clinical illness. Prior to inoculation, all animals were implanted with a subcutaneous transponder between the shoulders for monitoring body temperature and for animal identification. Ferrets were monitored daily for temperature changes, weight loss, and clinical signs of influenza infection over a 6-day period including nasal signs of infection and changes in activity related to disease, based on methods established by Reuman et al (Reuman, Keely, & Schiff, 1989). Briefly, nasal symptoms in ferrets were assessed and scored based on the following criteria: no evidence of nasal symptoms (0), nasal rattling or sneezing (1), nasal discharge on external nares (2), or evidence of mouth breathing (3). Changes in the ferret's level of activity were assessed and scored based on the following criteria; fully playful (0), responds to play overtures but does not initiate play (1), alert but not playful (2), or not playful nor alert (3).

Kinetics of virus replication. Two separate studies were performed in 37 ferrets; 12 ferrets in each group were inoculated intranasally (i.n.) with 0.2, 0.5, or 1.0 ml containing 10^6 $TCID_{50}$ of the H1N1pdm or H3N2v influenza virus. One ferret was mock-infected with 1 ml of diluent (Leibovitz-15 (L-15) medium (Invitrogen-GIBCO)). Four ferrets from each of the volume groups (0.2, 0.5, or 1.0 ml) were sacrificed 1, 3, or 6 days post-infection (p.i.) and the mock-infected control ferret was euthanized on day 6. Samples from the nasal turbinates (NT) and lungs were harvested and stored at -80°C. Tissue samples were thawed, weighed and homogenized in L-15 medium containing a 2X concentration of antibiotic-antimycotic (penicillin, streptomycin, and amphotericin B) (Invitrogen-GIBCO) to make 5% or 10% (wt./vol.) (NT) or 10% (wt./vol.) (lung) tissue homogenates. Tissue homogenates were clarified by centrifugation at 1,500 rpm for 10 min and titrated in 24-well and 96-well tissue culture plates

containing a monolayer of MDCK cells. The virus titers were calculated using the Reed and Muench method and expressed as $\log_{10}$ $TCID_{50}$/gram of tissue.

Histology. Sections of lungs (L) and NT were collected for histological evaluation as follows. Sections of the right middle, left cranial, and left caudal lung lobes were collected for microscopic evaluation. Prior to collection, the lung lobes (with trachea intact) were insufflated with 10% neutral buffered formalin (NBF) and thereafter submerged in 10% NBF for 2-3 days. After adequate fixation, the desired sections of lung were placed in tissue cassettes.

In order to collect the NT for histological evaluation, the animal's head was sectioned along the midline into equal halves. Nasal turbinate tissues from one half were removed with forceps and frozen for virus titration. The remaining half, with NT left *in situ*, were then placed in 10% NBF for 2-3 days followed by decalcifying solution (Richard-Allan Scientific) for 12-24 hours. The nasal passages were then sectioned transversely at three levels: (1) immediately caudal to the canine tooth, (2) bisecting the 2nd premolar, and (3) between the 3rd premolar and molar in order to permit examination of the differing epithelia within the rostral, middle and caudal aspects of the nasal passages. The tissues were embedded in paraffin and sectioned (5 μm), placed on glass slides, and stained with hematoxylin and eosin (H&E). The stained tissue sections were randomized and graded for the presence and severity of pathology as follows: a score of 1 for inflammatory changes in <20% of the examined section; a score of 2 for inflammation comprising 20-50% of the examined section and a score of 3 for inflammation comprising 50% or greater of the examined section.

Dye distribution study. To evaluate the role of volume on the spread of inoculum in the respiratory tract of the ferret, four adult ferrets (two male and two female) were lightly anesthetized via inhalation of isoflurane and inoculated i.n. with 0.2, 0.5, or 1.0 ml of a tissue marking dye (Polysciences Inc., Warrington PA). Following administration of tissue marking dye, ferrets were allowed to recover fully and move freely within their cages. Approximately 30 minutes later, animals were anesthetized and humanely euthanized and the entire length of the respiratory tract was opened (*in situ*) and assessed grossly for the presence and extent of tissue dye distribution.

Micro-CT (μCT) Imaging. Formalin-fixed lungs (with trachea attached) from four ferrets were transferred to 70% alcohol and imaged using an in-vivo micro scanner (SkyScan 1176, Bruker μCT Kontich, Belgium). The alcohol was removed from the airways and the trachea was intubated and attached to an oxygen source. The air pressure was increased until all lung lobes were distended. The inflated lungs were then placed in the image chamber and scanned for 3-4 hours at 18 μm using a 0.2 mm aluminum filter set at 45 kV (kilovoltz), 550 uA (milliamps) and at an exposure time of 180 milliseconds (ms). After scanning, lung images were reconstructed using the *Nrecon* software by Bruker μCT (Kontich, Belgium)and analyzed using manufacturer supplied software.

Statistical analysis. To examine the associations between response variables such as ferret weight, body temperature, nasal turbinate virus titer, right or left lung virus titer and the explanatory variables such as gender, day (post-infection), inoculum volume and virus subtype,

we used the linear mixed model. Statistical analysis was performed using the statistical software *Splus*. *P* values less than 0.01 were considered significant.

RESULTS

Clinical disease in ferrets following infection with H1N1pdm or H3N2v virus

Clinical data. Weight, temperature and clinical signs of influenza were monitored daily in experimentally infected ferrets.

H1N1pdm virus infection*:* All animals receiving 0.5 or 1.0 ml of inoculum lost weight, with a peak percent weight loss of 5.6 and 5.7%, respectively while 3 of 4 animals receiving 0.2 ml inoculum had peak loss of 3.4% (Fig. 1A). Animals in the 1.0 ml inoculum group exhibited elevations in body temperature that ranged from 1-2°C above baseline, first observed on day 1 post-infection (p.i.) and maintained through day 6 in all 4 animals (Fig. 2A). Fewer animals in the 0.2 ml (1/4) and 0.5 ml (3/4) groups had elevations in temperature above baseline (Fig. 2A). In addition, nearly all animals in the 0.2 and 0.5 ml inoculum groups with elevated body temperature, displayed a return to or below baseline by day 6 p.i. The method of virus propagation in eggs or MDCK cells and the source from which ferrets were procured were similar to published studies with the H1N1pdm virus (Duan et al., 2010; Huang et al., 2011; Ljungberg et al., 2012; Rowe et al., 2010; van den Brand et al., 2011).

Figure 1. Percent weight loss in ferrets inoculated i.n. with 0.2, 0.5, or 1.0 ml containing 10^6 $TCID_{50}$ of the pH1N1 or H3N2v influenza viruses.

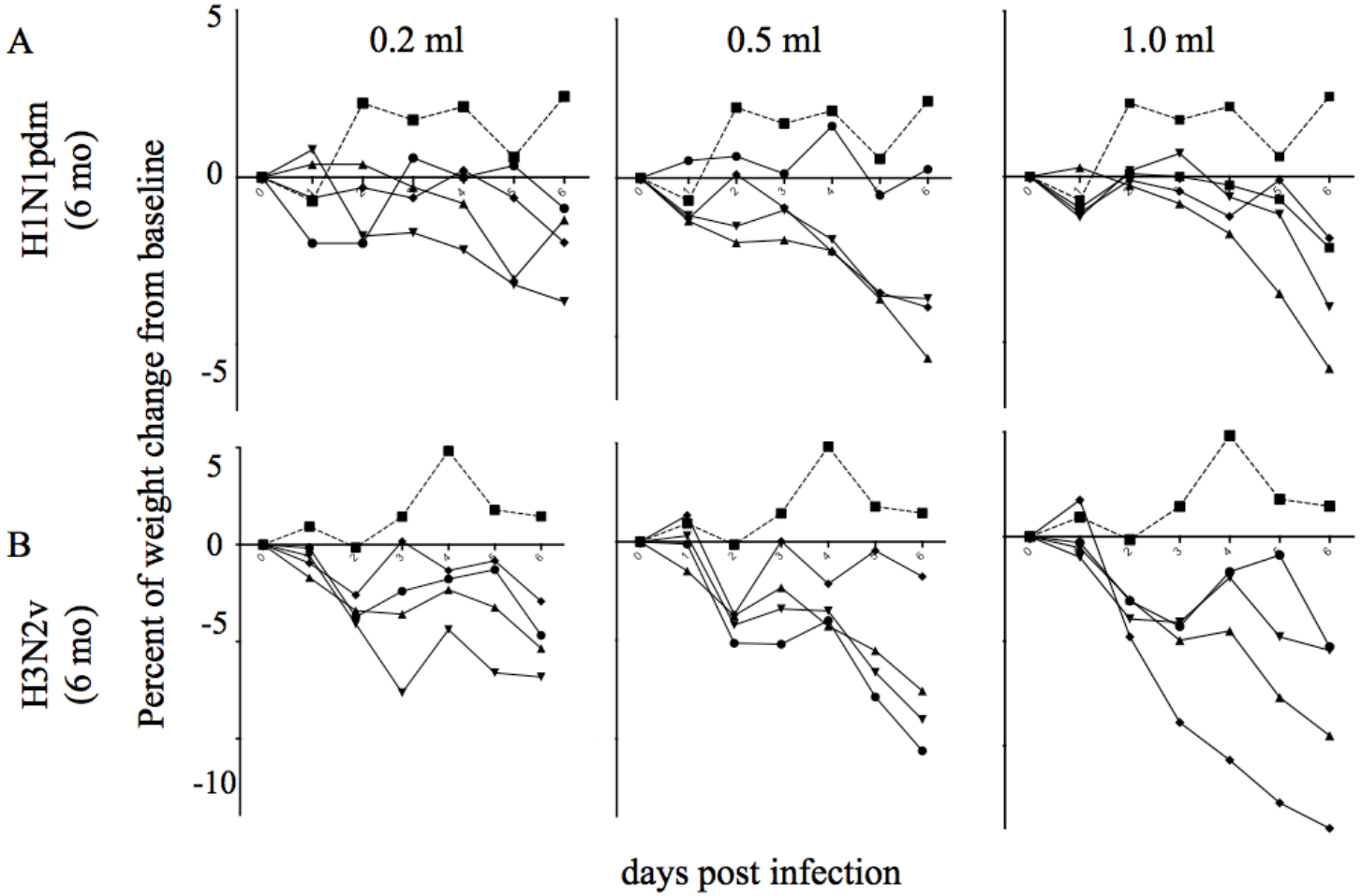

Figure 1 (cont'd)

Ferrets inoculated with either H1N1pdm (**A**) or H3N2v (**B**) were monitored daily for weight loss, and morbidity was recorded over a period of 6 days. Dotted lines represent the single mock-infected ferret, compared to animals that received virus at three different volumes (solid lines).

Figure 2. Change in body temperature in ferrets inoculated i.n. with 0.2, 0.5, or 1.0 ml containing 10^6 $TCID_{50}$ of the H1N1pdm or H3N2v influenza viruses.

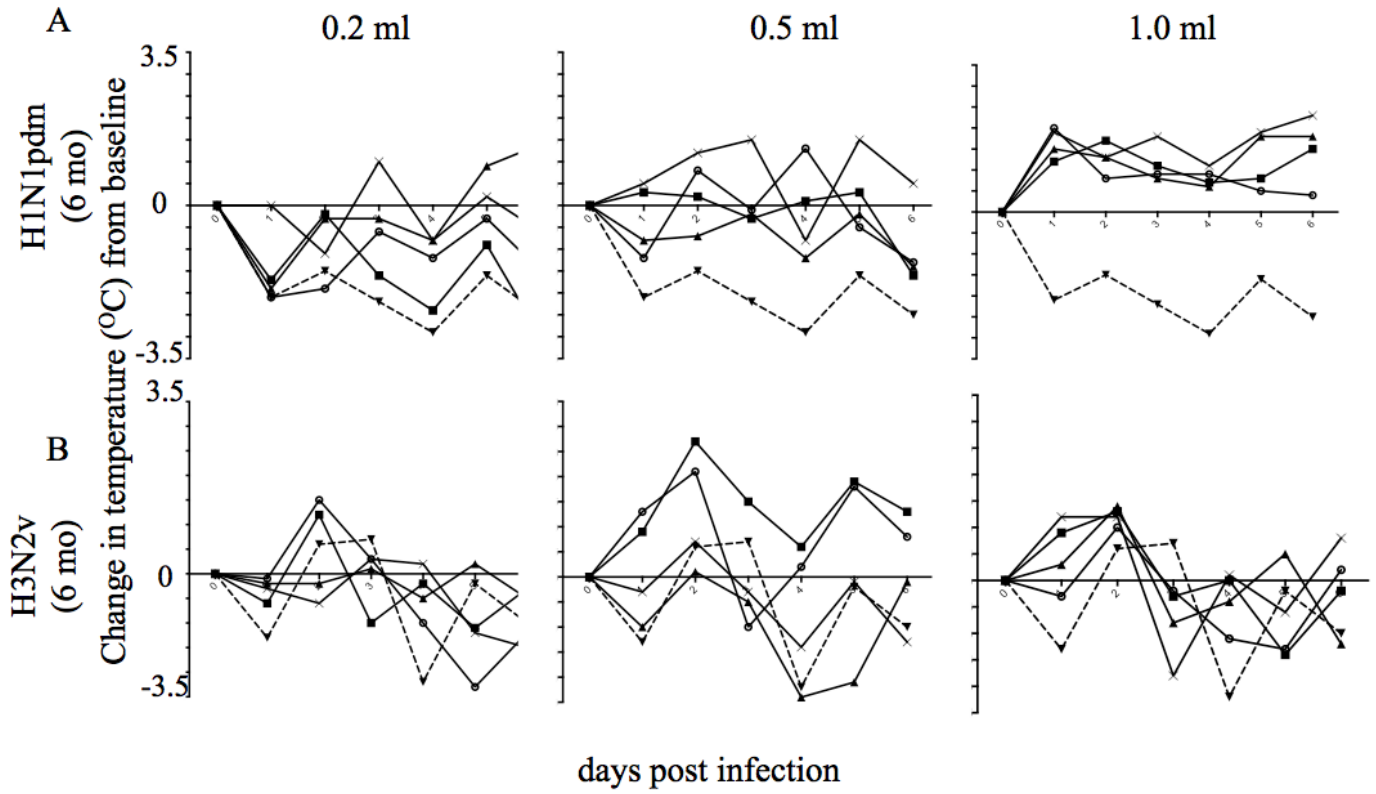

Figure 2 (cont'd)

Ferrets inoculated with either H1N1pdm (**A**) or H3N2v (**B**) were monitored daily for weight loss, and morbidity was recorded over a period of 6 days. Dotted lines represent the single mock-infected ferret, compared to animals that received virus at three different volumes (solid lines).

Ferrets that received 1.0 ml inoculum had a more substantial decrease in the level of activity (higher scores) than the other inoculum volume groups (0.2 and 0.5 ml) (Fig. 3A). Activity scores for the 0.2 and 0.5 ml groups ranged from clinically normal (0) to mild (1) or moderate (2). Nasal symptom scores were highest (3; most severe) on day 6 p.i. for animals in the 1.0 ml inoculum group, whereas nasal scores for the 0.2 and 0.5 ml groups ranged from clinically normal (0) to mild (1) or moderate (2) (Fig. 4A).

H3N2v virus infection. Weight loss was observed in all animals at each inoculum volume. Ferrets receiving 1.0 ml of inoculum reached a peak percent weight loss of 13.9% (4/4), while animals that received 0.2 ml and 0.5 ml had peak weight losses of 7.6% (4/4) and 10.6% (4/4), respectively (Fig. 1B). Peak elevations in body temperature occurred on day 2 p.i. for all inoculum groups (Fig. 2B). The largest increase in body temperature (~2.5°C above baseline) was observed in the 0.5 ml group and elevations in temperature were observed in 3/4 animals. All animals in the 1.0 ml inoculum group had elevations in body temperature that ranged from 1.0-1.5°C. Two of four animals in the 0.2 ml group exhibited elevations in body temperature above baseline (Fig. 2B). Although the magnitude of temperature elevation was greater in the 0.5 ml group, the consistency (day post infection and kinetics) with which the temperature elevation occurred was more appreciable in the animals that were administered 1.0 ml of virus inoculum. Additionally, we observed a relatively blunt response in body temperature change compared with weight change. The temperature was recorded using a subcutaneous transponder at a similar time each day. However, it is possible that a core body temperature may have been a more sensitive measure.

Clinical activity scores were similar for animals in the 0.5 and 1.0 ml inoculum groups, ranging from clinically normal (0) to mild (1) or moderate (2) and were observed as early as day 1 p.i. (Fig. 3B). Animals in the 0.2 ml group achieved activity scores similar to the 0.5 and 1.0 ml inoculum groups but the changes were of a shorter duration, and were observed only between days 2 and 4 p.i. (Fig. 3B). Nasal symptom scores were highest for animals in the 1.0 ml inoculum group and nasal symptoms were most severe on day 6 p.i. (3/4). The duration and degree of nasal symptoms was similar for animals in the 0.2 and 0.5 ml inoculum groups (Fig. 4B).

Figure 3. Activity scores for ferrets infected with the H1N1pdm or H3N2v influenza viruses.

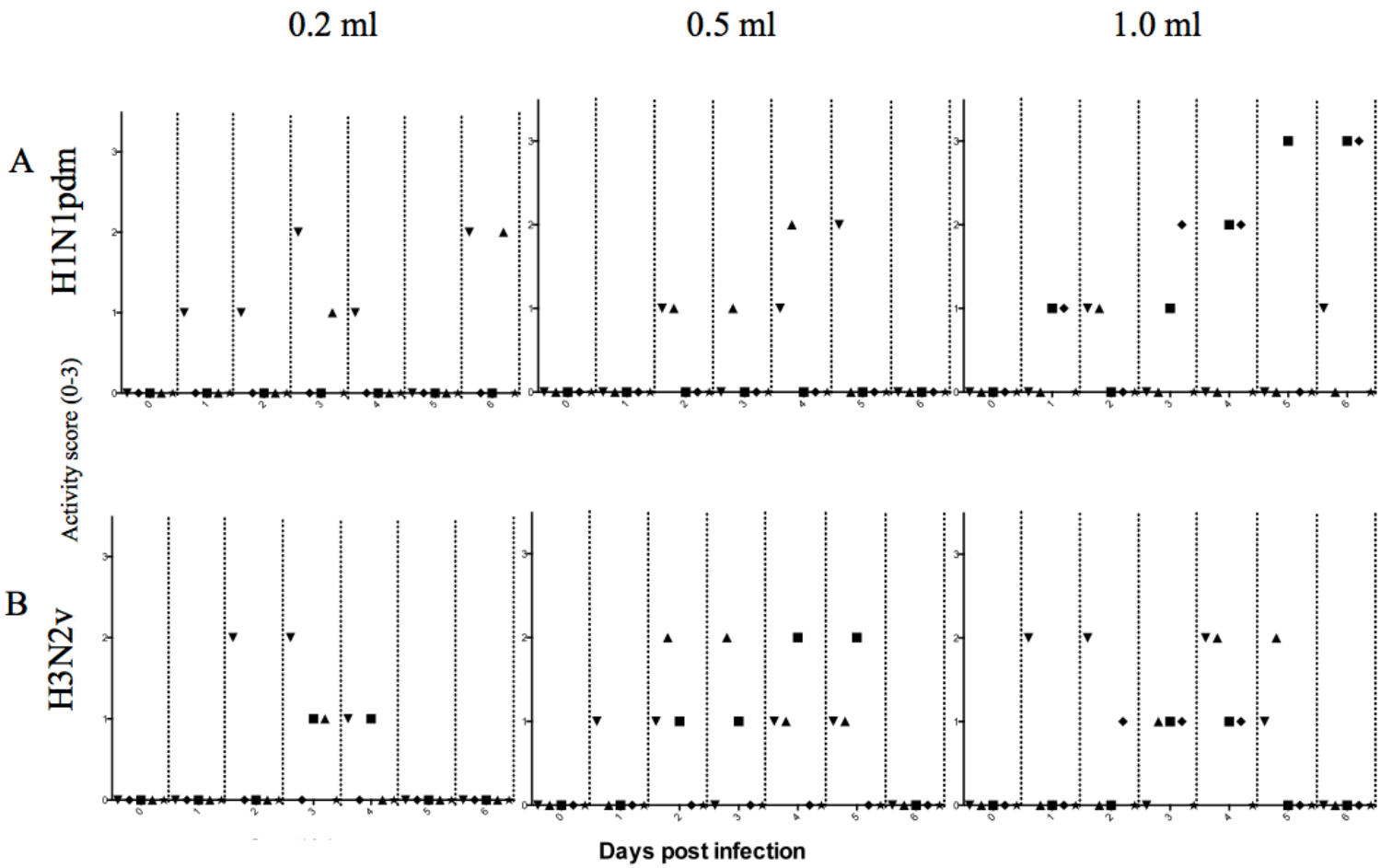

Figure 3 (cont'd)

Ferrets evaluated for level of activity following inoculation with the H1N1pdm (**A**) or H3N2v (**B**) influenza viruses. Activity scores range from 0 (within normal limits), 1 (mild), 2 (moderate), to 3 (severe; decrease in activity). Symbols represent activity scores for individual ferrets within each inoculum volume group and at a given timepoint.

Figure 4. Nasal symptom scores for ferrets infected with the H1N1pdm or H3N2v influenza viruses.

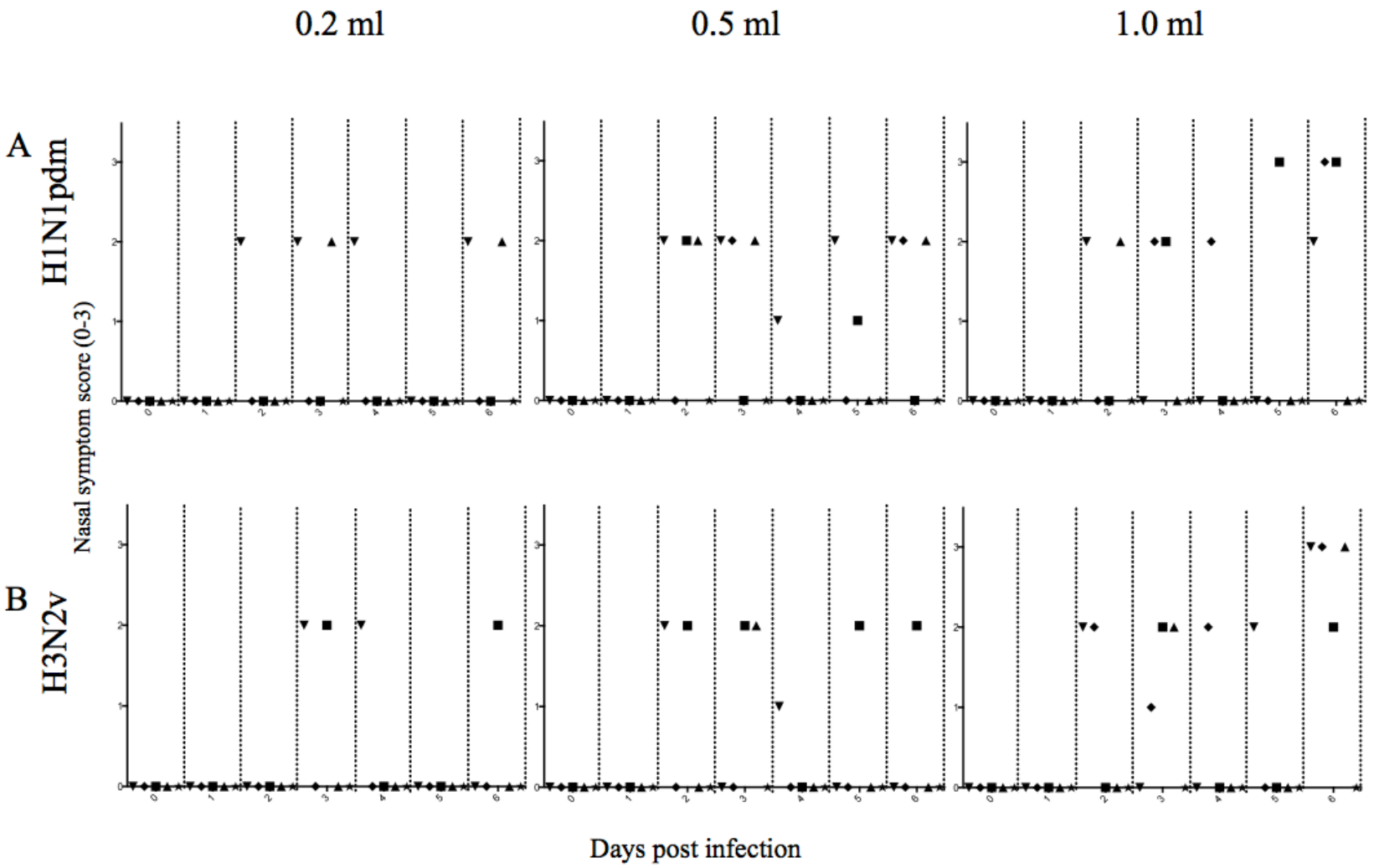

Figure 4 (cont'd) Ferrets evaluated for nasal symptoms following inoculation with the H1N1pdm (**A**) or H3N2v (**B**) influenza viruses. Nasal symptom scores range from 0 (within normal limits), 1 (mild), 2 (moderate), to 3 (severe). Symbols represent nasal scores for individual ferrets within each inoculum volume group and at a given timepoint.

Viral replication in the upper and lower respiratory tract

H1N1pdm virus infection. In the NT, the H1N1pdm virus replicated to high titers at all inoculum volumes and in all animals inoculated (Fig. 5A). Animals that received 0.2 ml inoculum (4/4) had a mean virus titer of $10^{7.5}$ $TCID_{50}$/g on day 1 p.i. Similar levels of virus replication were observed in animals that received the virus in volumes of 0.5 ml (4/4; $10^{7.4}$ $TCID_{50}$/g) on d3 p.i. and 1.0 ml (4/4; $10^{6.6}$ $TCID_{50}$/g) on d1 p.i. (Fig. 5A).

In the lower respiratory tract (LRT), sections of right middle (RM) and left cranial (LCr) lung lobes were sampled. The kinetics and level of virus replication for animals in the 1.0 ml inoculum group were similar when comparing right and left lung lobes. The mean titer on the day that the highest titer was achieved in the 1.0 ml group was $10^{5.1}$ $TCID_{50}$/g for the right and $10^{5.2}$ $TCID_{50}$/g for the left lung (Fig. 5A). The mean titer on the days that the highest titer was achieved for animals in the 0.5 ml group were $10^{3.3}$ $TCID_{50}$/g and $10^{3.8}$ $TCID_{50}$/g for right and left lung lobes, respectively. Animals in the 0.2 ml group showed the most noticeable disparity in viral replication between the two sides of the lung, with mean peak titers of $10^{2.5}$ $TCID_{50}$/g for the right lung versus $10^{3.8}$ $TCID_{50}$/g for the left lung samples (Fig. 5A). At all inoculum volumes, viral titers in the lungs declined sharply or were undetectable by day 6 p.i.

H3N2v virus infection. Similar to the replication in H1N1pdm virus infected animals, the H3N2v virus replicated efficiently and to high titers at all inoculum volumes. Animals in the 0.5 ml and 1.0 ml group showed the highest titers of virus in the NT (10^{8} and $10^{7.9}$ $TCID_{50}$/g, respectively) followed by the 0.2 ml group ($10^{7.2}$ $TCID_{50}$/g). In contrast to the consistent

decline in viral titers observed with the H1N1pdm virus, virus was detected at moderate to high levels on day 6 p.i. in the 0.5 and 1.0 ml inoculum groups (Fig. 5B).

In the LRT, peak mean virus titers were achieved on day 1 p.i. for the 1.0 ml group and the titers for the right and left lung were of similar magnitude, with $10^{7.1}$ $TCID_{50}$/g for the right and $10^{7.3}$ $TCID_{50}$/g for the left lung. Similar to observations made in H1N1pdm infected animals, the two smaller inoculum groups (0.2 and 0.5 ml) showed more noticeable inconsistencies in the amount of virus isolated between right and left lung samples (Fig. 5B). The mean titer on the day that the highest titer was achieved for the 0.5 ml group was $10^{3.1}$ in the right lung and $10^{5.3}$ $TCID_{50}$/g in the left lung. Similar to the level of inconsistent virus replication observed in the 0.2 ml group for animals infected with H1N1pdm virus, the peak mean virus titers from the right and left lung in the 0.2 ml group were $10^{2.7}$ and $10^{4.1}$ $TCID_{50}$/g, respectively. In all inoculum volume groups, viral titers decreased to levels near the limit of detection (LOD) by day 6 p.i.

Figure 5. Replication kinetics of H1N1pdm or H3N2v influenza viruses in ferrets following i.n. inoculation of 10^6 $TCID_{50}$/virus.

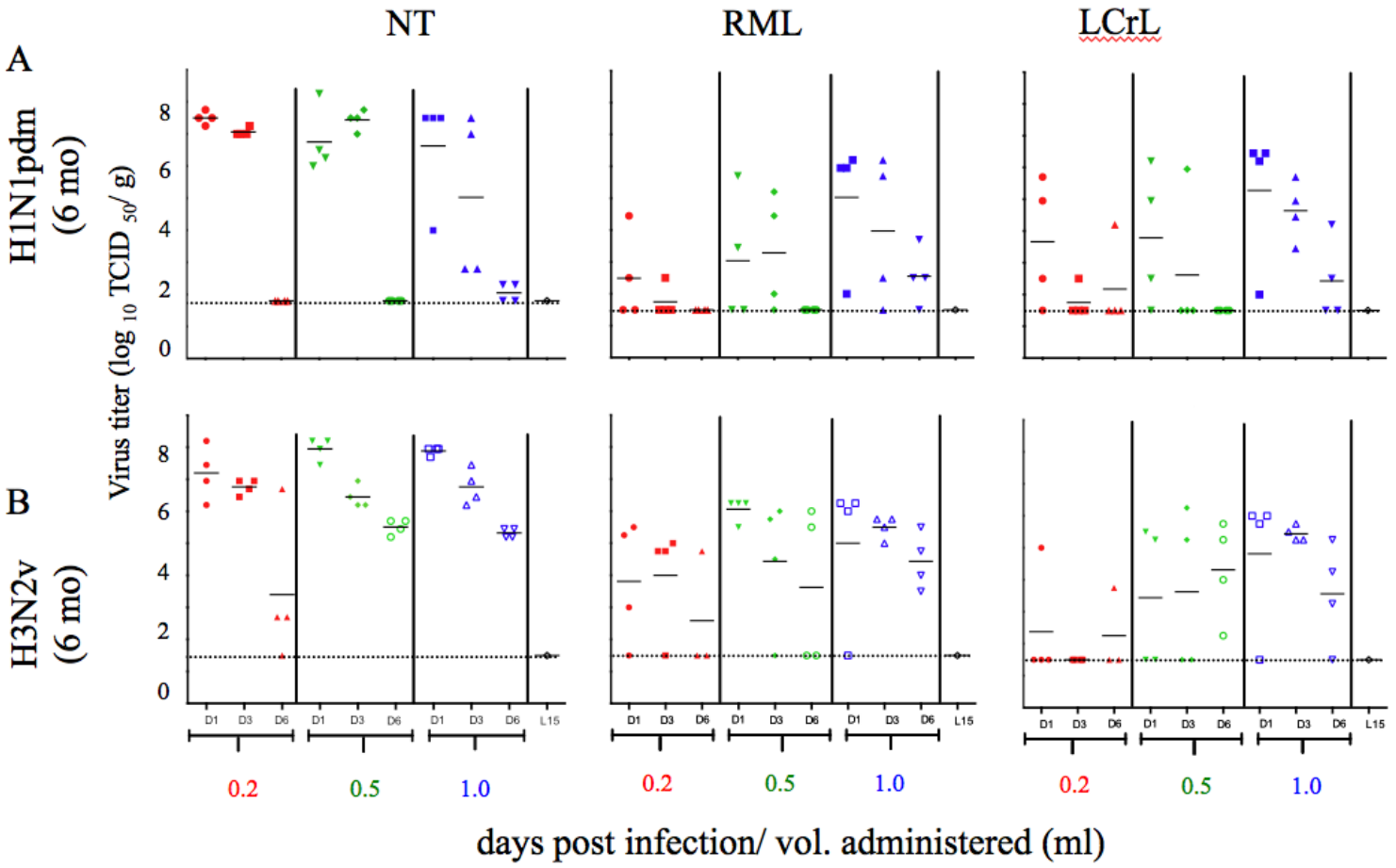

Figure 5 (cont'd)

Virus titers in the nasal turbinates (NT) and lungs (right middle [RML] and left cranial [LCr]) lobes of 4 ferrets per group that were euthanized on 1, 3, and 6 dpi are expressed as $\log_{10}$ $TCID_{50}$/gram of tissue. Ferrets were intranasally infected with either the H1N1pdm (**A**) or H3N2v (**B**) influenza viruses. Bars represent mean titers and symbols represent titers from individual ferrets. The dashed horizontal line indicates the lower limit of detection, $10^{1.8}$ and $10^{1.5}$ $TCID_{50}$ per gram for the NT and lungs, respectively.

Histopathology of the upper and lower respiratory tract

As previously described, the nasal turbinates (URT) were sectioned at 3 specific levels that would allow visualization of the different URT epithelia and to evaluate the tropism of the virus and the degree of pathology resulting thereafter. This method of histopathological evaluation of the URT of ferrets facilitates consistent and accurate tissue sampling and comparison of kinetics of viral replication with subsequent pathological changes. The landmarks for histopathology sectioning of the URT are: (1) immediately caudal to the canine tooth, (2) bisecting the 2nd premolar, and (3) between the 3rd premolar and molar (Fig. 6).

Figure 6. Sectioning of the nasal turbinates of ferrets for histologic evaluation.

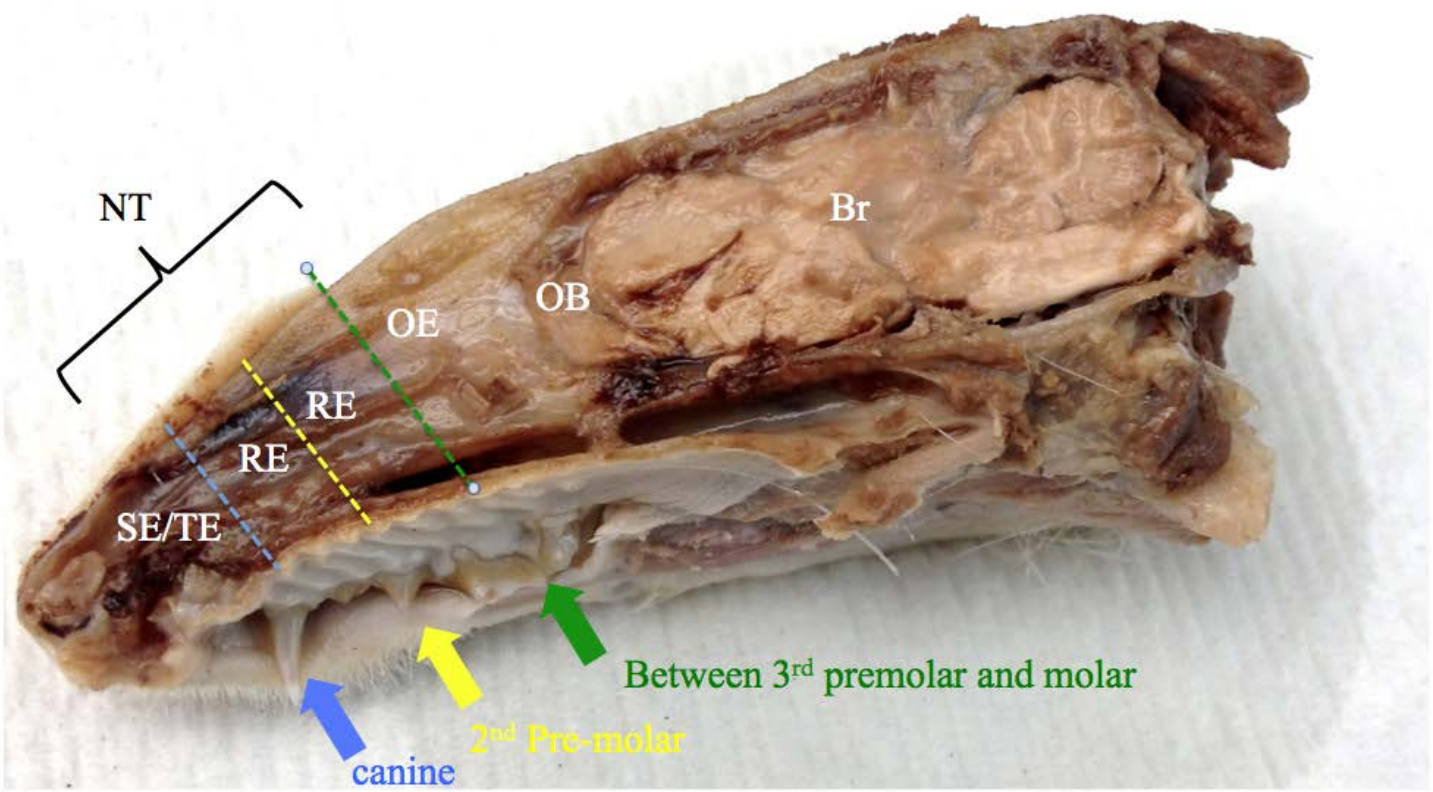

Figure 6 (cont'd)

Nasal turbinate tissues for virus titration and histopathology were collected at 3 specific levels of the nasal passages, which contain multiple epithelial cells types including squamous epithelium (SE), respiratory epithelium (RE), and olfactory epithelium (OE). Influenza viruses typically target the ciliated RE. The landmarks for consistent sectioning and sampling of the RE are; 1) caudal to the canine tooth, 2) bisecting the 2nd premolar and 3) between the 3rd premolar and 1st molar.

H1N1pdm virus infection

Sections of NT from animals infected with the H1N1pdm virus were sampled on days 1, 3 and 6 p.i. and examined histologically. In the sections of NT from day 6 p.i., the inflammatory changes were most intense and were often associated with abundant cellular debris that, in some cases, completely filled the NT lumina (Fig. 7A). The overlying respiratory epithelium consistently displayed regions of both cellular hyperplasia and occasional areas of squamous metaplasia; intact ciliated cells were infrequently observed. Inflammation was first observed on day 3 p.i. and was characterized by marked expansion and infiltration of the submucosal stroma by edema fluid and inflammatory cells (Fig. 7A). Ciliated cells along the mucosal surface were variably sloughed or intact and necrotic. In many cases, the lumina of the NT contained variable amounts of viable and degenerate neutrophils and admixed necrotic cellular debris. Sections of NT from animals on day 1 p.i. in all three groups were within normal limits, without evidence of inflammation (Fig 7A).

Figure 7. Pathology of the H1N1pdm and H3N2v influenza viruses in the nasal turbinate (NT) of ferrets following i.n. inoculation of 10^6 $TCID_{50}$/virus administered in 0.2, 0.5, or 1.0 ml volumes.

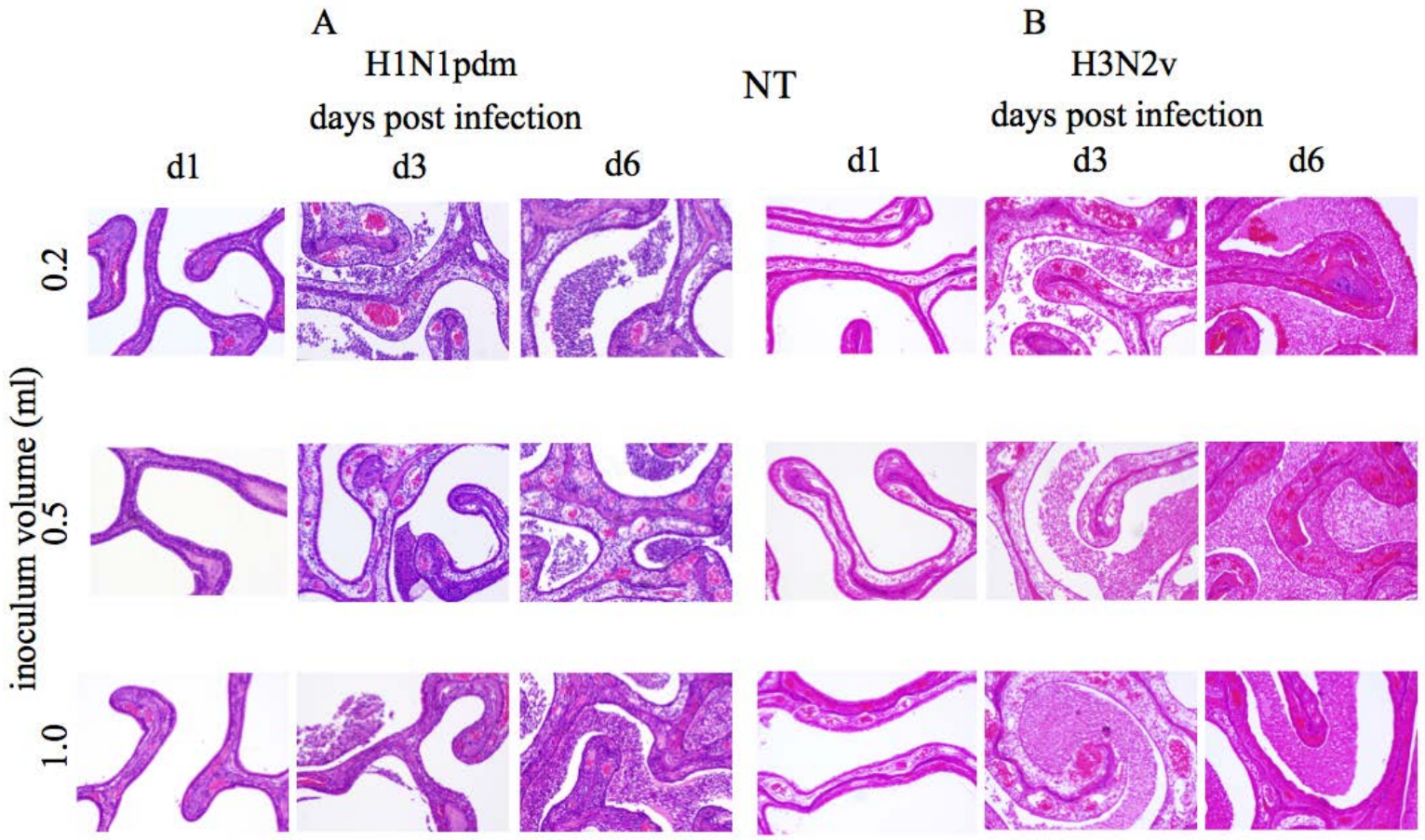

Figure 7 (cont'd)

Animals were euthanized on 1, 3, and 6 dpi. Photomicrographs are representative of the histopathological changes present in tissues from the 4 ferrets per group that were euthanized on 1, 3, and 6 following infection with either the H1N1pdm (**A**) or H3N2v (**B**) influenza viruses.

Sections of the right middle, left cranial, and left caudal lung lobes from four animals in each group at each of the three timepoints (1, 3, and 6 days p.i.) were sampled for histological evaluation. The presence and general degree of inflammation within the sections of lung examined correlated with the volume of inoculum administered. Lung pathology was widespread and most severe for the 1.0 ml group, while the 0.2 and 0.5 ml groups showed less severe pathology and fewer lung lobes affected (Table 1). While the frequency of lesions differed by volume, the cellular composition of the inflamed regions and the localization of the inflammatory lesions were consistent at all inoculum volumes. Similar to the kinetics of pathology in the upper respiratory tract (URT), inflammatory changes were most intense in the lung by day 6 p.i. (Fig. 8A). The regions immediately surrounding the bronchi were often characterized by expansion and infiltration of the peribronchial stroma by edema and an abundant mixed cellular infiltrate composed of neutrophils, macrophages, lymphocytes and plasma cells. In most cases, within these inflammatory foci, the submucosal glands (SMG) exhibited variable degrees of neutrophilic inflammation and necrosis (Fig. 8A). Sections of lung from day 3 p.i. exhibited a more extensive inflammatory process characterized by intense peribronchiolar inflammation that also extended into and expanded the alveolar interstitium adjacent to the affected airways (Fig. 8A). Inflammatory changes in the lung were present as early as day 1 p.i. (Fig. 8A), and began with a mild and predominantly neutrophilic and lesser histiocytic (alveolar macrophage) infiltrate in both peri- and intra-bronchiolar regions.

Figure 8. Pathology of the H1N1pdm and H3N2v influenza viruses in the lungs (LG) of ferrets following i.n. inoculation of 10^6 $TCID_{50}$/virus administered in 0.2, 0.5, or 1.0 ml volumes.

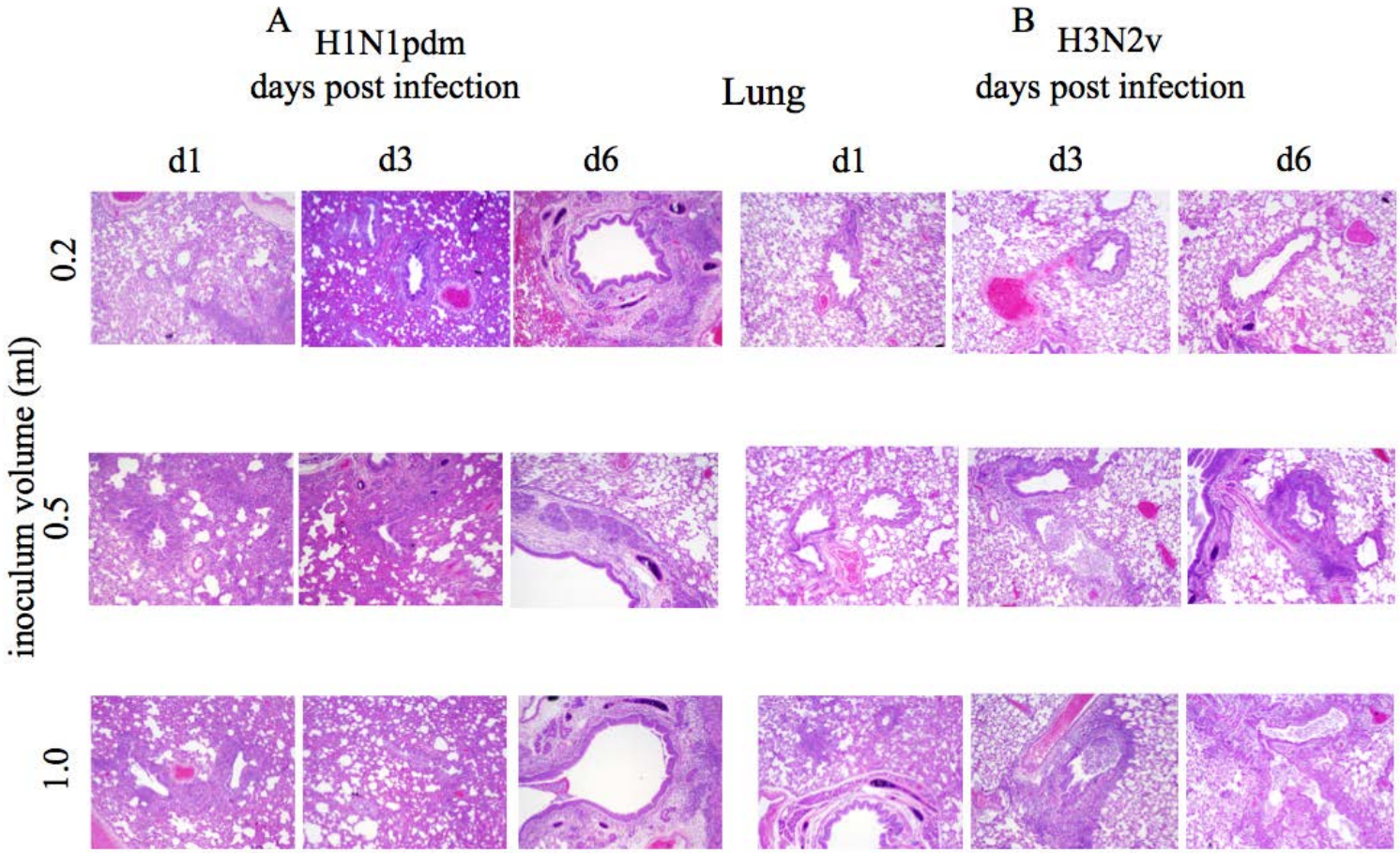

Figure 8 (cont'd)

Animals were euthanized on 1, 3, and 6 following infection with either the H1N1pdm (**A**) or H3N2v (**B**) influenza viruses. Photomicrographs are representative of the histopathological changes present in tissues from the 4 ferrets per group that were sacrificed on 1, 3, and 6 dpi.

H3N2v virus infection. Similar to URT findings with the H1N1pdm virus, infection with the H3N2v virus resulted in NT inflammation that was first observed on day 3 p.i. but was most severe on day 6 p.i. Sections of NT from day 6 p.i. were characterized by an intense neutrophilic inflammatory infiltrate that often completely filled the nasal passages. Frequently, the mucosa within these intensely inflamed regions was devoid of ciliated cells and displayed both epithelial hyperplasia and squamous metaplasia (Fig. 7B). On day 3, sections were characterized by expansion and infiltration of the submucosal stroma by edema and inflammatory cells. The overlying respiratory epithelium was often segmentally populated by ciliated cells and those exhibiting changes were histologically consistent with degeneration and necrosis. Sections of NT from day 1 p.i. showed no evidence of inflammation (Fig. 7B).

We found that, similar to animals infected with the H1N1pdm virus, lung pathology was more severe and more widespread, affecting a larger proportion of the lung sections examined, as the inoculum volumes were increased (Table 1). In the case of H3N2v, inflammatory lesions were most severe on day 6 for animals that received virus at volumes of 0.5 ml and 1.0 ml (Fig. 8B). These inflammatory foci were intensely neutrophilic and were closely associated with the bronchi and bronchioles. Day 3 p.i. (0.5 ml) was the earliest timepoint at which inflammation was observed and consisted of variably dense neutrophilic and, to a lesser extent, histiocytic infiltrates that were situated intimately around small bronchi and bronchioles (Fig. 8B). In contrast to H1N1pdm, inflammation was minimal to absent at all timepoints in animals that received virus in 0.2 ml.

Table 1. Distribution and severity of pathology in the lungs of ferrets infected with the H1N1pdm or H3N2v influenza viruses administered at different volumes.

		Volume of inoculum administered (ml)								
Virus	Animal ID	0.2			0.5			1.0		
		Necropsy on indicated days p.i.			Necropsy on indicated days p.i.			Necropsy on indicated days p.i.		
		D1	D3	D6	D1	D3	D6	D1	D3	D6
		Number of lung lobes affected* / lung pathology score (range 0-3) in each lobe examined (x, y)**								
H1N1pdm	1	0 / 0	1 / 1	1 / 1	1 /3	0 /0	2 / 2, 2	1/ 1	2 / 2, 1	2 / 3, 3
	2	1 / 1	1 / 1	1 / 1	0 / 0	1 / 1	2 / 3, 2	2 / 1, 1	1 / 1	2 / 3, 3
	3	1 / 1	1 / 2	1 / 3	1 / 1	1 / 1	2 / 2, 2	2 / 3, 1	2 / 3, 2	2 / 3, 3
	4	0 / 0	1 / 1	0 / 0	0 / 0	1 / 2	2 / 2, 3	1 / 2	2 / 2, 1	2 / 3, 2
H3N2v										
	1	1 / 1	0 / 0	0 / 0	0 / 0	0 / 0	2 / 2, 1	0 / 0	1 / 1	2 / 3, 1
	2	0 / 0	0 / 0	0 / 0	0 / 0	1 / 1	1 / 2	0 / 0	1 / 1	2 / 1, 3
	3	0 / 0	0 / 0	0 / 0	1 / 1	1 / 1	1 / 1	1 / 2	1 / 2	2 / 2, 2
	4	0 / 0	0 / 0	0 / 0	0 / 0	1 / 2	1 / 1	1 / 2	1 / 3	2 / 3, 2

Table 1 (cont'd)

*Two sections of lung (right middle and left cranial (caudal half) were sampled for animals infected with the H1N1pdm or H3N2v influenza viruses. **Lung pathology scores ranged from 0 (minimal) to 3 (severe) and were based on the extent of pathology present in each tissue section examined; 0= within normal histologic limits, 1= 5-25%, 2= 25-50%, 3= 50% or greater.

Distribution of inoculum in the ferret respiratory tract

In order to determine the basis for differences in viral replication and distribution of pathology in the respiratory tract, we sought to investigate the ability of different inoculum volumes to coat the URT and LRT. We inoculated ferrets intranasally with tissue staining dye in volumes of 0.2, 0.5, or 1.0 ml. Introduction of this dye into the nasal passages, at different volumes, allowed us to characterize the spread and localization of inoculum immediately following administration.

At all three volumes, dye was detected in the upper respiratory tract (URT) and in the esophagus. However, we cannot estimate the proportion of the inoculum that was swallowed. Animals in the 0.2 ml inoculum group showed small accumulations of dye in the rostral-most regions of the nasal passages (Fig. 9). Inoculum was also present in the proximal esophagus, but not in the trachea (Fig. 9). Animals in the 0.5 ml group showed dye over a greater area of the nasal passages, and abundant staining of the esophageal mucosa but no evidence of dye in the trachea. In the 1.0 ml group, dye coverage of the URT was extensive, extending caudally towards the margin of the cribriform plate. The dye was present throughout the length of the esophagus and the full length of the trachea and was also observed grossly within the parenchyma of the left caudal lung lobe (Fig. 9). On cut section, dye was present within the lung parenchyma (Fig. 9 [inset].

Figure 9. Distribution of a mock inoculum within the upper and lower respiratory tract of ferrets.

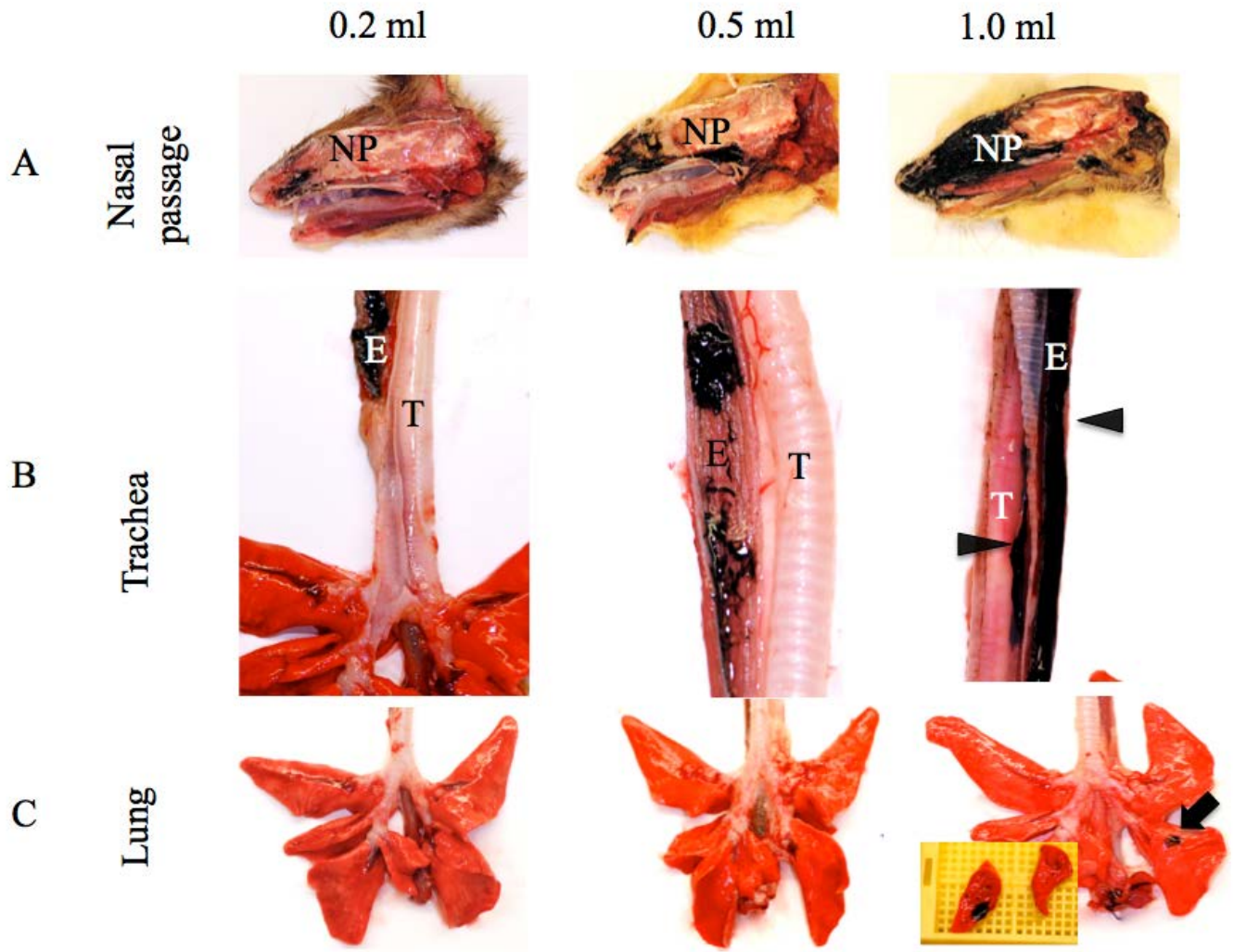

Figure 9 (cont'd)

Tissue staining dye was administered i.n. to 4 ferrets per group in 0.2 (A), 0.5 (B), or 1.0 (C) ml volumes. Thereafter, animals were euthanized and gross examination of the respiratory tract was conducted. Examined tissues included nasal passage (NP), trachea (T), esophagus (E) and lungs. Arrowheads indicate deposition of tissue dye within the trachea and esophagus and stars indicate localization of dye in the lung. Dye can be observed from the surface of the lung (arrow) and on cut sections within lung parenchyma (inset).

Micro-CT (μCT) imaging and analysis of the ferret respiratory tract

Using Micro-Computed Tomography (μCT) we found that, consistent with published data, ferrets and humans share a number of anatomic similarities of the lung (Baric, 2006), characterized by three right (cranial, middle, caudal) lung lobes and two left (cranial and caudal) lung lobes. Interestingly, we found that the diameter of the right main stem bronchus was considerably and consistently larger than left. In addition, the right bronchus arose from the tracheal bifurcation at an angle with a more pronounced lateral deviation and one that is more acute than the left bronchus, whereas, the narrower left bronchus consistently arose from the bifurcation in a straighter fashion, projecting towards the left caudal lung lobe (Fig. 10).

Figure 10. Maximum intensity projection (MIP) of normal ferret lung anatomy.

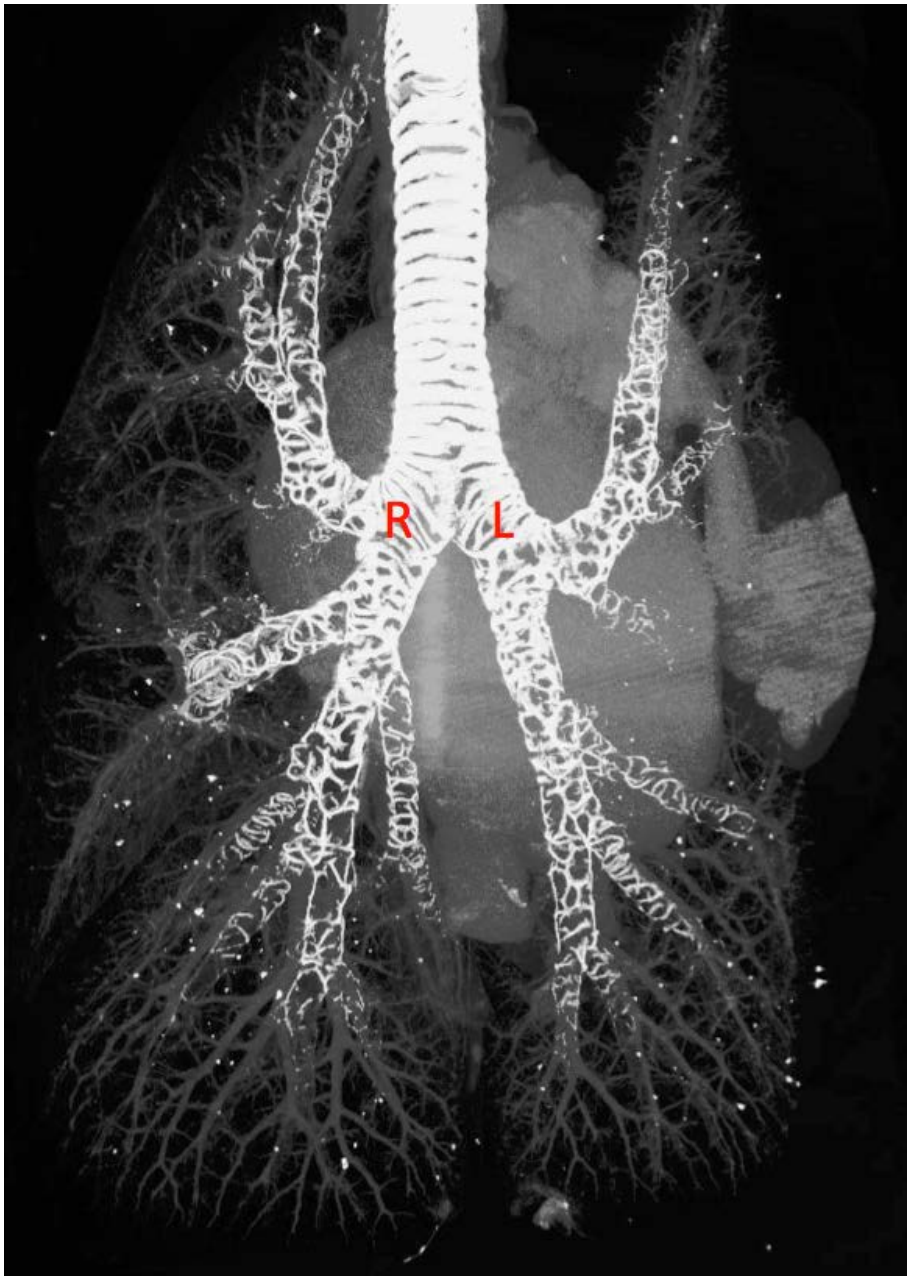

Figure 10 (cont'd)

Lungs from uninfected adult ferrets were imaged (ex-vivo) using a modified air bronchogram method and Micro-computed Tomography (μCT) to assess the normal anatomy and conformation of the ferret LRT. Letters indicate the location of the ostia of the right (R) and left (L) mainstem bronchi as they arise from their origin at the tracheal bifurcation.

SUMMARY

-Inoculum volume, irrespective of virus subtype, had a significant effect on the level and consistency of viral replication in the LRT of ferrets.

-Smaller inoculum volumes (0.2 and 0.5 ml) were associated with less consistent viral replication and pathology in the lungs than in animals that received 1.0 ml inoculum. We found that a dose of 10^6 $TCID_{50}$ of virus was sufficient to induce reproducible clinical disease and pulmonary pathology in ferrets.

-We found that collecting the right middle and a caudal portion of the left cranial lung lobe for virus titration provides a more comprehensive assessment of viral replication in the lungs.

-Micro-CT analysis of the ferret lung identified unique anatomical features of the ferret respiratory tract; specifically, that the right mainstem bronchus was consistently larger in diameter than the left mainstem bronchus and arose from the tracheal bifurcation earlier and at a more acute angle, whereas, the left bronchus often exhibited a straighter projection into the caudal lung lobe.

DISCUSSION

In this study we demonstrate that inoculum volume affects the severity of clinical disease in ferrets experimentally infected with two different influenza viruses. Understanding the contribution of inoculum volume to disease outcomes in this model will reduce the level of variability in clinical disease and viral replication and lead to standardization of the model. Miller *et al*. (Miller, Kok, & Li, 2013) demonstrated variable clinical outcomes in mice infected with an H3N2 influenza A virus (X31) that was administered to mice intranasally at a dose of 10^3 $TCID_{50}$ in volumes of 25, 35 or 50µl. They found that mice infected with virus in a volume of 25 µl readily recovered from disease, while the same dose of virus administered in 35 µl and 50 µl volumes was associated with fatal outcome. Cook *et al*. (Cook, Eglin, & Easton, 1998) also reported considerable variations in clinical disease outcomes in mice that were infected with 120 plaque forming units of pneumovirus administered in 10, 25, and 50 µl. Lowering the inoculum volume from 50 to 25 µl diminished the severity and duration of clinical signs. Further reduction of inoculum to 10 µl completely abolished signs of disease.

Importantly, in addition to clinical observations, we found that inoculum volume had a significant effect on the level and consistency of viral replication in the LRT of ferrets. Furthermore, we found that smaller inoculum volumes (0.2 and 0.5 ml) were associated with less consistent viral replication in the lungs than in animals that received 1.0 ml inoculum. In some cases, animals that received 0.2 or 0.5 ml inoculum had 10,000 to 100,000-fold differences in virus titer between the right and left lung lobes. Differences of this magnitude were rarely observed in the 1.0 ml group, demonstrating that the largest inoculum volume resulted in more uniform viral replication in the LRT, likely a result of more uniform distribution of inoculum. van den Brand *et al.* (van den Brand, Stittelaar, Leijten, et al., 2012) reported inconsistencies in

the ability to elicit clinical signs of disease in ferrets using a seasonal human influenza virus administered intranasally at a dose of 10^6 $TCID_{50}$. Thereafter, they modified their experimental design to intratracheal administration of 10^9 $TCID_{50}$ of virus in an inoculum volume of 3 ml. However, we found that a dose of 10^6 $TCID_{50}$ of virus administered intranasally in a volume of 1.0 ml was sufficient to induce clinical disease and pulmonary pathology in ferrets.

The H1N1pdm and H3N2v viruses replicated to high titers in the NT, though the H3N2v virus replicated to levels that were significantly (p= 0.0016) higher than the H1N1pdm virus. Animals that received H1N1pdm virus in 0.2 ml of inoculum had viral titers that were slightly higher than animals that received this virus in 0.5 or 1.0 ml volumes. Furthermore, the level of virus replication in the animals in the 0.2 ml group (n=4) was more consistent than that observed in the 0.5 and 1.0 ml groups. In contrast, NT virus titers for animals infected with the H3N2v influenza virus were highest and most consistent for the 0.5 and 1.0 ml groups and slightly lower (10 to 100 - fold) and less consistent than in animals that received virus at the lowest inoculum volume (Fig. 5). The H3N2v virus replicated to levels that were significantly higher than those of the H1N1pdm virus in the NT, but in the LRT, both viruses replicated poorly except when the inoculum volume was 1.0 ml. Smith *et al.* (J. H. Smith et al., 2011) also reported that when ferrets were infected with a dose of 10^2 $TCID_{50}$/ ml in 0.2 ml, the H1N1pdm virus replicated well (~6 logs) in the NT but virus was not isolated from the lungs of any of the animals. However, in contrast to my findings, Pearce *et al.* (Pearce et al., 2012) reported that the influenza A/MN/10 (H3N2v) virus replicated to high titers in the NT but was undetectable in the lungs of ferrets that were infected intranasally with 10^6 PFU administered in 1.0 ml volume. It is possible that their inability to detect viral replication in the LRT was influenced by sampling of lung

tissue for virus titration because we noted significant differences in the level of virus replication between the right and left lung samples, irrespective of virus subtype. We found that collecting the right middle and a caudal portion of the left cranial lung lobe for virus titration provides a more comprehensive assessment of viral replication in the lungs. We also found that when we compared the pathology associated with the two viruses in the LRT of ferrets, pathological changes were minimal in the 0.2 ml inoculum group but were more severe and evenly distributed (between right and left lung) when animals received either virus in a 1.0 ml volume (Table 1). In a multivariate analysis when we examined gender, day (p.i.), inoculum volume and virus subtype, we found that both day p.i. and inoculum volume, were significant predictors of level of virus replication in the lung of ferrets experimentally infected with either virus subtype. Specifically, we found that increasing the inoculum volume led to significant increases in the virus titer in both right (p=<0.0001) and left (p=0.0001) lung lobes. In addition, we found that over the 6-day period, there was a significant decrease in virus in both the right (p=0.0001) and left (p=<0.0001) lung lobes.

These observations prompted us to investigate the anatomy of the ferret's respiratory tract in order to determine whether anatomical features contribute to the variable distribution of inoculum in the LRT of the ferret model. Micro-CT analysis of the ferret lung demonstrated that the right mainstem bronchus of ferrets (n=4; irrespective of gender) consistently had a larger diameter than the left mainstem bronchus and often arose from the tracheal bifurcation earlier and at a more acute angle, whereas, the left bronchus often exhibited a straighter projection into the caudal lung lobe. In addition to the observations made on μCT, we examined gross specimens (n=10) and found that at the level of the tracheal bifurcation the mean diameter of the left mainstem bronchus was 3.08± 0.12 mm and the right mainstem bronchus was approximately

1.5 times larger than the left mainstem bronchus, measuring 4.85 ± 0.20 mm in diameter. Irrespective of virus subtype, there was significantly higher titer of virus in both the right and left lung lobes based on the volume of inoculum administered. In addition, we noted that at the two smaller inoculum volumes (0.2 and 0.5 ml) there was a trend towards higher virus titers in the left lung lobe, irrespective of the virus subtype administered. However, the variability in virus titer was reduced when a volume of 1.0 ml of inoculum was administered. We speculate that the conformation of the conducting airways influences the distribution of inoculum in the LRT

Ferrets are commonly held in an upright position while inoculum is instilled into the nasal passages and they are maintained in this position long enough to ensure full inhalation of the inoculum. It is possible that anatomical features of the ferret airways, in conjunction with the vertical positioning and the administration of a particular volume of inoculum, could influence the direction and immediate localization of inoculum in the LRT. Swallowing of inoculum likely contributes to the high variability of virus titers in the lung and volume-dependent differences in clinical disease severity when smaller inoculum volumes are administered. Three of four animals that received 1.0 ml of dye showed evidence of staining in the LRT in addition to a considerable amount of dye in the esophagus. It is likely that the larger volume of inoculum easily reaches the lower respiratory tract, though a significant proportion of the inoculum is swallowed. It is important to note that the dye inoculation study only shows the immediate distribution of an inert inoculum; clearly, influenza virus administered in 0.2 or 0.5 ml is able to infect the LRT despite my inability to detect dye in the LRT of ferrets immediately following administration. The association of clinical signs with the larger volume of inoculum suggests that the virus replication and inflammatory changes that occur in the LRT are important determinants of clinical illness.

In the lung, both influenza viruses were associated with a predominantly neutrophilic inflammatory response at the mid and late timepoints of the study. However, the severity and distribution of inflammation in the lung was greater in the animals infected with the H1N1pdm virus. The H1N1pdm virus was associated largely with changes in the pulmonary interstitium at early timepoints and became more airway-centered by day 6 p.i. A remarkable feature of H1N1pdm virus infection at day 6 p.i. was the presence of submucosal gland (SMG) inflammation and viral antigen. Bissel et al (Bissel et al., 2014) also identified H1N1pdm virus within the SMG of experimentally infected ferrets between days 2-3 p.i. by *in situ* hybridization (ISH). The significance of inflammation at this location is not well understood, however the localization of viral antigen in the submucosal glands has been demonstrated in humans who succumbed to H1N1pdm infection (Guarner & Falcon-Escobedo, 2009; Sheng et al., 2011; van Riel et al., 2007), ferrets infected with seasonal human H3N2 virus (Schrauwen et al., 2011), and in formalin fixed paraffin-embedded (FFPE) tissues from humans and mice infected *in-vitro* with H5N1 virus using immunohistochemistry (van Riel et al., 2007).

Ferrets express influenza virus SA receptors in a pattern that is similar to that of the humans. In general, human influenza viruses preferentially bind α2,6 SA, that are found in the URT while avian influenza viruses preferentially bind α2,3 SA that are much more prevalent in the LRT. In this study, I did not examine the effect of inoculum volume on infection with seasonal human influenza viruses or avian influenza viruses that differ significantly in their sialic acid receptor preference. However, in a separate study, I observed that a highly pathogenic H5N1 influenza virus administered in 0.2 ml caused only mild clinical disease in ferrets (unpublished data) while the same amount of virus administered in an inoculum volume of 0.5 ml caused neurological disease including hind limb paresis (Suguitan et al., 2012). Taken

together with the findings from the current study, it is likely that the animals that received 0.2 ml of the H5N1 virus had milder clinical disease than the animals that received 0.5 ml inoculum because the smaller volume did not efficiently infect the LRT where the α2,3 SA receptors predominate.

In summary, I have demonstrated the importance and influence of inoculum volume on clinical illness and pathology and viral replication in ferrets experimentally infected with two different influenza A viruses. I have shown the importance of using a 1.0 ml volume of inoculum to deliver virus to the LRT. In addition, I have identified anatomical features of the ferret LRT that influence the disease process. Therefore, I recommend administering 1.0 ml of inoculum intranasally for experimental infection in ferrets, particularly when clinical disease outcomes are a desired study parameter.

CHAPTER 3: Clinical disease outcomes in influenza virus-infected ferrets based on age

INTRODUCTION

In Chapter 2, I described detailed clinical and pathological outcomes of experimental infection with the H1N1pdm and H3N2v influenza viruses in 6 month old ferrets. In my review of literature related to the use of ferret model in the investigation of H1N1pdm pathogenesis, I also identified age as a potential contributor to the severity of clinical disease. In order to evaluate this parameter, I will compare and contrast the disease outcomes of 8 week old ferrets infected with either the H1N1pdm or H3N2v influenza viruses, to that previously described in older (6 month old) animals infected with these viruses. This chapter will be focused on the severity of clinical disease in ferrets based on animal age. Specifically, I will assess clinical disease, kinetics of virus replication, pathology of the respiratory tract, and distribution of influenza virus receptors, immune response, and the role of lung development on clinical disease outcomes.

ABSTRACT

Ferrets are a valuable model for influenza pathogenesis, virus transmission and antiviral therapy studies. Analysis of the current literature related to the use of the ferret model shortly after the emergence of the 2009 H1N1 pandemic (H1N1pdm) influenza virus, revealed substantial variation in clinical disease in ferrets that were administered similar H1N1pdm viruses intranasally at a dose of 10^6 $TCID_{50}$. In a previous study (I. N. Moore et al., 2014), it was shown that increasing inoculum volume while using the same amount of virus was associated with increased efficiency and consistency of virus replication in the lower respiratory tract and increased severity of clinical disease with two influenza viruses [H1N1pdm (A/California/07/2009) and H3N2-variant (H3N2v) (A/Minnesota/11/2010)]. Interestingly, comparison of published studies revealed that the severity of clinical disease differed between animals of different ages following experimental infection. Therefore, I sought to assess the role of age on the severity of clinical disease in ferrets experimentally infected with influenza viruses. The H1N1pdm and the H3N2v influenza viruses were administered intranasally to young (8 week old) and old (6 month old) ferrets in a range of inoculum volumes (0.2, 0.5, or 1.0 ml) and viral replication, clinical disease, and pathology was followed over 6 days. I observed that clinical illness and respiratory tract pathology were most severe and most consistent in old (6 month old) ferrets. In order to determine the biological basis for the age-related difference in disease severity, I examined the anatomy of the respiratory tract and the immune responses in the two groups of ferrets. A modified method of micro-CT imaging showed that the distal regions of the conducting airways of old ferrets, consistently displayed a more complex and extensive pattern of airway branching compared to younger ferrets. These anatomic features likely

influence the distribution of inoculum in the lower respiratory tract. Immune responses differed between the two age groups, with pro-inflammatory or anti-viral focused responses in old and young ferrets, respectively. These findings highlight important anatomical features of the ferret lung that influence the kinetics of viral replication, clinical disease severity and lung pathology.

MATERIALS AND METHODS

Viruses. Influenza A viruses, A/CA/07/2009 (H1N1pdm) and A/MN/11/2010 (H3N2v), were propagated in the allantoic cavity of 9 to 11 day old specific-pathogen-free embryonated hen's eggs (Charles River Laboratories, Franklin, CT) at 37°C. Virus titers were determined in Madin-Darby canine kidney (MDCK) cells (ATCC, Manassas, VA) and calculated using the Reed and Muench method (Reed, 1938). Ferret experiments were conducted in an approved animal care facility at the National Institutes of Health (NIH). The method of virus propagation in eggs or MDCK cells and the source from which ferrets were procured were similar to published studies with the H1N1pdm virus (Duan et al., 2010; Huang et al., 2011; Ljungberg et al., 2012; Rowe et al., 2010; van den Brand et al., 2011).

Animals. Eight week old and six month old male and female ferrets (Triple F Farms, Sayre, PA) were used and all animal experiments were performed at the NIH with approval of and in compliance with the guidelines of the NIAID/NIH institutional animal care and use committee. All of the ferrets, in each of the respective groupings, were born on the same day. All ferrets were seronegative for hemagglutination inhibition (HAI) antibodies against currently circulating human H1N1 and H3N2 viruses.

Experimental influenza virus infection. Studies with each influenza virus were conducted in 36 8-week-old ferrets and 36 6-month-old ferrets (male: female; 1:1), therefore the data presented represent 4 separate experiments. All ferrets were lightly anesthetized via inhalation of isoflurane and held in an upright position and inoculated intranasally (i.n.) with 0.2, 0.5, or 1.0

ml containing 10^6 $TCID_{50}$ of the H1N1pdm or H3N2v influenza virus. The diluent was Liebovitz-15 Medium (L15; (Invitrogen-GIBCO)). A total of 6 mock-infected ferrets (4 8 week old and 2 6 month olds) were administered 1 ml of diluent only. The total volume of each inoculum was administered in roughly equal portions into the two nares. The ferrets were held upright for 10-15 seconds after virus administration, to allow a few normal breaths before they were placed prone in their cage. The ferrets were sedated deeply enough to suppress sneezing and they regained consciousness within 5 minutes of intranasal administration of the inoculum.

Clinical illness. Prior to inoculation, all animals were implanted with a subcutaneous transponder between the shoulders for monitoring body temperature and for animal identification. Ferrets were monitored daily for temperature changes, weight loss, and clinical signs of influenza infection over a 6-day period including nasal signs of infection and changes in activity related to disease, based on methods established by Reuman et al (Reuman et al., 1989). Briefly, nasal signs in ferrets were assessed and scored based on the following criteria: no evidence of nasal signs (0), nasal rattling or sneezing (1), nasal discharge on external nares (2), or evidence of mouth breathing (3). Changes in the ferret's level of activity were assessed and scored based on the following criteria; fully playful (0), responds to play overtures but does not initiate play (1), alert but not playful (2), or not playful nor alert (3).

Kinetics of virus replication. Four separate studies were performed using 36 ferrets each; 12 ferrets in each group were inoculated intranasally (i.n.) with 0.2, 0.5, or 1.0 ml containing 10^6 $TCID_{50}$ of the H1N1pdm or H3N2v influenza virus. Four ferrets from each of the inoculum

volume groups (0.2, 0.5, or 1.0 ml) were euthanized 1, 3, or 6 days post-infection (p.i.) and mock-infected control ferrets were sacrificed on day 6. Samples from the nasal turbinates (NT) and lungs (right middle lung [RML] or left cranial lung [LCrL]) were harvested and stored at -80°C. Tissue samples were thawed, weighed, and homogenized in L-15 medium containing a 2X concentration of antibiotic-antimycotic (penicillin, streptomycin, and amphotericin B) (Invitrogen-GIBCO) to make 5% or 10% (wt./vol.) (NT) or 10% (wt./vol.) (lung) tissue homogenates. Tissue homogenates were clarified by centrifugation at 1,500 rpm for 10 min and titrated in 24-well and 96-well tissue culture plates containing a monolayer of MDCK cells. The virus titers were calculated using the Reed and Muench method (Reed, 1938) and expressed as $\log_{10}$ $TCID_{50}$/gram of tissue.

Histology and immunohistochemistry. Section of lungs (L) and NT were collected for histological evaluation as follows. Sections of the right middle, left cranial and left caudal lung lobes were collected for microscopic evaluation. Prior to collection, the lung lobes (with trachea intact) were insufflated with 10% neutral buffered formalin (NBF) and thereafter submerged in 10% NBF for 2-3 days. After adequate fixation, the desired sections of lung were placed in tissue cassettes.

In order to collect the NT for histological evaluation, the animal's head was sectioned along the midline into equal halves. Nasal turbinate tissues from one half were removed with forceps and frozen for virus titration. The remaining half, with NT left in situ, were then placed in 10% NBF for 2-3 days followed by decalcifying solution (Richard-Allan Scientific) for 12-24 hours. The nasal passages were then sectioned transversely at three levels: (1) immediately caudal to the canine tooth, (2) bisecting the 3rd premolar and (3) bisecting the molar, to permit

examination of the differing epithelia within the rostral, middle and caudal aspects of the nasal passages and to facilitate consistent sampling of the cell type (respiratory) which are the primary targets of virus infection.

The tissues were embedded in paraffin and sectioned (5μm), placed on glass slides, and stained with hematoxylin and eosin (H&E). The stained tissue sections were graded for the presence and severity of pathology as follows: a score of 1 for inflammatory changes in <20% of the examined section; a score of 2 for inflammation comprising 20-50% of the examined section and a score of 3 for inflammation comprising 50% or greater of the examined section.

Evaluation of sialic acid and sialyltransferase distribution in the ferret RT. For lectin histochemistry, unstained sections of formalin-fixed paraffin-embedded (FFPE) lung tissue (previously described) were deparaffinized and rehydrated using sequential treatments of xylene and graded alcohol series, respectively. Endogenous peroxidase activity was blocked using hydrogen peroxide (3%) for 10 minutes. For antigen retrieval, slides were incubated in sodium citrate buffer for 30 minutes at 95°C. Non-specific lectin binding was blocked using Carbo-free blocking solution for 1hour at room temperature (RT) and sections were then incubated with biotin-labelled Sambucus nigra agglutinin (SNA) or Maackia amurensis agglutinin 2 (MAAII) (Vector, Burlingame, CA), respectively for 1 hour, in a humid chamber, at RT at a dilution of 1:100. Indirect immunoperoxidase staining was performed using the Vectastain ABC system (Vector, Burlingame, CA) with DAB (diaminobenzidine) substrate. Sections were incubated with DAB substrate for 3-5 minutes and counterstained with Hematoxylin QS (Vector, Burlingame, CA) for 30 seconds at RT. Tissues were washed in a 1% hydrochloric acid (HCL) solution followed by Scott's Tap Water (Leica Biosystems, Richmond, IL). All stained sections

were then dehydrated using a sequential graded alcohol series and xylene and coverslipped using Permount (Fischer, Fair Lawn, NJ) histological mounting medium.

For detection of sialyltransferases (SAt) by immunohistochemistry (using an IHC protocol kindly provided by Dr. John Nicholls from the University of Hong Kong) (Jia et al., 2014), unstained sections of formalin-fixed paraffin-embedded (FFPE) lung tissue (previously described) were deparaffinized and rehydrated using sequential treatments of xylene and graded alcohol series, respectively. Endogenous peroxidase activity was blocked using hydrogen peroxide (3%) for 10 minutes. For antigen retrieval, I incubated the slides in aliquots of sodium citrate buffer for 30 minutes at 95°F. Tissue sections were blocked with normal donkey serum (10 %) and allowed to incubate for 20 minutes at room temperature (RT) and then were incubated with a rabbit polyclonal antibody (pAb) to ST3GAL3 (1°) (Novus Biologicals LLC, Littleton CO) or a goat pAb to ST6GAL1 (1°) (Novus Biologicals LLC, Littleton CO) for 1 hour at RT at a dilution of 1:200 or 1:50, respectively. Sections incubated with the anti-ST3GAL3 Ab were then incubated with a biotinylated donkey anti-rabbit gamma immunoglobulin (2°) (GE Healthcare Bio-Sciences, Piscataway NJ) for 30 minutes at RT at a dilution of 1:100 and sections incubated with anti-ST6GAL1 Ab were incubated for 30 minutes at RT at a dilution of 1:100 with a biotinylated donkey anti-goat gamma immunoglobulin (Life technologies, Eugene Oregon). Antigen-antibody reactions were visualized using the Vectastain ABC system (Vector, Burlingame, CA) with DAB (diaminobenzidine) substrate. Sections were incubated with DAB substrate for 3-5 minutes and then counterstained with Hematoxylin QS (Vector, Burlingame, CA) for 30 seconds at RT. Tissues were washed in a 1% hydrochloric acid (HCL) solution followed by Scott's Tap Water (Leica Biosystems, Richmond, IL). All stained sections were

rehydrated using sequential alcohol washes and xylene and then coversliped using Permount (Fischer, Fair Lawn, NJ) histological mounting medium.

Micro-CT (μCT) Imaging. Formalin-fixed lungs (with trachea attached) from four ferrets were transferred to 70% alcohol and imaged using an in-vivo micro scanner (SkyScan 1176, Bruker μCT Kontich, Belgium). The alcohol was evacuated from the airways and trachea using an endotracheal tube attached to a large volume syringe. The intact respiratory tract specimen (trachea, heart, and lungs) was subsequently re-intubated and attached to an oxygen source. The air pressure was increased steadily until all lung lobes were fully distended. The inflated lungs were then placed (ventral side up) in a hollowed, halved, Styrofoam tube that mimics the natural orientation and shape of the lung within the thoracic cavity. The lung and Styrofoam container were gently wrapped in parafilm (Parafilm "M", Pechiney Plastic Packaging, Chicago, IL) to prevent desiccation of the lung tissue. The lungs were placed in the image chamber and scanned for 3-4 hours at 18 μm using a 0.2 mm aluminum filter set at 45 kV (kilovoltz), 550 uA (milliamps) and an exposure time of 180 milliseconds (ms). After scanning, lung images were reconstructed using the Nrecon software by Bruker μCT (Kontich, Belgium) and analyzed using manufacturer's software.

Cytokine mRNA quantification by quantitative real-time RT-PCR. These experiments were undertaken in collaboration with Drs. Veronika von Messling and Theresa Enkirch from the Paul Ehrlich Institute in Germany. RNA was isolated from frozen lung tissue samples by disrupting the tissue in lysing matrix tubes (Lysing matrix D, MP Biomedicals) and subsequently following the manufactuers's instructions for the RNeasy Mini kit (Qiagen). RNA standards were produced

by in vitro transcription from expression plasmids encoding the respective gene using T7 RNA polymerase (New England Biolabs). Cytokine mRNAs and serial dilutions of the RNA standards were analyzed by real-time RT-PCR using a QuantiTect SYBR Green RT-PCR kit (Qiagen). For each reaction, 10 ng of RNA was mixed with the appropriate amount of PCR reagents following the manufacturer's instructions. The primers used for the respective cytokines were published previously (Danesh et al., 2008; Svitek & von Messling, 2007), and each experiment was performed in duplicate. The mean of the two values was used for the calculation of the RNA copy number according to the following formula: number of copies = amount of RNA (ng) x 6.022×10^{23} / gene length (bp) x 10^{9} x 340. The relative quantity (RNA copy number) of each cytokine in the lung tissues was compared to a standard curve.

Statistical analysis. A linear mixed model was used to examine the associations between response variables such as ferret weight, body temperature, nasal turbinate virus titer, right or left lung virus titer and the explanatory variables such as gender, day (post-infection), inoculum volume and virus subtype. Statistical analysis was performed using the statistical software *Splus*. The Wilcoxon-signed rank test to assess differences in cytokine mRNA levels between ferrets of different ages (8 wk. vs. 6 mo.). P values less than 0.01 were considered significant.

RESULTS

Clinical disease in ferrets following infection with H1N1pdm or H3N2v virus

Clinical data. Weight, temperature and clinical signs of influenza were monitored daily in groups of 8 week and 6 month old ferrets that were experimentally infected with either the H1N1pdm or H3N2v influenza viruses.

H1N1pdm virus infection. All 8 week old ferrets that received the H1N1pdm virus gained weight throughout the 6 day course, irrespective of volume of inoculum administered (Figure 11A). All animals in the 1.0 ml group (4/4) exhibited elevations in body temperature that ranged from 0.5- 0.75°C, while only 1/4 animal in the 0.2 ml (2.0°C) and 2/4 0.5 ml (1.0°C) groups exhibited elevations in body temperature (Fig. 12A). Clinical signs of influenza were minimal to absent at all inoculum volumes in 8 week old ferrets (Figs. 13A and 15A).

With the exception of 1 animal (0.5 ml), all 6 month old animals receiving 0.5 or 1.0 ml of inoculum lost weight, with a peak percent weight loss of 5.6 and 5.7%, respectively while 4 of 4 animals receiving 0.2 ml inoculum had peak loss of 3.4% (Fig. 11B). Animals in the 1.0 ml inoculum group exhibited elevations in body temperature that ranged from 1-2°C above baseline, first observed on day 1 post-infection (p.i.) and maintained through day 6 in all 4 animals (Fig. 12B). Fewer animals in the 0.2 ml (1/4) and 0.5 ml (3/4) groups had elevations in temperature above baseline (Fig. 12B). In addition, nearly all animals in the 0.2 and 0.5 ml inoculum groups with elevated body temperature, displayed a return to or below baseline by day 6 p.i.

Figure 11. Percent weight loss in 8 week old and 6 month old ferrets inoculated i.n. with 0.2, 0.5, or 1.0 ml containing 10^6 $TCID_{50}$ of the H1N1pdm influenza virus.

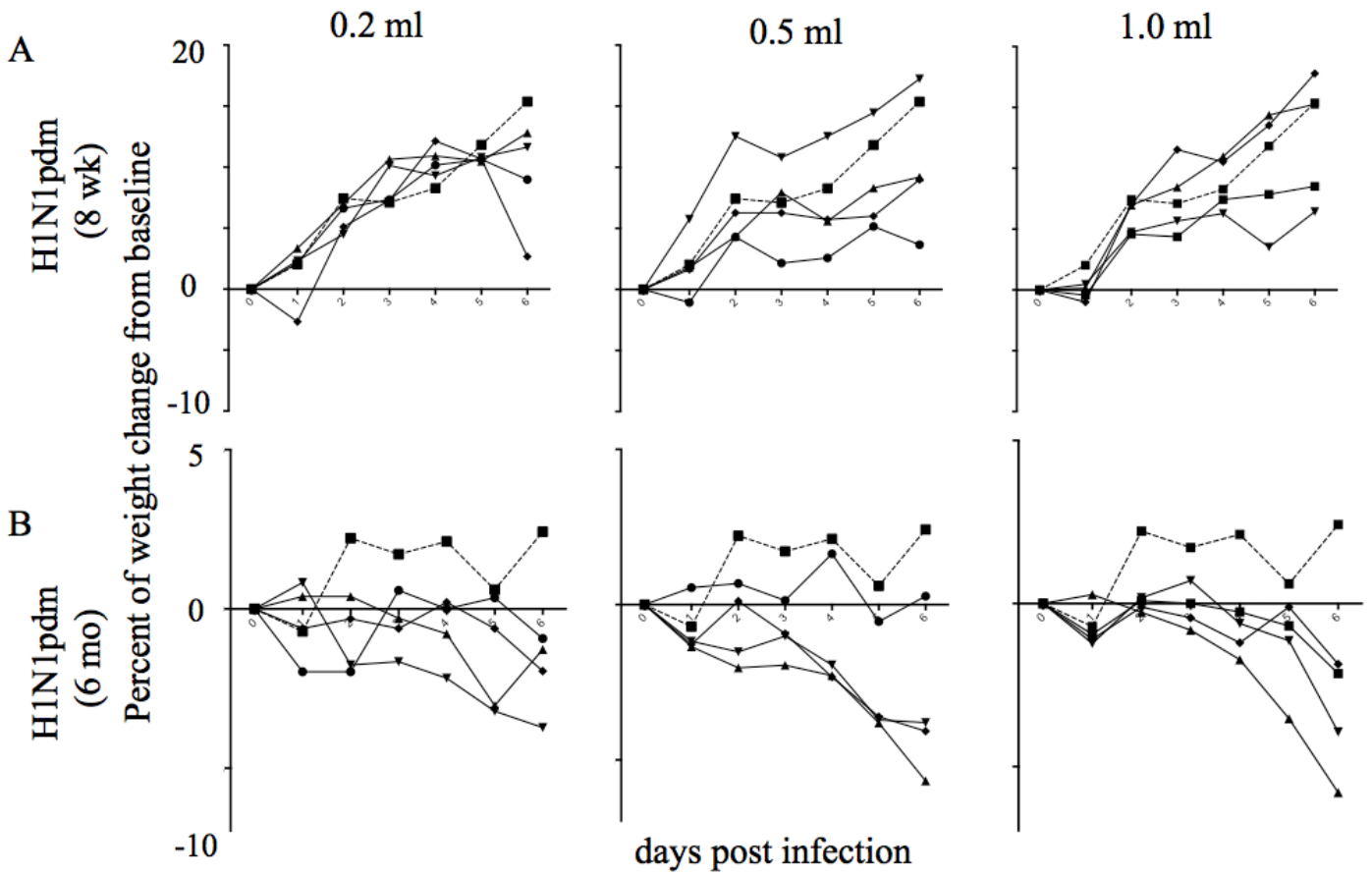

Figure 11 (cont'd)

Eight week old (**A**) and 6 month old (**B**) ferrets were monitored daily for weight loss, and morbidity was recorded over a period of 6 days. Dotted lines represent the single mock-infected ferret, compared to animals that received virus at three different volumes (solid lines).

Figure 12. Change in body temperature in 8 week old and 6 month old ferrets inoculated i.n. with 0.2, 0.5, or 1.0 ml containing 10^6 $TCID_{50}$ of the H1N1pdm influenza virus.

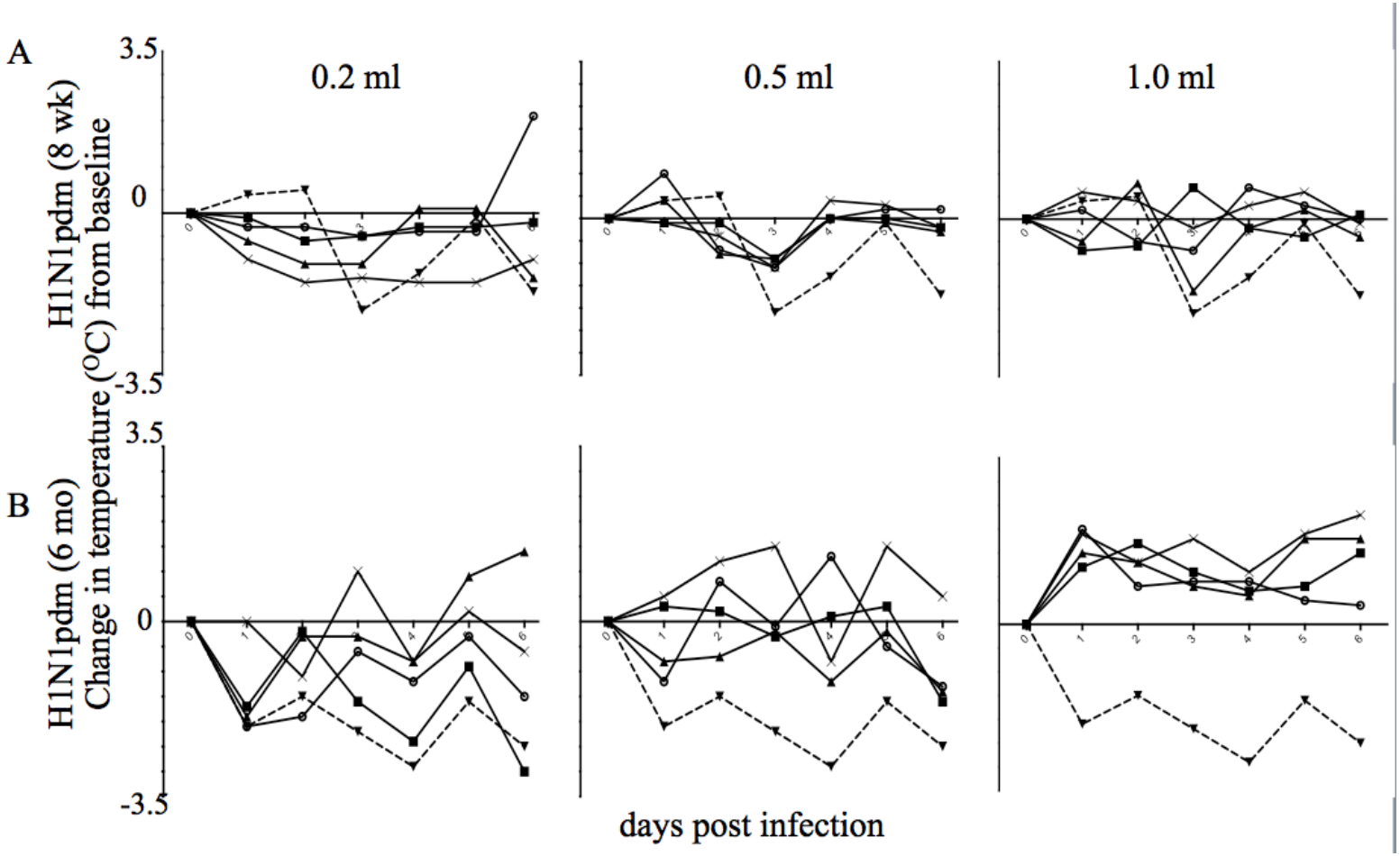

Figure 12 (cont'd)

Eight week old (**A**) and 6 month old (**B**) ferrets were monitored daily for weight loss, and morbidity was recorded over a period of 6 days. Dotted lines represent the single mock-infected ferret, compared to animals that received virus at three different volumes (solid lines).

Ferrets that received 1.0 ml inoculum had a more substantial decrease in the level of activity (higher scores) than the other inoculum volume groups (0.2 and 0.5 ml) (Fig. 14A). Activity scores for the 0.2 and 0.5 ml groups ranged from clinically normal (0) to mild (1) or moderate (2). Nasal symptom scores were highest (3; most severe) on day 6 p.i. for animals in the 1.0 ml inoculum group, whereas nasal scores for the 0.2 and 0.5 ml groups ranged from clinically normal (0) to mild (1) or moderate (2) (Fig. 5).

H3N2v virus infection. In 8 week old ferrets that received the H3N2v influenza virus, peak weight losses of 7.5% and 6.5% were observed in the 0.5 (3/4) and 1.0 ml (1/4) groups, respectively (Fig. 17A). There was no significant weight loss observed in animals that were inoculated with 0.2 ml (Fig. 17A). Mild elevations in body temperature were observed at all inoculum volumes, with the greatest elevation observed were in the 1.0 ml (1/4) group (1.5°C); slightly lower elevations were observed in the 0.5 ml (2/4) (1.0°C) and 0.2 ml (1/4) (0.5°C) groups (Fig 18A). Clinical signs of influenza were minimal to absent at all inoculum volumes in 8 week old ferrets (Figs. 13B and 15B).

Figure 13. Activity scores for 8 week old ferrets infected with the H1N1pdm or H3N2v influenza viruses.

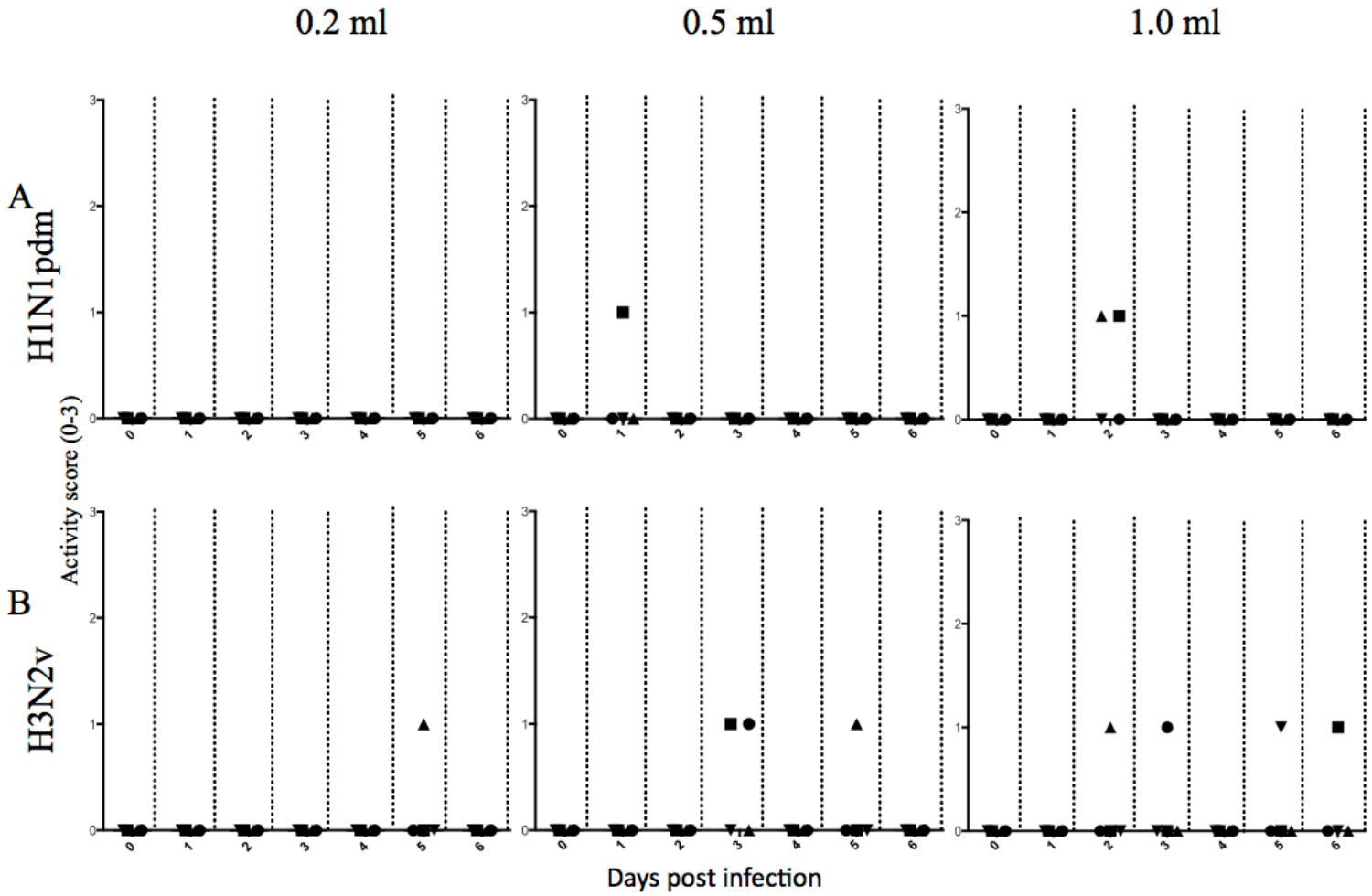

Figure 13 (cont'd)

Eight week old ferrets evaluated for level of activity following inoculation with the H1N1pdm (**A**) or H3N2v (**B**) influenza viruses. Activity scores range from 0 (within normal limits), 1 (mild), 2 (moderate), to 3 (severe; decrease in activity). Symbols represent activity scores for individual ferrets within each inoculum volume group and at a given timepoint.

Figure 14. Activity scores for 6 month old ferrets infected with the H1N1pdm or H3N2v influenza viruses.

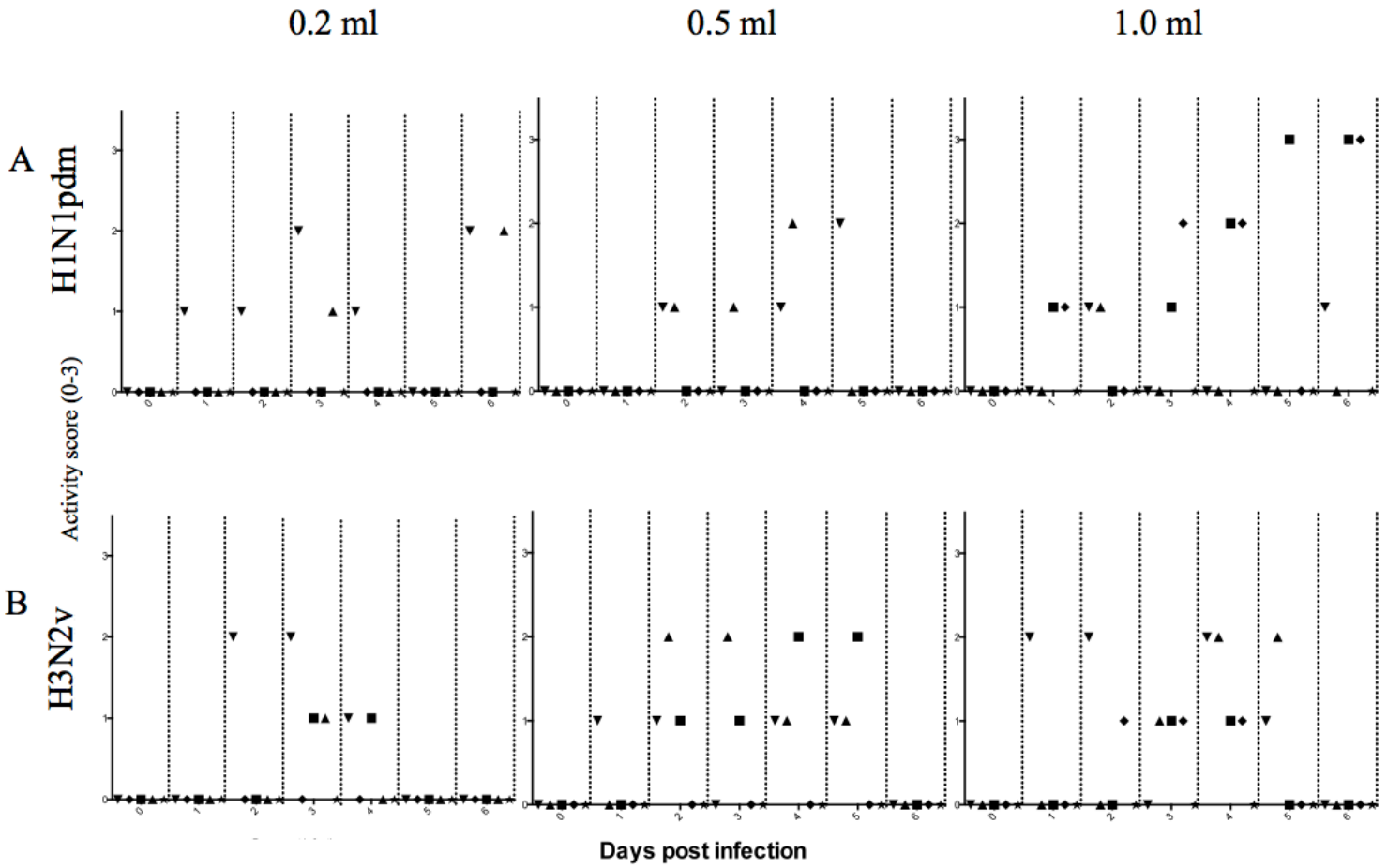

Figure 14 (cont'd)

Six month old ferrets evaluated for level of activity following inoculation with the H1N1pdm (**A**) or H3N2v (**B**) influenza viruses. Activity scores range from 0 (within normal limits), 1 (mild), 2 (moderate), to 3 (severe; decrease in activity). Symbols represent activity scores for individual ferrets within each inoculum volume group and at a given timepoint.

Figure 15. Nasal symptom scores for 8 week old ferrets infected with the H1N1pdm or H3N2v influenza viruses.

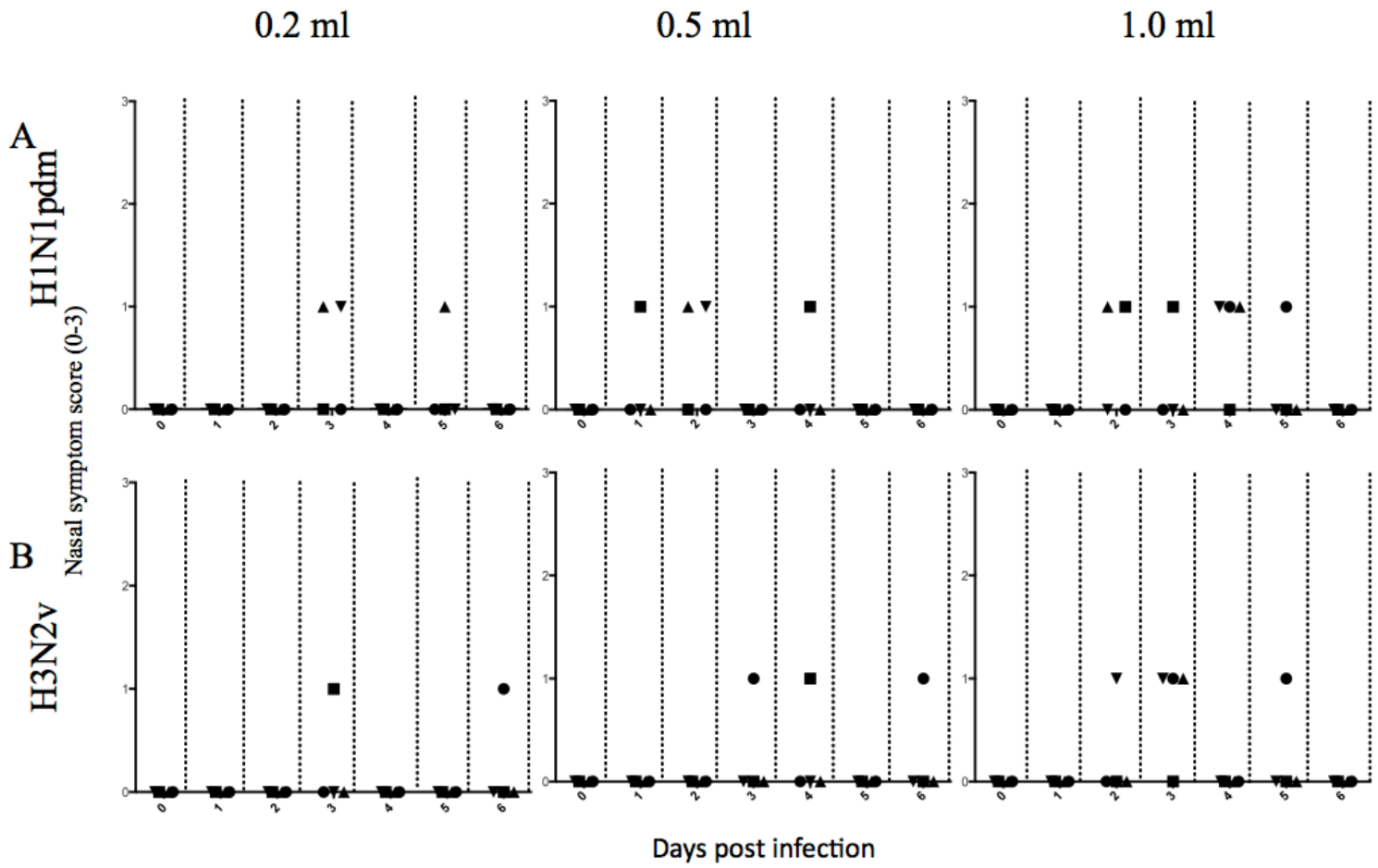

Figure 15 (cont'd)

Eight week old ferrets evaluated for nasal symptoms following inoculation with the H1N1pdm (**A**) or H3N2v (**B**) influenza viruses. Nasal symptom scores range from 0 (within normal limits), 1 (mild), 2 (moderate), to 3 (severe). Symbols represent nasal scores for individual ferrets within each inoculum volume group and at a given timepoint.

Figure 16. Nasal symptom scores for ferrets infected with the H1N1pdm or H3N2v influenza viruses.

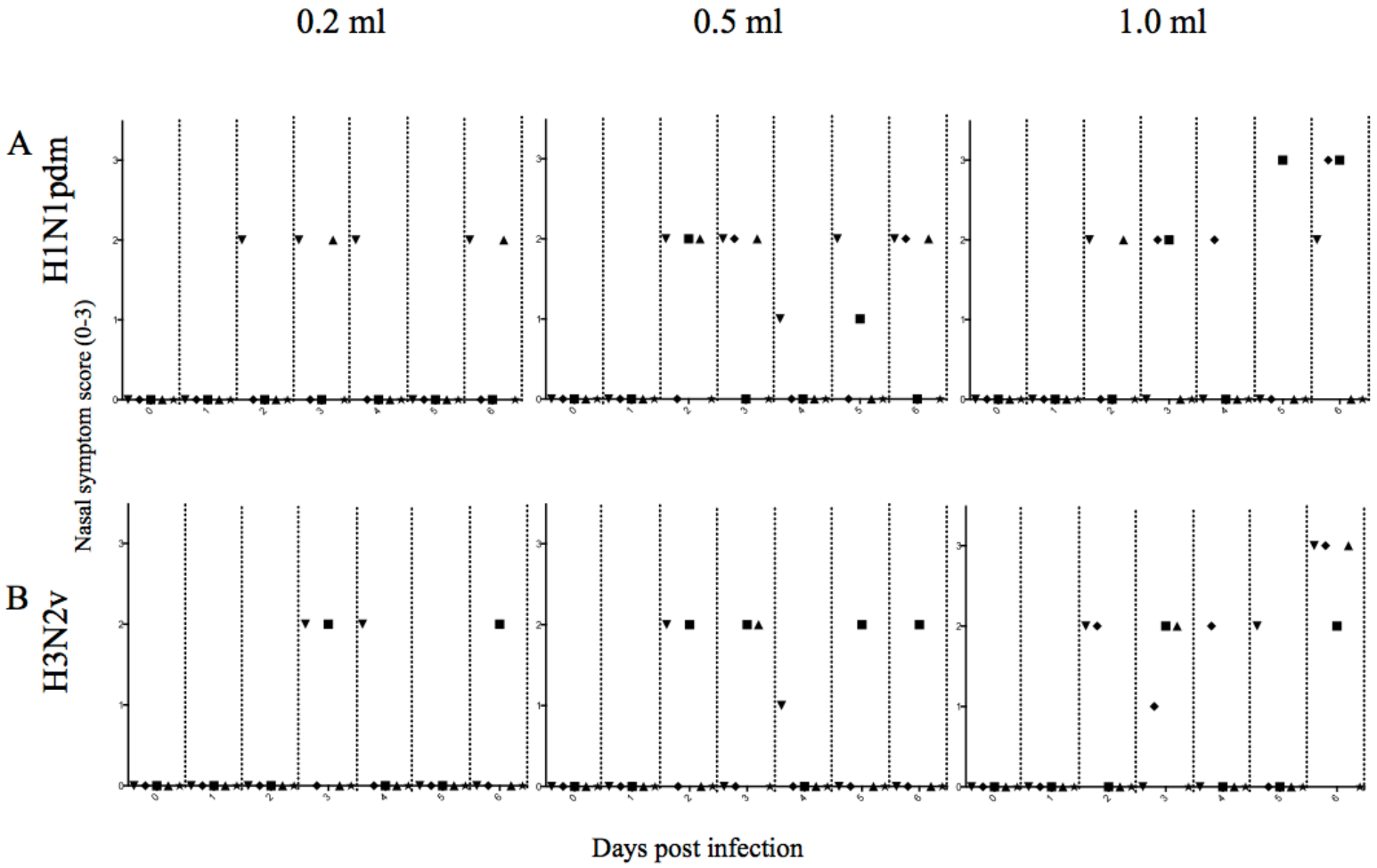

Figure 16 (cont'd)

Ferrets evaluated for nasal symptoms following inoculation with the H1N1pdm (**A**) or H3N2v (**B**) influenza viruses. Nasal symptom scores range from 0 (within normal limits), 1 (mild), 2 (moderate), to 3 (severe). Symbols represent nasal scores for individual ferrets within each inoculum volume group and at a given timepoint.

In 6 month old ferrets infected with the H3N2v virus, weight loss was observed in all animals at each inoculum volume. Ferrets receiving 1.0 ml of inoculum reached a peak percent weight loss of 13.9% (4/4), while animals that received 0.2 ml and 0.5 ml had peak weight losses of 7.6% (4/4) and 10.6% (4/4), respectively (Fig. 17B). Peak elevations in body temperature occurred on day 2 p.i. for all inoculum groups (Fig. 18B). The largest increase in body temperature (~2.5°C above baseline) was observed in the 0.5 ml group and in 3/4 animals. All animals in the 1.0 ml inoculum group had elevations in body temperature that ranged from 1.0-1.5°C and 2/4 animals in the 0.2 ml group exhibited elevations in body temperature above baseline (Fig. 18B). Although the magnitude of temperature elevation was greater in the 0.5 ml group, the consistency in kinetics of temperature elevation was greater in the 1.0 ml group. Additionally, there was a relatively blunt response in body temperature change compared with weight change when the temperature was recorded using a subcutaneous transponder at a similar time each day. It is possible that a core body temperature may have been a more sensitive measure.

Clinical activity scores were similar for animals in the 0.5 and 1.0 ml inoculum groups, ranging from clinically normal (0) to mild (1) or moderate (2) and were observed as early as day 1 p.i. (Fig. 14B). Animals in the 0.2 ml group achieved activity scores similar to the 0.5 and 1.0 ml inoculum groups but the changes were of a short duration, between days 2 and 4 p.i. (Fig. 14B). Nasal scores were highest for animals in the 1.0 ml inoculum group and nasal symptoms were most severe on day 6 p.i. (3/4). The duration and degree of nasal symptoms was similar for animals in the 0.2 and 0.5 ml inoculum groups (Fig. 16B).

Therefore, in summary, 8 week old ferrets had minimal or no clinical signs of infection, weight loss and increase in body temperature following infection with the H1N1pdm or H3N2v

influenza viruses. In contrast, 6 month old ferrets lost weight, had increased body temperature, decreased activity and nasal symptoms following infection with both viruses. As described in Chapter 2 the larger inoculum volume was associated with more severe and consistent signs of illness.

Figure 17. Percent weight loss in 8 week old and 6 month old ferrets inoculated i.n. with 0.2, 0.5, or 1.0 ml containing 10^6 $TCID_{50}$ of the H3N2v influenza virus.

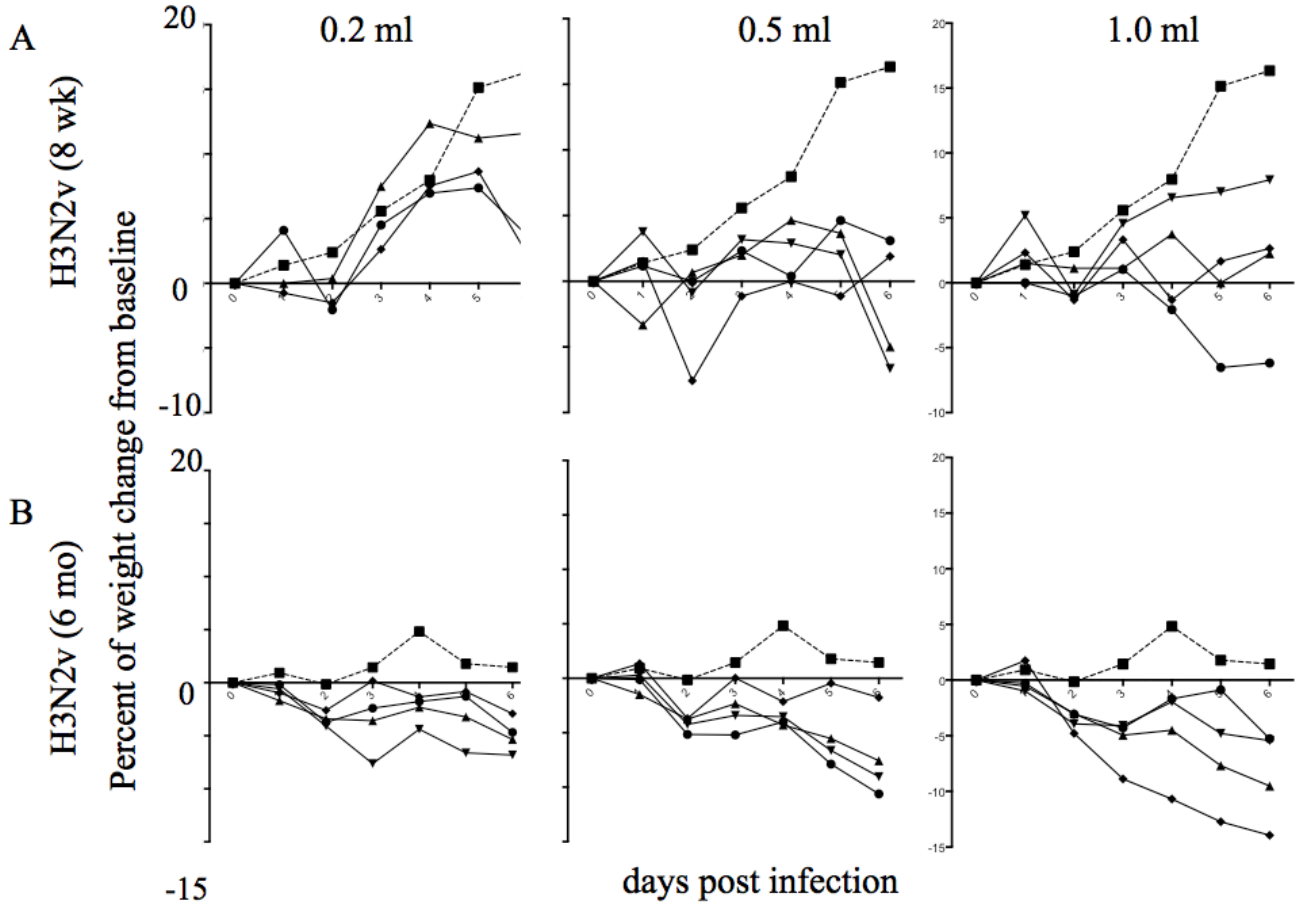

Figure 17 (cont'd)

Eight week old (**A**) and 6 month old (**B**) ferrets were monitored daily for weight loss, and morbidity was recorded over a period of 6 days. Dotted lines represent the single mock-infected ferret, compared to animals that received virus at three different volumes (solid lines)

Figure 18. Change in body temperature in 8 week old and 6 month old ferrets inoculated i.n. with 0.2, 0.5, or 1.0 ml containing 10^6 $TCID_{50}$ of the H3N2v influenza virus.

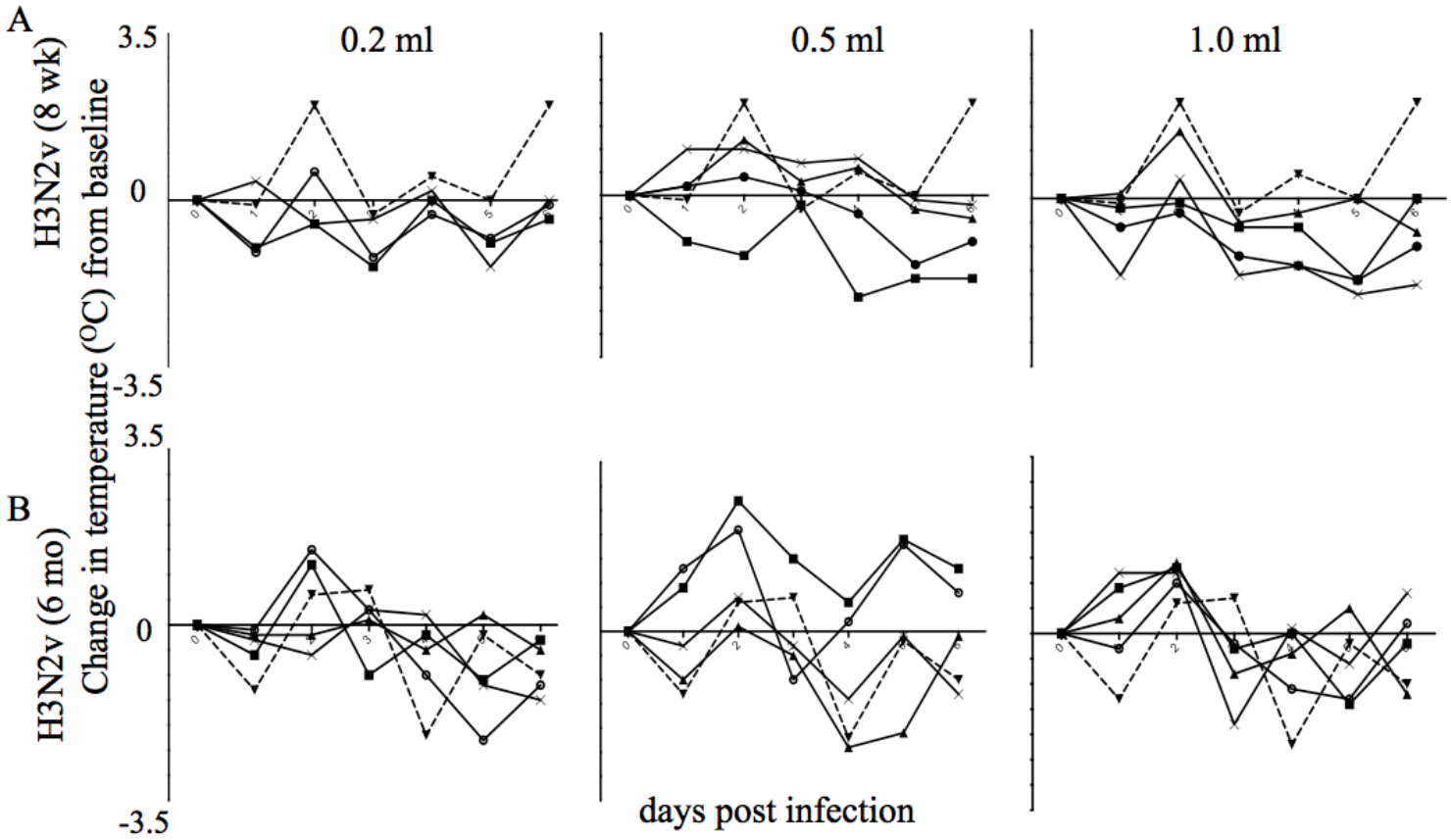

Figure 18 (cont'd)

Eight week old (**A**) and 6 month old (**B**) ferrets were monitored daily for weight loss, and morbidity was recorded over a period of 6 days. Dotted lines represent the single mock-infected ferret, compared to animals that received virus at three different volumes (solid lines).

Viral replication in the upper and lower respiratory tract

H1N1pdm virus infection. The H1N1pdm virus replicated efficiently and to high titer in the nasal turbinates (NT) of 8 week old ferrets at all inoculum volumes (Fig. 19A). A mean peak titer of $10^{6.3}$ $TCID_{50}$/g was observed in ferrets that received 0.2 ml or 1.0 ml on days 1 and 3 p.i., respectively (Figure 19A). Animals that received the H1N1pdm virus in a volume of 0.5 ml had similar titers ($10^{6.1}$ $TCID_{50}$/g) on d1 p.i.

Figure 19. Replication kinetics of H1N1pdm influenza virus in 8 week old and 6 month old ferrets following i.n. inoculation of 10^6 $TCID_{50}$/virus.

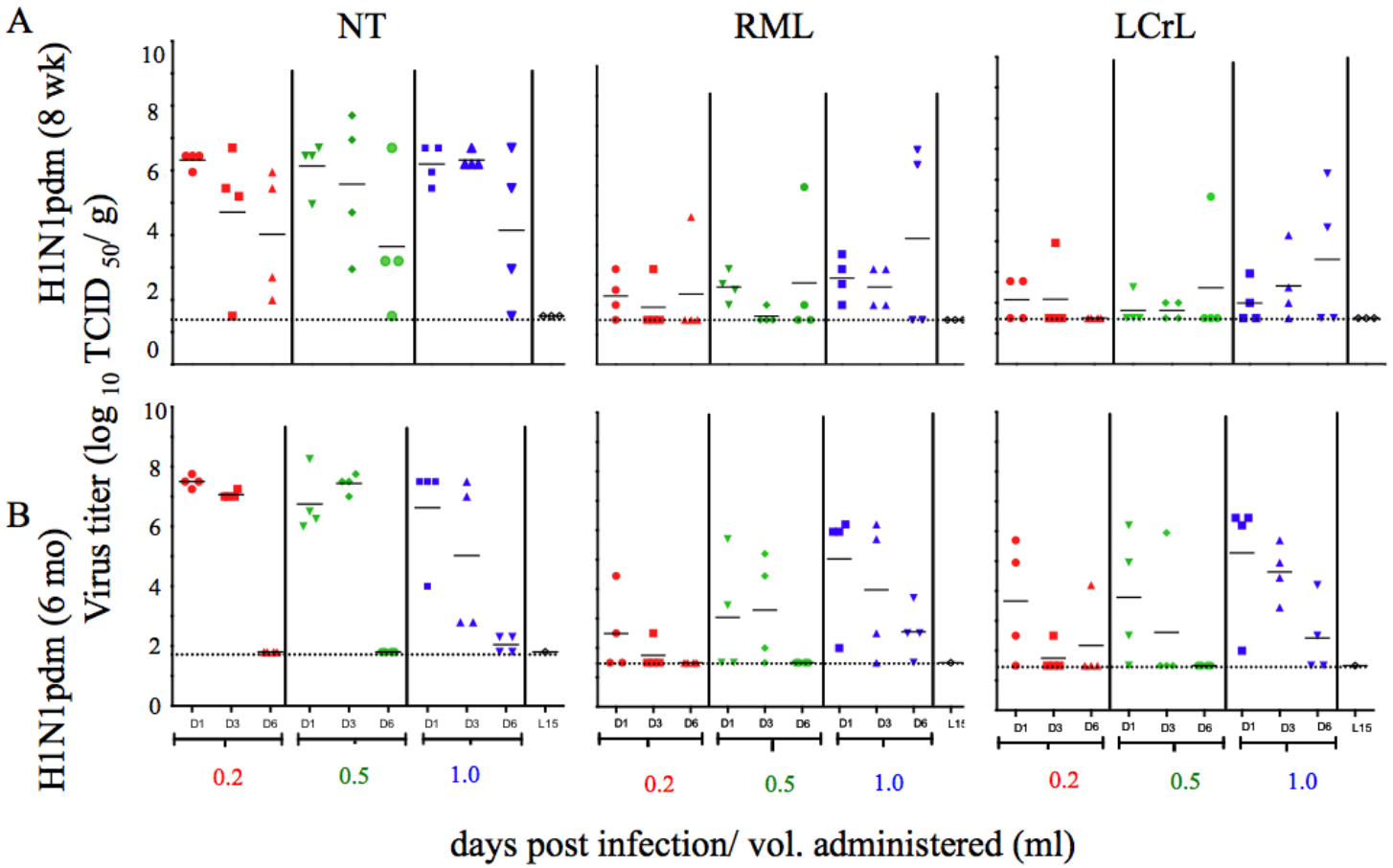

Figure 19 (cont'd)

Virus titers in the nasal turbinates (NT) and lungs (right middle [RML] and left cranial [LCr]) lobes of 8 week old (**A**) and 6 month old (**B**) 4 ferrets infected with the H1N1pdm influenza virus. Four ferrets per group were euthanized on 1, 3, and 6 dpi and virus titers in the tissues are expressed as $\log_{10}$ $TCID_{50}$/gram of tissue. Bars represent mean titers and symbols represent titers from individual ferrets. The dashed horizontal line indicates the lower limit of detection, $10^{1.8}$ and $10^{1.5}$ $TCID_{50}$ per gram for the NT and lungs, respectively.

In the lower respiratory tract (LRT), sections of right middle (RM) and left cranial (LCr) lung lobes were sampled. The kinetics and level of virus replication, in the right and left lung lobes, were most similar for 8 week old animals that received the H1N1pdm virus in a volume of 1.0 ml (Figure 19A). The mean peak titers in the 1.0 ml group were $10^{4.1}$ $TCID_{50}$/g and $10^{3.5}$ $TCID_{50}$/g for the right and left lung lobes, respectively (Figure 19A). The mean peak titers in the 0.5 ml group were $10^{2.5}$ $TCID_{50}$/g and $10^{3.5}$ $TCID_{50}$/g for the right and left lung lobes, respectively. Virus replication in the 0.2 ml group was relatively low, with $10^{2.2}$ and $10^{2.1}$ $TCID_{50}$/g in the right and left lung lobes, respectively. Viral in the 0.5 and 1.0 ml groups increased over the 6 days post infection and peaked on d6 p.i (Figure 19A).

Six month old ferrets had levels of virus replication in the URT that was similar to that in younger ferrets (Figure 19B). In the NT, the H1N1pdm virus replicated to high titers at all inoculum volumes and in all animals. Animals that received 0.2 ml inoculum (4/4) had a mean virus titer of $10^{7.5}$ $TCID_{50}$/g on day 1 p.i. Similar titers were observed in animals that received 0.5 ml (4/4; $10^{7.4}$ $TCID_{50}$/g) on d3 p.i. and 1.0 ml (4/4; $10^{6.6}$ $TCID_{50}$/g) on d1 p.i. (Fig. 19B).

In the LRT, the kinetics and titers for animals in the 1.0 ml inoculum group were similar in the right and left lung lobes. The mean peak titer in the 1.0 ml group was $10^{5.1}$ $TCID_{50}$/g (Fig. 19B). The mean peak titers for animals in the 0.5 ml group were $10^{3.3}$ and $10^{3.8}$ $TCID_{50}$/g for right and left lung lobes, respectively. Animals in the 0.2 ml group showed the most noticeable disparity in titers between the right and left lung, with mean peak titers of $10^{2.5}$versus

$10^{3.8}$ $TCID_{50}$/g, respectively (Fig. 19B). At all inoculum volumes, viral titers in the lungs declined sharply or were undetectable by day 6 p.i.

H3N2v virus infection. In the NT of 8 week old ferrets, the H3N2v influenza virus replicated efficiently and to high titers at all inoculum volumes (Fig. 20A). Animals in the 0.5 (4/4) and 1.0 ml (4/4) inoculum groups showed the highest mean titer ($10^{7.3}$ $TCID_{50}$/g) on d1 p.i. Animals in the 0.2 (4/4) ml group had a peak mean titer of $10^{6.7}$ $TCID_{50}$/g observed on d1 p.i. (Figure 20A).

Figure 20. Replication kinetics of the H3N2v influenza viruses in 8 week old and 6 month old ferrets following i.n. inoculation of 10^6 $TCID_{50}$/virus.

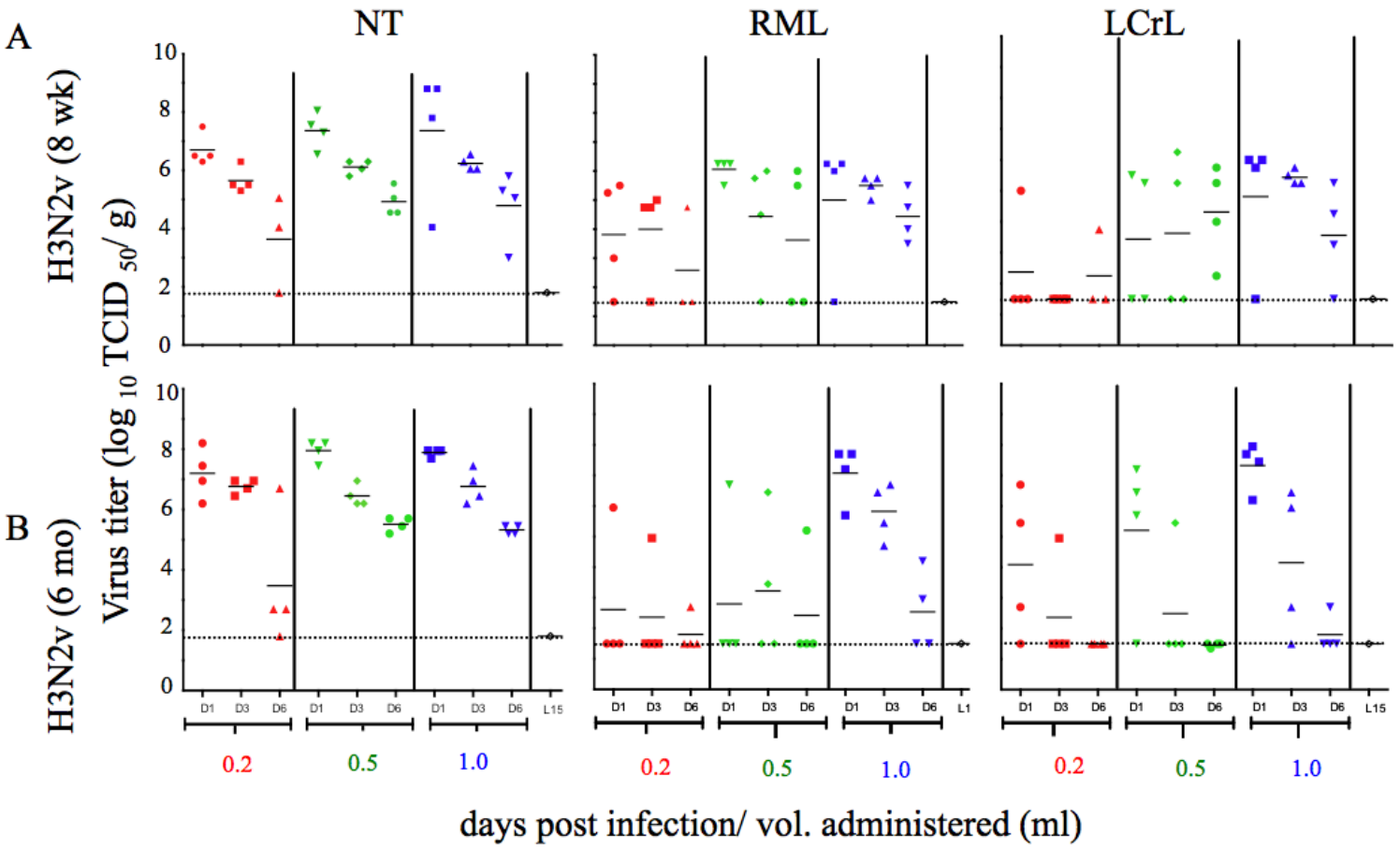

Figure 20 (cont'd)

Virus titers in the nasal turbinates (NT) and lungs (right middle [RML] and left cranial [LCr]) lobes of 8 week old (**A**) and 6 month old (**B**) ferrets infected with the H3N2v influenza virus. Four ferrets per group euthanized on 1, 3, and 6 dpi and virus titers in the tissues are expressed as $\log_{10}$ $TCID_{50}$/gram of tissue. Bars represent mean titers and symbols represent titers from individual ferrets. The dashed horizontal line indicates the lower limit of detection, $10^{1.8}$ and $10^{1.5}$ $TCID_{50}$ per gram for the NT and lungs, respectively.

In the LRT, young animals that received the H3N2v virus in a volume of 1.0 ml had the greatest consistency in the level and kinetics of virus replication, between right and left lung lobes (Figure 20A). In the 1.0 ml group, peak titers of ~ $10^{5.5}$ $TCID_{50}$/g occurred on d3 p.i. For both the 0.2 and 0.5 ml groups, mean peak titers occurred on different days post infection. With the exception of the 0.5 ml group (LCr), all viruses showed a decline in the level of replication over the 6 days (Figure 20A).

In 6 month old ferrets, the H3N2v virus replicated efficiently and to high titers ($10^{7.2}$ and 10^{8} $TCID_{50}$/g) at all inoculum volumes (Fig. 20B). In contrast to the decline in titers observed with the H1N1pdm virus, the H3N2v virus was detected at moderate to high levels on day 6 p.i. in the 0.5 and 1.0 ml inoculum groups (Fig. 20B).

In the LRT, mean peak virus titers were achieved on day 1 p.i. in the 1.0 ml group and the titers for the right and left lung were of similar magnitude. Similar to observations made in H1N1pdm infected animals, the two smaller inoculum groups (0.2 and 0.5 ml) showed more noticeable inconsistencies in titers between right and left lung (Fig. 20B). Within all inoculum volume groups, viral titers decreased to levels near the limit of detection (LOD) by day 6 p.i.

Histopathology in URT and LRT

H1N1pdm virus infection. As previously described, the nasal turbinates (URT) were sectioned at 3 specific levels, to facilitate the evaluation virus tropism in the nasal passages, using the previously described anatomic landmarks (Fig. 21).

Figure 21. Sectioning of the nasal turbinates of ferrets for histologic evaluation.

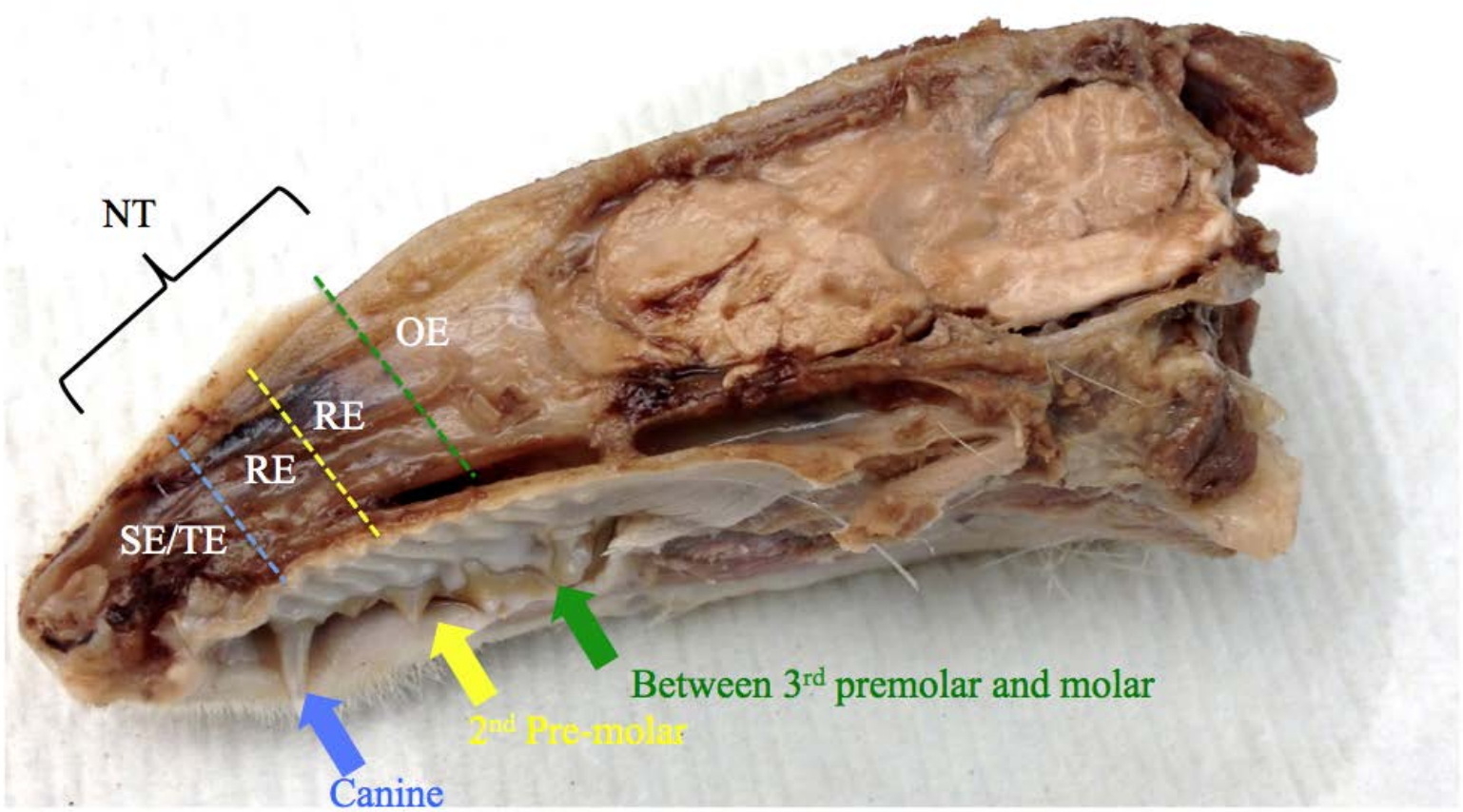

Figure 21 (cont'd)

Nasal turbinate tissues for virus titration and histopathology were collected at 3 specific levels of the nasal passages, which contain multiple epithelial cells types including squamous epithelium (SE), respiratory epithelium (RE), and olfactory epithelium (OE). Influenza viruses typically target the ciliated RE. The landmarks for consistent sectioning and sampling of the RE are; 1) caudal to the canine tooth, 2) bisecting the 2^{nd} premolar and 3) between the 3^{rd} premolar and 1^{st} molar.

Sections of nasal turbinates (NT) from 8 week old ferrets (day 1, 3, and 6 p.i.) were examined histologically. Inflammatory changes associated with H1N1pdm infection were characterized by a predominantly neutrophilic cellular infiltrate, mild to moderate expansion of the submucosal stroma with edema and variable degrees of respiratory epithelial cell necrosis and loss (Figure 22A). The most abundant inflammatory infiltrate was observed in sections of NT from animals in the 1.0 ml group on d3 p.i. (Figure 22A) There was abundant submucosal edema and numerous viable and degenerate neutrophils admixed with cellular debris in the turbinate lumens. Sections of NT from the 0.5 ml group exhibited similar, but less severe, inflammatory changes, also first observed on d3 p.i. There was no evidence of significant inflammation observed at any timepoint in the NT in the 0.2 ml group (Figure 22A).

Figure 22. Pathology of the H1N1pdm influenza virus in the nasal turbinate (NT) of 8 week old and 6 month old ferrets following i.n. inoculation of 10^6 $TCID_{50}$/virus administered in 0.2, 0.5, or 1.0 ml volumes.

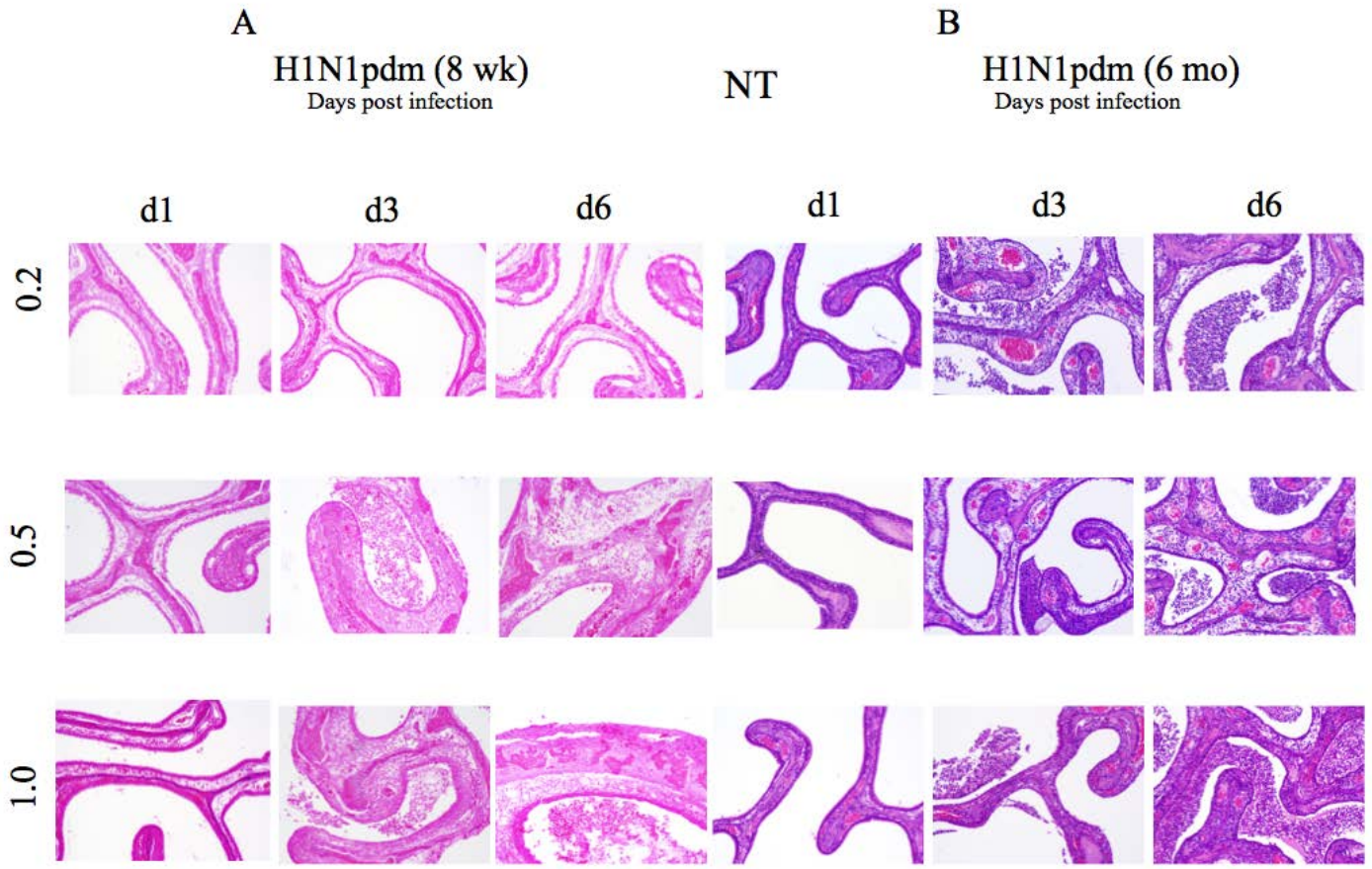

Figure 22 (cont'd)

Eight week old (**A**) and 6 month old (**B**) ferrets were euthanized on 1, 3, and 6 dpi. Photomicrographs are representative of the histopathological changes present in tissues from the 4 ferrets per group that were euthanized on 1, 3, and 6 dpi.

Sections of right middle (RML), left cranial (LCr) and left caudal (LCau) lung lobe for animals in each inoculum group and at each timepoint (1, 3, and 6 days p.i.) were sampled for histopathology. Pulmonary inflammation was predominantly neutrophilic with infiltrates largely concentrated on small airways (bronchioles) and to a less extent, the large airways (bronchi) with some extension into the alveolar interstitium (Figure 23A). In the 1.0 ml group, inflammation was observed at all three timepoints (days 1, 3, and 6 p.i.). The abundance and distribution of inflammation increased over the 6 days. In the 0.5 ml group inflammation was first observed on d3 p.i. Inflammation in the 0.2 ml group was minimal or absent in the sections of lung examined histologically (Figure 23A).

In the URT of 6 month old ferrets, inflammatory changes were most intense in sections of NT from d6 p.i. and were often associated with abundant cellular debris that, in some cases, completely filled the NT lumina (Fig. 22B). The overlying respiratory epithelium consistently displayed regions of both cellular hyperplasia and occasional areas of squamous metaplasia; intact ciliated cells were infrequently observed. Inflammation was first observed on day 3 p.i. and was characterized by marked expansion and infiltration of the submucosal stroma by edema fluid and inflammatory cells (Fig. 22B). Ciliated cells along the mucosal surface were variably sloughed or intact and necrotic. In many cases, the lumina of the NT contained variable amounts of viable and degenerate neutrophils and admixed necrotic cellular debris. Sections of NT from animals on day 1 p.i. in all three groups were within normal limits, without evidence of inflammation (Fig 22B).

The presence and general degree of inflammation within the sections of lung examined correlated with the volume of inoculum administered. Lung pathology was widespread and most

severe for the 1.0 ml group, while the 0.2 and 0.5 ml groups showed less severe pathology and fewer lung lobes were affected (Table 1). Moreover, the cellular composition and the localization of the inflammatory lesions were consistent at all inoculum volumes. Similar to the kinetics of pathology in the upper respiratory tract (URT), inflammatory changes were most intense in the lung by day 6 p.i. (Fig. 22B). The regions immediately surrounding the bronchi were often characterized by expansion and infiltration of the peribronchial stroma by edema and an abundant mixed cellular infiltrate composed of neutrophils, macrophages, lymphocytes and plasma cells. In most cases, within these inflammatory foci, the submucosal glands (SMG) exhibited variable degrees of neutrophilic inflammation and necrosis (Fig. 23B). Sections of lung from day 3 p.i. exhibited a more extensive inflammatory process characterized by intense peribronchiolar inflammation that also extended into and expanded the alveolar interstitium adjacent to the affected airways (Fig. 23B). Inflammatory changes in the lung were present as early as day 1 p.i. (Fig. 23B), and began with a mild and predominantly neutrophilic and lesser histiocytic (alveolar macrophage) infiltrate in both peri- and intra-bronchiolar regions.

In the sections of URT and LRT from young and old ferrets infected with the H1N1pdm, the onset and general distribution of inflammation was similar for animals of both age groups. However, the severity of inflammation was greater in the URT and LRT of older ferrets.

Figure 23. Pathology of the H1N1pdm influenza virus in the lungs (LG) of 8 week old and 6 month old ferrets following i.n. inoculation of 10^6 $TCID_{50}$/virus administered in 0.2, 0.5, or 1.0 ml volumes.

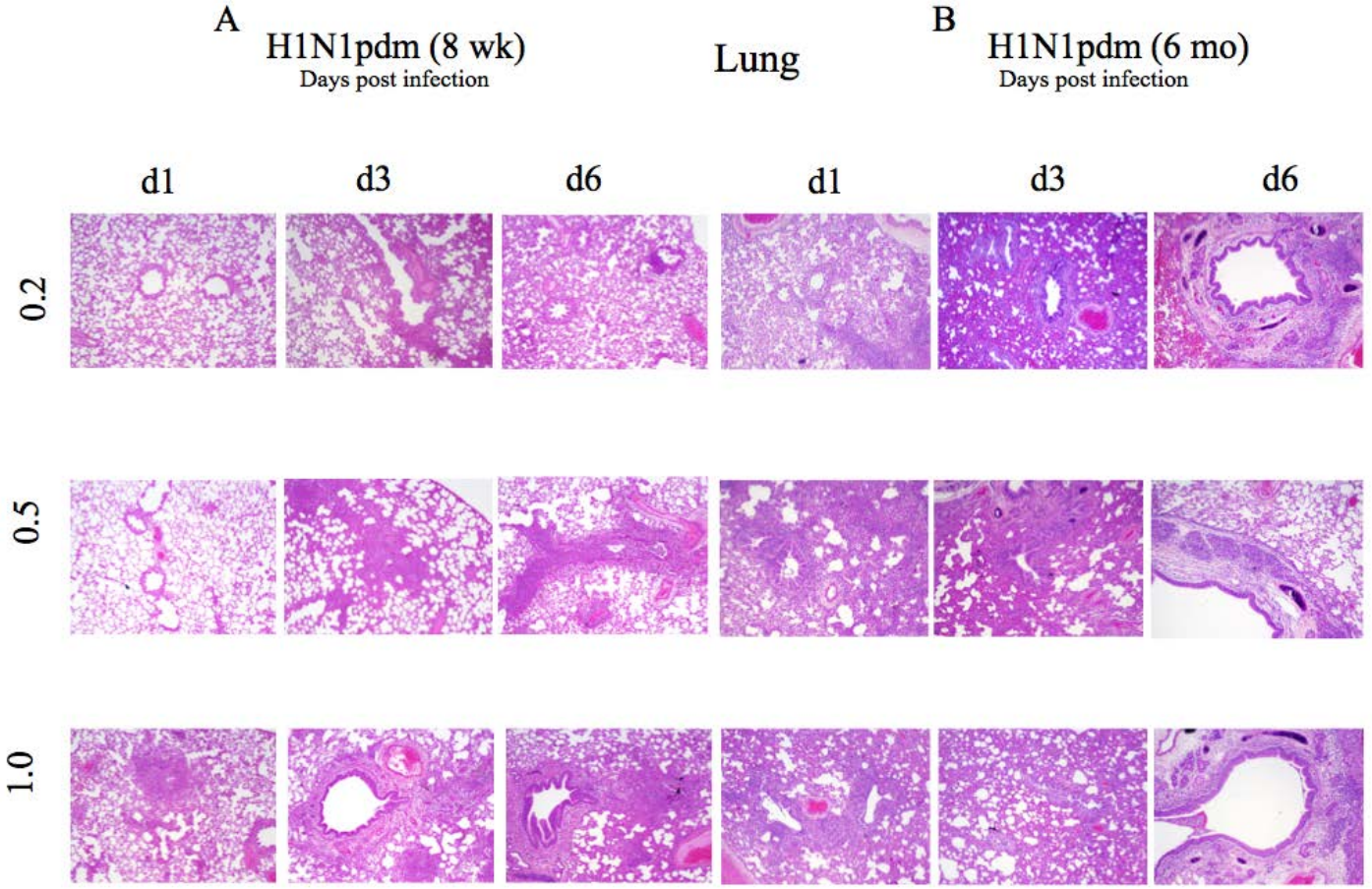

Figure 23 (cont'd)

Eight week old (**A**) and 6 month old (**B**) ferrets were euthanized on 1, 3, and 6 dpi. Photomicrographs are representative of the histopathological changes present in tissues from the 4 ferrets per group that were euthanized on 1, 3, and 6 dpi.

H3N2v virus infection. Inflammatory changes associated with H3N2v virus infection in the URT of 8 week old ferrets were characterized by a predominance of infiltrating neutrophils, submucosal edema, and respiratory epithelial cell necrosis and loss. Inflammation was most abundant in 8 week old ferrets in the 1.0 ml group and was first observed on d3 p.i (Fig. 24A). Viable and degenerate neutrophils and cellular debris were regularly observed in the turbinate airway spaces. On d6 p.i., the neutrophilic inflammatory infiltrate and cell debris was more abundant and often completely filled the airways, there were also occasional areas of epithelial cell hyperplasia, which were consistent with epithelial regeneration (Fig. 24A).

Figure 24. Pathology of the H3N2v influenza virus in the nasal turbinate (NT) of 8 week old and 6 month old ferrets following i.n. inoculation of 10^6 $TCID_{50}$/virus administered in 0.2, 0.5, or 1.0 ml volumes.

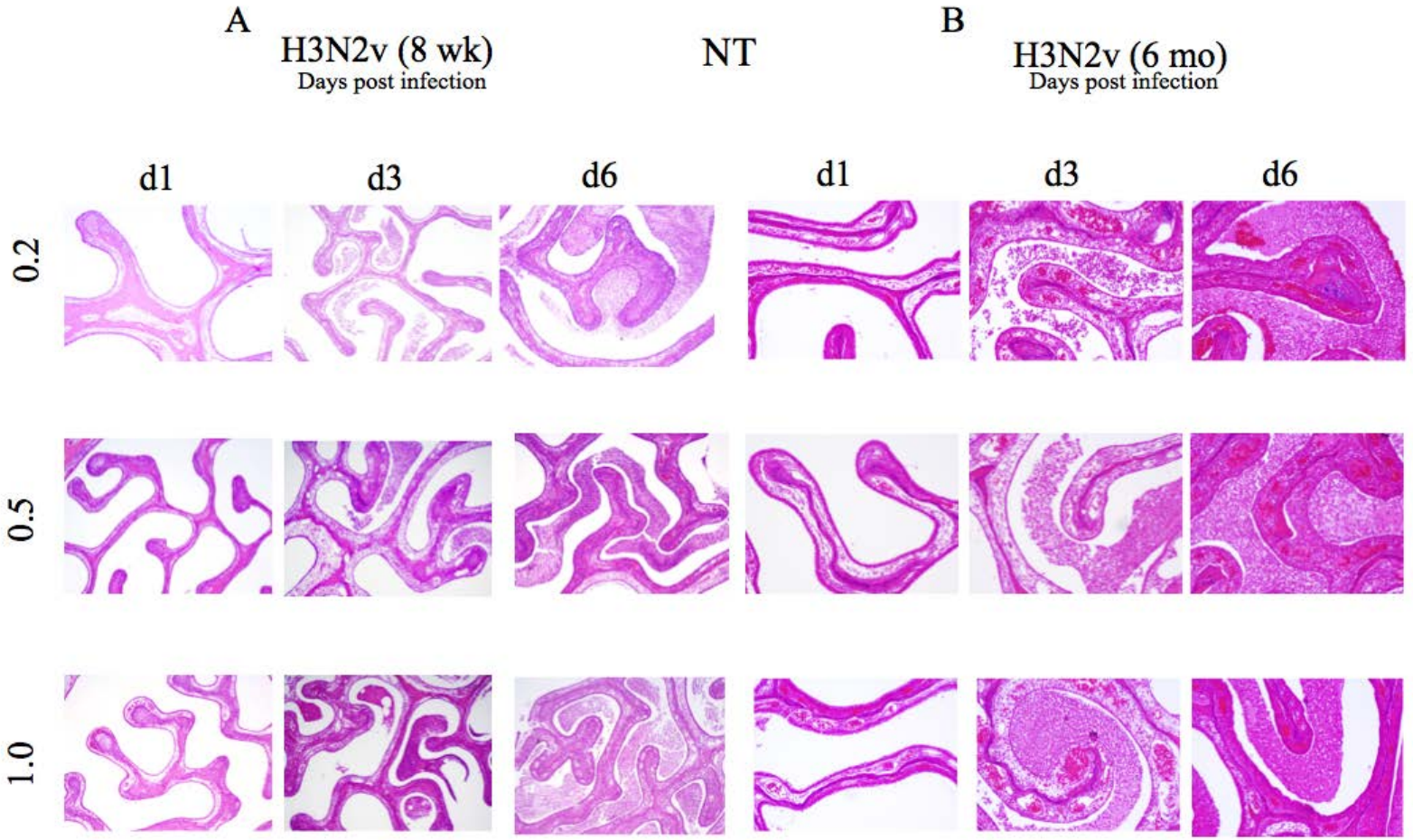

Figure 24 (cont'd)

Eight week old (**A**) and 6 month old (**B**) ferrets were euthanized on 1, 3, and 6 dpi. Photomicrographs are representative of the histopathological changes present in tissues from the 4 ferrets per group that were euthanized on 1, 3, and 6 dpi.

In the lung of 8 week old ferrets, the H3N2v virus was associated with a mild to moderate neutrophilic infiltrate that was most abundant in the 1.0 ml group at all three timepoints (Fig. 25A). On d1 p.i., inflammation was mild and often limited to the regions immediately surrounding small bronchioles. Day 3 sections exhibited more abundant inflammatory infiltrates that both surrounded and filled the lumens of smaller airways. Many of the affected airways exhibited variable degrees of bronchial and bronchiolar epithelial necrosis and loss. By d6 p.i., small airway inflammation was less frequently observed and larger airways (bronchi) were often highlighted by cellular infiltrates that were often intimately associated with the submucosal glands (SMG). The affected SMG were often obscured by the infiltrating cells and exhibited varying degrees of glandular epithelial cell necrosis. In the lung sections from 8 week old ferrets administered virus in 0.5 and 0.2 ml groups, inflammation was less abundant and was first observed on d3 and d6 p.i., respectively (Figure 25A).

Infection of 6 month old ferrets with the H3N2v virus resulted in NT inflammation that was first observed on day 3 p.i. but was most severe on day 6 p.i. Sections of NT from day 6 p.i. were characterized by an intense neutrophilic inflammatory infiltrate that often completely filled the nasal passages. Frequently, the mucosa within these intensely inflamed regions was devoid of ciliated cells and displayed both epithelial hyperplasia and squamous metaplasia (Fig. 24B). On day 3, sections were characterized by expansion and infiltration of the submucosal stroma by edema and inflammatory cells. The overlying respiratory epithelium was often segmentally populated by ciliated cells and those exhibiting changes were histologically consistent with degeneration and necrosis. Sections of NT from day 1 p.i. showed no evidence of inflammation (Fig. 24B).

Lung pathology was more severe and more widespread, affecting a larger proportion of the lung sections examined, as the inoculum volumes were increased (Table 1). In the case of H3N2v infection, inflammatory lesions in the lung of 6 month old ferrets, were most severe on day 6 in the 0.5 ml and 1.0 ml groups (Fig. 25B). The inflammatory foci were intensely neutrophilic and were closely associated with the bronchi and bronchioles. Day 3 p.i. (0.5 ml) was the earliest timepoint at which inflammation was observed and consisted of variably dense neutrophilic and, to a lesser extent, histiocytic infiltrates that were situated intimately around small bronchi and bronchioles (Fig. 25B). In contrast to H1N1pdm virus infection, inflammation was minimal to absent at all timepoints in animals that received the H3N2v virus in 0.2 ml.

Inflammation in the URT and LRT of animals infected with H3N2v influenza virus showed similarities in the onset, severity, and distribution of inflammation in the examined tissues. The differences in clinical disease between the two age groups, despite similar RT pathology, are indicative of other mediators of disease in the ferret model.

Figure 25. Pathology of the H3N2v influenza virus in the lungs (LG) of 8 week old and 6 month old ferrets following i.n. inoculation of 10^6 $TCID_{50}$/virus administered in 0.2, 0.5, or 1.0 ml volumes.

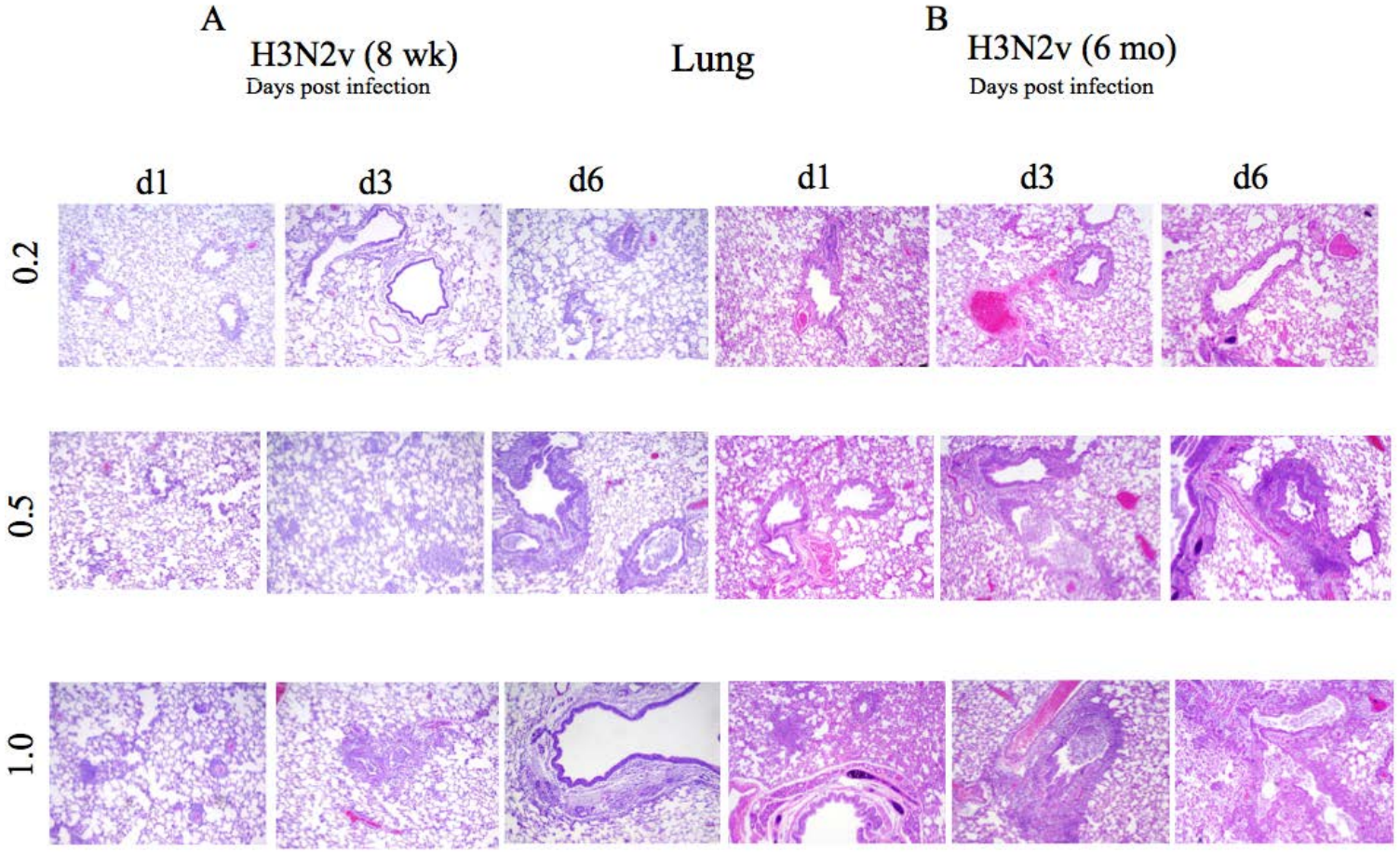

Figure 25 (cont'd)

Eight week old (**A**) and 6 month old (**B**) ferrets were euthanized on 1, 3, and 6 dpi. Photomicrographs are representative of the histopathological changes present in tissues from the 4 ferrets per group that were euthanized on 1, 3, and 6 dpi.

Sialic acid and sialyltransferase distribution

The possibility that the remarkable age-related difference in response to experimental influenza virus infection was due to differences in the distribution of sialic acid receptors in the tow age groups of ferrets was investigated. Plant lectins specific for mammalian-like sialic acids (α2,6-linked) (*Sambucus nigra agglutinin* (SNA)) and avian-like sialic acids (α2,3-linked) (*Maackia amurensis agglutinin* II (MAAII)), were used to stain sections of formalin-fixed paraffin-embedded (FFPE) lung tissue from 8 week old and 6 month old ferrets for the presence and distribution of influenza virus receptors.

In the of lungs of 8 week old ferrets, the epithelial cells of the bronchus, bronchiole, alveolar tissues and the submucosal glands showed positive staining for α2,6-linked SA receptor (SNA). In the bronchus sections, SNA staining was strong in both goblet cells and ciliated respiratory epithelial cells whereas the MAAII lectin primarily stained goblet cells (Fig. 26A). Within the bronchioles, intense staining was observed along the apical surfaces of the simple cuboidal cells lining the airways. In contrast, bronchioles did not stain with the MAAII lectin. Sections of lung from 8 week old ferrets showed diffuse and intense staining of the alveolar capillaries with both the SNA and MAAII lectins (Fig. 26A). SNA stained the SMG intensely and the margins of gland lumens and regularly labeled the acini of some glandular lobules, however the SMGs in the lung sections did not stain with the MAAII lectin (Fig. 26A).

In lungs from 6 month old ferrets, the bronchus, bronchiole, alveolar tissues and SMG were positive for α2,6-linked SA receptors (SNA) (Fig. 26B). In the bronchus, SNA staining was strong and diffuse within ciliated respiratory epithelial cells and staining was less intense in the goblet cells (Fig. 26B). In identical sections evaluated with the MAAII lectin, positive staining was primarily associated with goblet cells. Within the bronchiolar regions, intense staining was observed along the apical surfaces of the simple cuboidal cells lining the airways. Similar to the lung of 8 week old ferrets, bronchiolar regions in 6 month old ferret lungs were negative when evaluated with the MAAII lectin. There was diffuse and intense staining of the alveolar capillaries with both SNA and MAAII. The SMG showed intense staining of the margins of gland lumens and regularly labeled the acini of some glandular lobules, however lung sections containing SMG were often negative for the MAAII lectin (Fig. 26B).

In the URT and LRT tissues examined, I evaluated tissue sections with plant lectins specific for α3,6-linked and α2,6-linked SA receptors and it was determined that sialic acid distribution did not differ between ferrets of different ages and therefore did not contribute to the age-related differences in clinical disease.

Figure 26. Histochemical evaluation of sialic acid distribution in the lung of 8 week old and 6 month old ferrets.

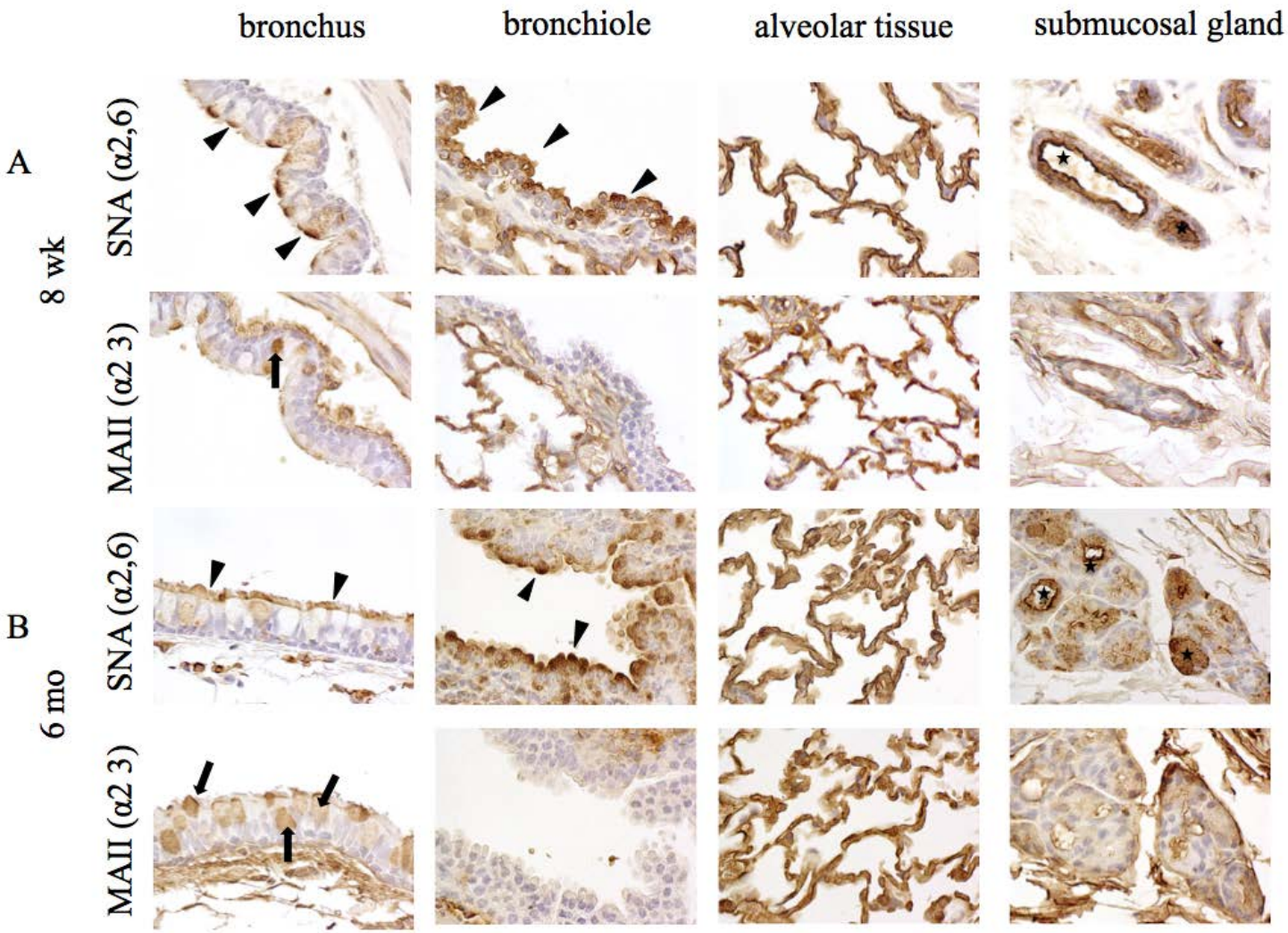

Figure 26 (cont'd)

Lung tissue from 8 week old (**A**) and 6 month old (**B**) ferrets were evaluated histochemically with the plant lectins SNA (*sambucus nigra agglutinin*) or MAAII (*maackia amurensis agglutinin* II) which are specific for mammalian-like sialic acids (α2,6) and avian-like sialic acids (α2,3), respectively. Histology sections contained bronchus, bronchiole, alveolar tissue, and submucosal glands (SMG). Arrow-heads indicate positive staining associated with ciliated bronchial or cuboidal bronchiolar epithelial cells while arrows denote positive staining in goblet cells of the bronchus. Stars indicate positive staining within regions of the SMGs.

In addition to SA receptor distribution inferred by lectin staining, I sought to determine if sialyltransferases (*SAt*) distribution and abundance differed with age. Sections of lung tissue were evaluated for the presence of the *SAt*, enzymes that catalyze the transfer of SA from the nucleotide sugar donor CMP-Sia to acceptor oligosaccharides found on oligosaccharides (Kornfeld & Kornfeld, 1985; J. E. Sadler, Rearick, & Hill, 1979). Using immunohistochemical methods (kindly provided by Dr. John Nicholls, University of Hong Kong) (Jia et al., 2014), I employed antibodies specific for specific for both the α2,3-associated *SAt* (ST3GAL3) and the α2,6-associated *SAt* (ST6GAL1). In general, the distribution of *SAt* in the lung of 8 week old (Fig. 27A) and 6 month old (Fig. 27B) ferrets did not differ significantly and was similar to the pattern of SA distribution revealed by lectin staining. In lung sections labeled with α-ST3GAL3, there was strong diffuse labeling of the bronchial epithelium, bronchiolar epithelium, alveolar tissue and submucosal gland (SMG) epithelium (Figs. 27A and 27B). Lung sections labeled with α-ST6GAL1, showed strong labeling of the bronchiolar epithelium and SMG epithelium and less intense labeling of the bronchial epithelium and the alveolar tissues. The labeling observed in the bronchiolar epithelial cells was diffuse and cytoplasmic, while labeling in the SMG was distributed in a stippled to coarsely-clumped pattern, often associated with the nucleus of the glandular epithelial cells (Figs. 27A and 27B).

Thus, the presence or distribution of sialic acid receptors or sialyltransferases did not account for the age-related difference in clinical illness or pathology in ferrets infected with influenza viruses.

Figure 27. Immunohistochemical evaluation of labeling in the lung of 8 week and 6 month old ferrets for Sialyltransferases.

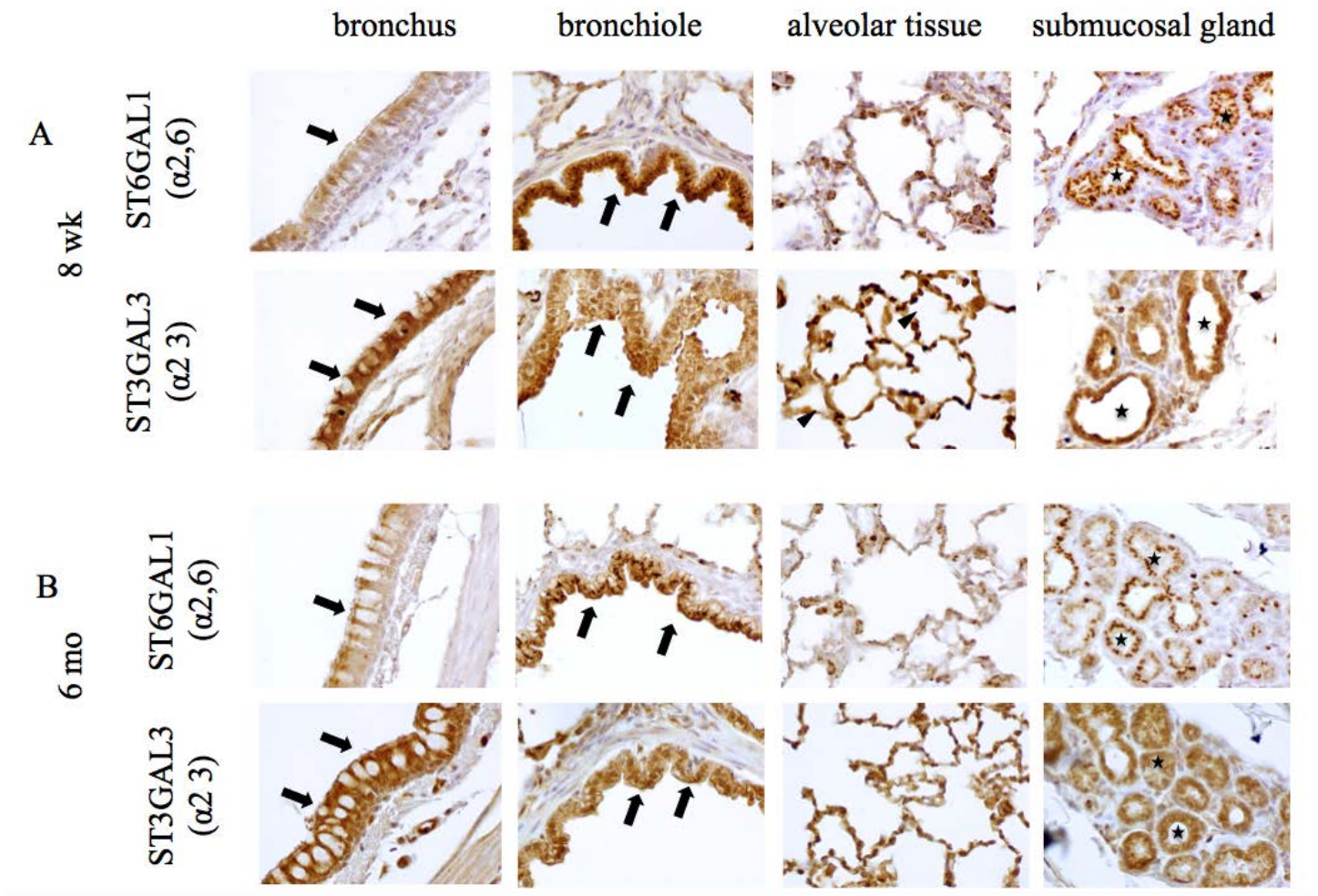

Figure 27 (cont'd)

Lung tissue from 8 week old (**A**) and 6 month old (**B**) ferrets were evaluated immunohistochemically with antibodies specific for the α2,3-associated Sialyltransferase (*SAt*) enzyme, ST3GAL3 and for the α2,6-associated *SAt* enzyme, ST6GAL1. Histology sections contained bronchus, bronchiole, alveolar tissue, and submucosal glands (SMG). Arrows indicate positive staining associated with ciliated (bronchus) or cuboidal (bronchiolar) epithelial cells. Stars indicate positive staining within regions of the SMG.

Evaluation of lung tissue for cytokine mRNA levels

Cytokine data. Because the histopathologic changes associated with influenza virus infection were more severe in older ferrets, frozen lung samples were evaluated for changes in the levels of several cytokines and chemokines (IL-6, IL-8, TNF- α, IFN-α, IFN-β, IFN-γ, IL-10 and CXCL10 (IP-10)).

In H1N1pdm infection, 6 month old ferrets had significantly elevated levels of IL6 and CXCL10 (IP10) and IL6 mRNA levels were significantly higher in older ferrets on day 3 ($p=0.0003$) and day 6 ($p=0.0029$) post infection, compared to younger ferrets (Figs. 28A and 28B). There were no significant differences observed between the age groups for the remaining cytokines; IL-8, TNF- α, IFN-α, IFN-β, IFN-γ, IL-10.

Figure 28. Cytokine mRNA transcript levels of IL-6 and CXCL10 in the lungs of 8 week and 6 month old ferrets following infection with the H1N1pdm influenza virus.

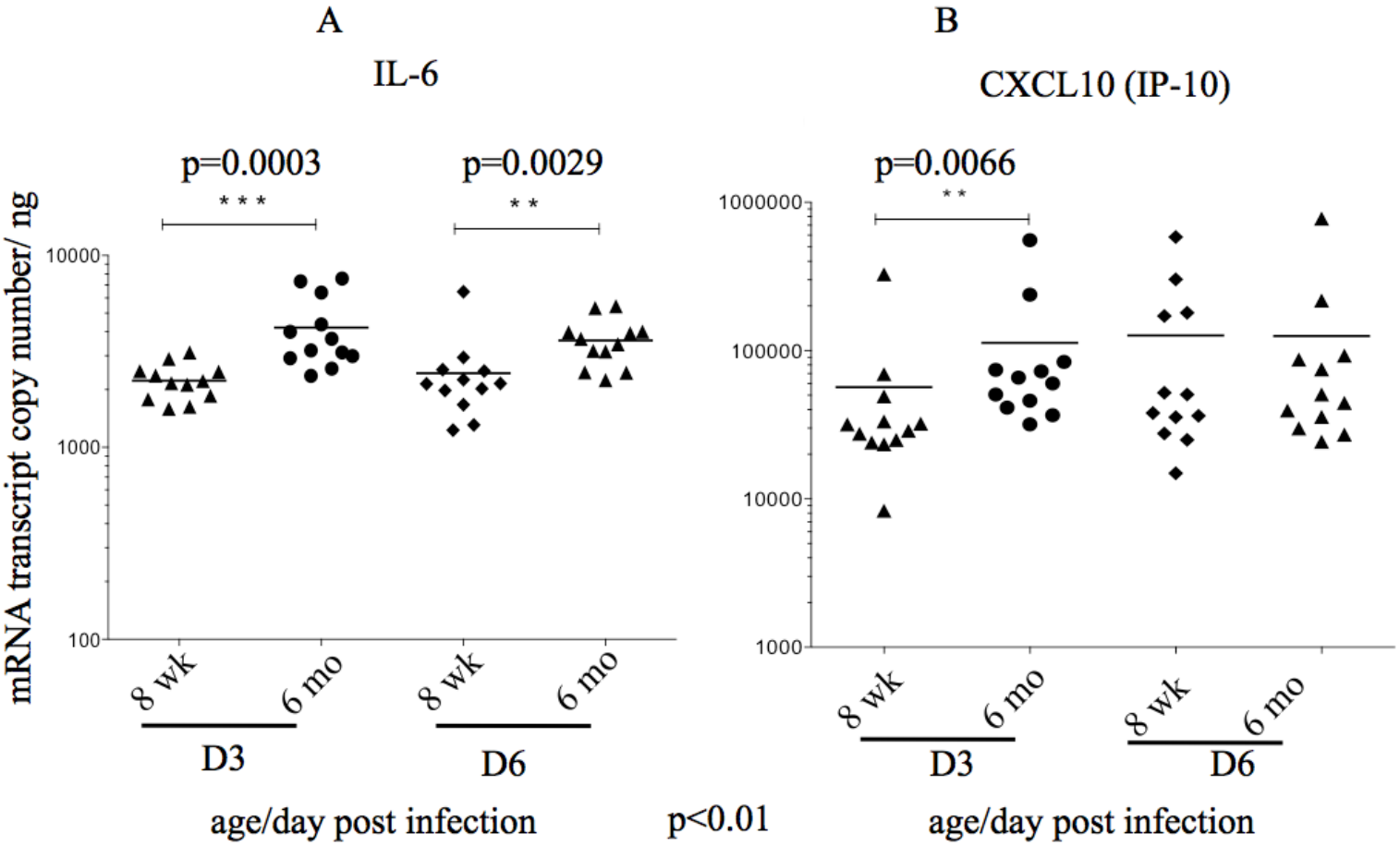

Figure 28 (cont'd)

Transcript levels for Interleukin-6 (IL-6) (**A**) and CXC motif chemokine-10 or Interferon-gamma induced protein-10 (CXCL10/ IP-10) (**B**) in the lung of 8 week old and 6 month old ferrets on days 3 and 6 following inoculation with the H1N1pdm influenza virus. Symbols represent individual animals within each (day) group. Bar represents group mean. **p <0.01, ***p <0.001 based on Wilcoxon signed-rank test.

In the ferrets infected with the H3N2v influenza virus, there were no significant differences observed for any of the cytokines evaluated. However, both IFN-γ (Fig. 29A) and TNF-α (Fig. 29B) were of borderline significance on day 1 ($p=0.012$) and day 3 ($p=0.015$), respectively.

Figure. 29. Cytokine mRNA transcript levels of IFN-β and TNF-α in the lungs of 8 week and 6 month old ferrets following infection with the H3N2v influenza virus.

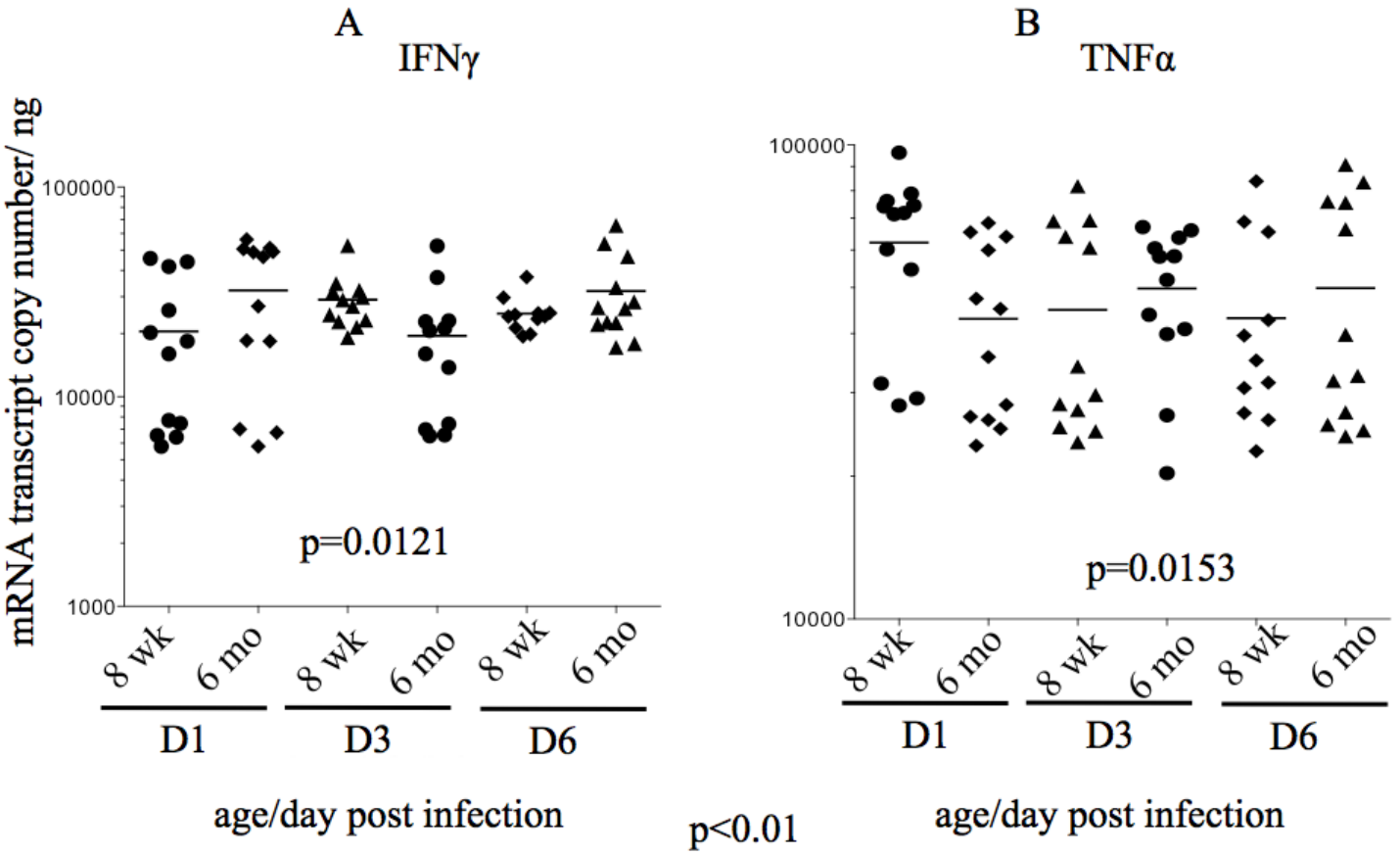

Figure 29 (cont'd)

Transcript levels for Interferon –beta (IFN-β) (**A**) and Tumor necrosis factor-alpha (TNF-α) (**B**) in the lung of 8 week old and 6 month old ferrets on days 3 and 6 following inoculation with the H3N2v influenza virus. Symbols represent individual animals within each (day) group. Bar represents group mean. $p < 0.01$ based on Wilcoxon signed-rank test.

Micro-CT imaging and analysis of the ferret respiratory tract

Having found no difference in the presence or distribution of viral receptors to account for the age-related difference in clinical illness I used Micro-Computed Tomography (μCT) to determine if anatomical differences could account for the lack of clinical disease in young ferrets. Ferrets like humans, (Johnson-Delaney & Orosz, 2011), have three right (cranial, middle, caudal) lung lobes and two left (cranial and caudal) lung lobes. Interestingly, irrespective of animal age and gender, the diameter of the right main stem bronchus was considerably and consistently larger than left. In addition, the right bronchus arose from the tracheal bifurcation at an angle more acute and pronounced lateral deviation than the left, whereas, the left bronchus consistently arose from the bifurcation in a straighter fashion, projecting towards the left caudal lung lobe (see Fig. 10).

Using a novel method of positive pressure inflation, I intubated formalin-fixed lungs were distended and imaged (Figs. 30A and 30B). The lungs of 4 ferrets (two from each age group) were imaged and a noticeable difference in the degree of airway branching was observed, (particularly beyond the level of the segmental bronchus) with more branching in the older animals (Figs. 31A-C). Features of the conducting and respiratory regions of the airways were analyzed as regions of interest (ROI), in order to calculate the total airway volume (Figs. 32A and 32B). Three-dimensional (3D) models of the lungs of an 8 week old and 6 month old ferret were compared (Figs. 33Aand 33B). Using Amira® software, the airway branching was quantified and the generations of respiratory tree branching in young and old animals were compared. The Amira® software generated a nodal map of the conducting (proximal) and respiratory (distal) regions of the ferret airway. Each node represented a point at which airways branched and further analysis of the nodes allowed the number of branches, the mean length of

the airways, mean radius of the airways segments, and total length of the airway segments to be calculated. A comparison of these measurements permitted an assessment of the lung remodeling that occurs in ferrets as they age (Fig. 34).

Overall, the total airway volume increased with age. Specifically, the number of airway branches in the 6 month old animal was 315,592 compared to 93,340 branching events in the 8 week old ferret. The 6 month old animal had a total airway volume of 1,271.453 mm^3 compared to 1,022.675 mm^3 in the 8 week old ferret. Additionally, as a consequence of branching, the mean length of the airways decreased with age (8 wk; 1.08709 mm, 6 mo; 0.7119mm) and the mean radius of the airways decreased with age (8 wk; 0.0900 mm, 6 mo; 0.0639 mm), while the total length of airway segments increased with age (8 wk; 47,914.85 mm, 6 mo; 178,599.25 mm).

Figure 30. Ex-vivo imaging of formalin fixed ferret lungs using a modified method of positive pressure inflation.

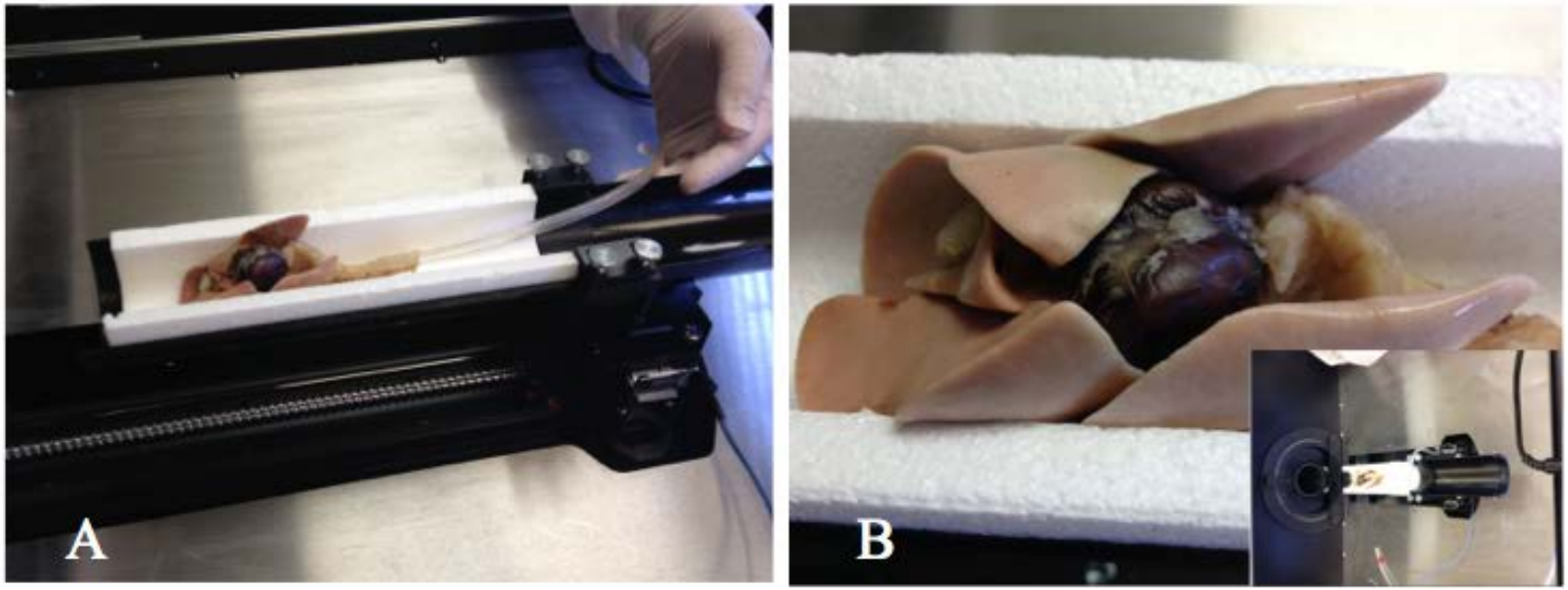

Figure 30 (cont'd)

Whole Lungs from 8 week old and 6 month old ferrets were removed from the thoracic cavity (with trachea and heart intact), formalin fixed, and drained prior to imaging. The airway was intubated (**A**) and attached to a constant pressure oxygen source, re-inflated, and placed in the Micro-CT scanner (**B**).

Figure 31. Micro-CT images of 8 week and 6 month old ferret lung branching.

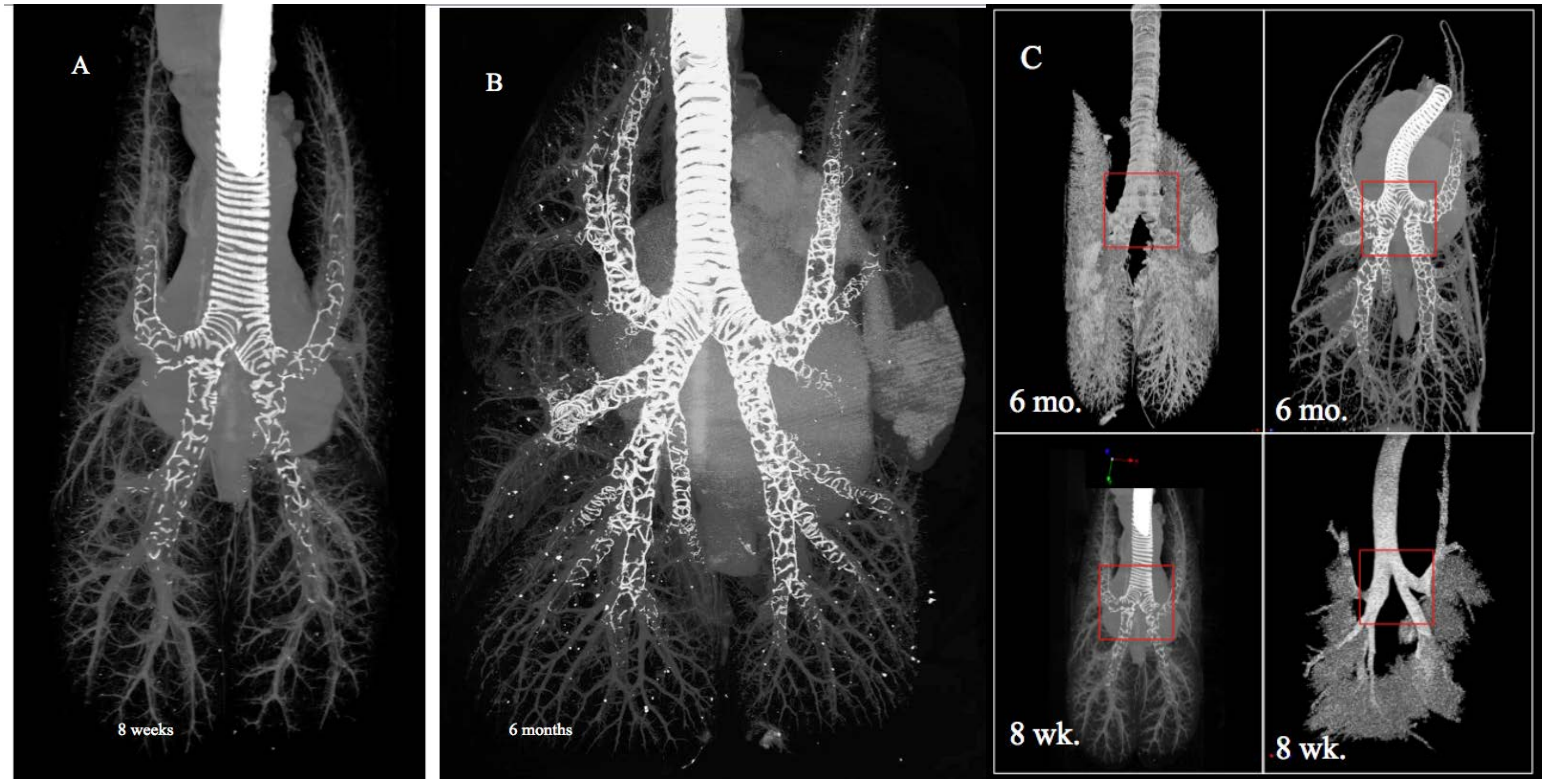

Figure 31 (cont'd)

Maximum intensity projection (MIP) comparing the normal anatomy and airway branching for 8 week old (**A**) and 6 month old (**B**) ferrets. Panel illustrating the degree of lung branching in multiple ferrets of different ages (**C**) using different imaging modalities. All lungs harvested from uninfected ferrets were imaged (ex-vivo) using a modified air bronchogram method and Micro-computed Tomography (μCT).

Figure 32. Morphometric analysis of the ferret lung.

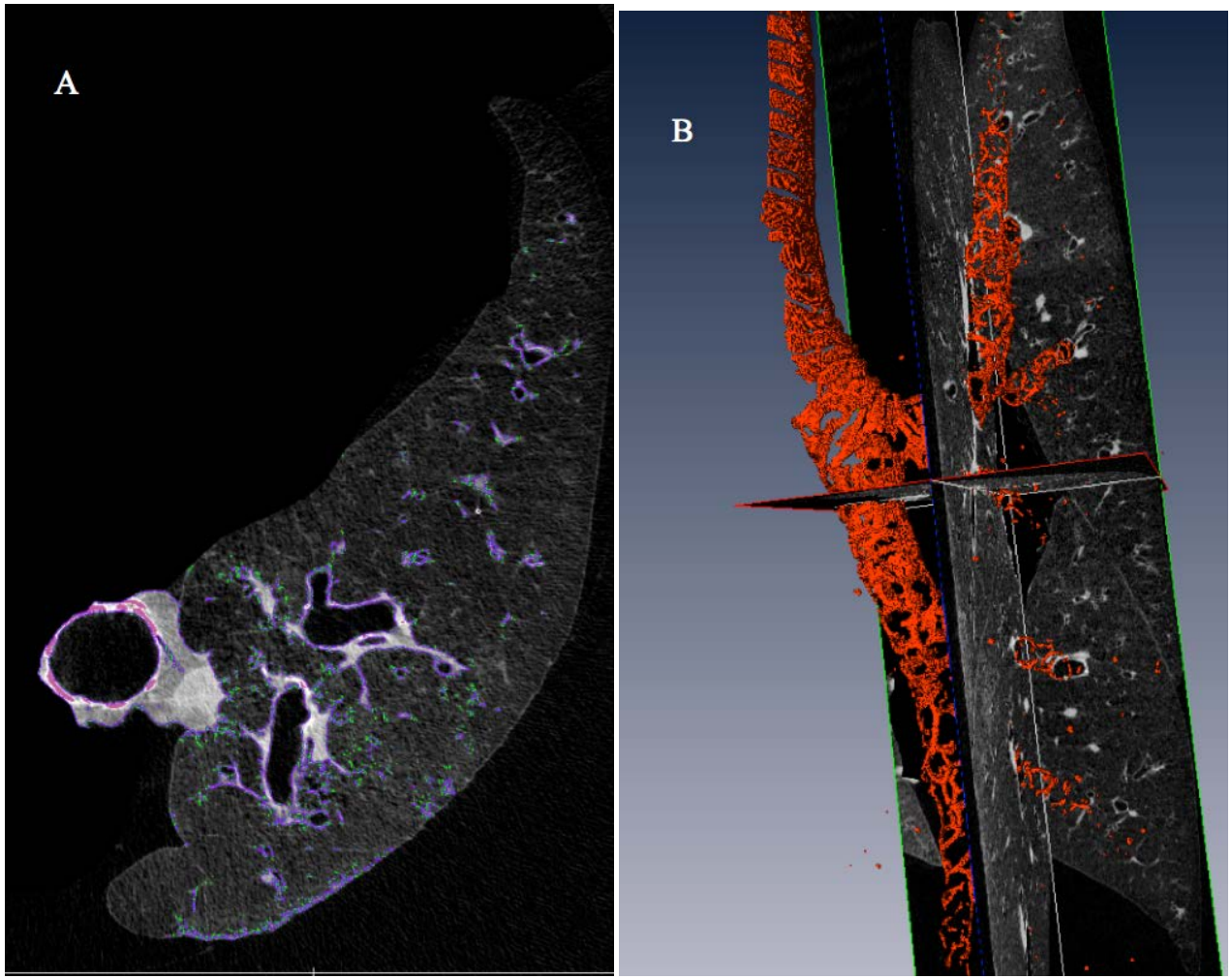

Figure 32 (cont'd)

Region of interest (ROI) generated from μCT scans of ferret lung (**A**) are analyzed via a series of image thresh-holdings in order to identify the conducting and respiratory regions of the airways. The selected areas are then reconstructed and analyzed using the Amira® image analysis software (**B**).

Figure 33. Computer generated three-dimensional (3D) volumetric reconstructions of 8 week old and 6 month old ferret lung branching.

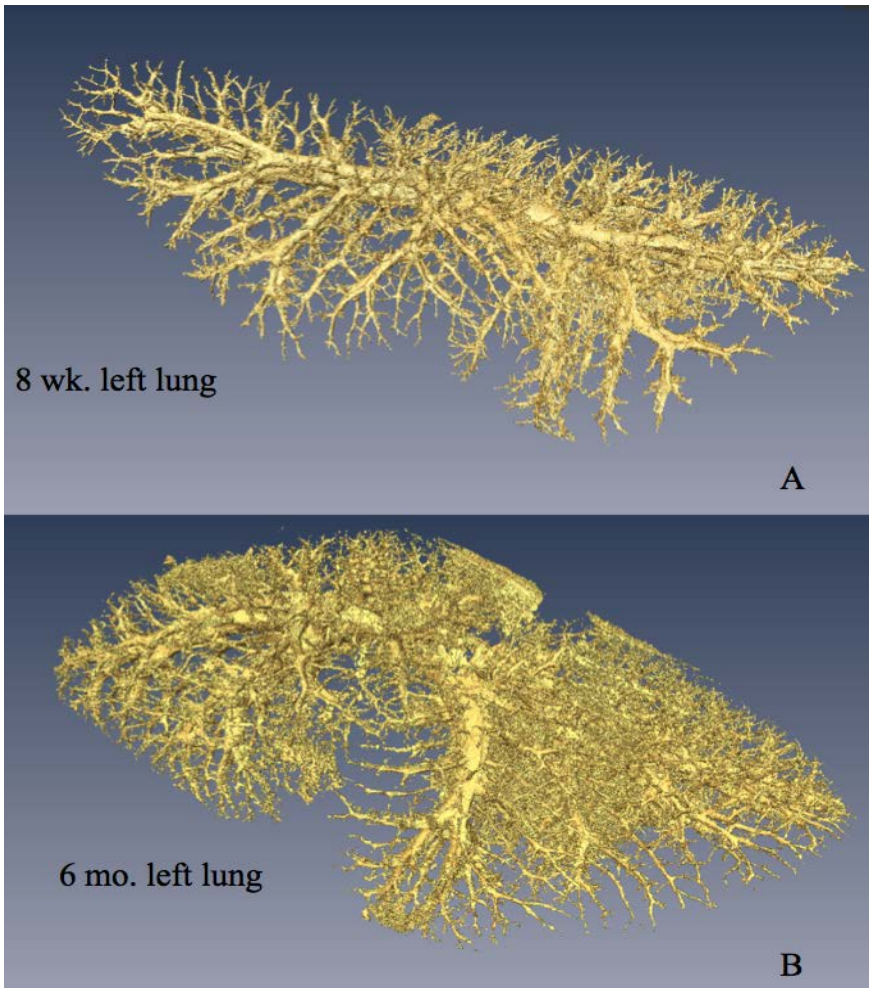

Figure 33 (cont'd)

Uninfected lungs from 8 week old (**A**) and 6 month old (**B**) ferrets were imaged using Micro-Computed Tomography (μCT) and three-dimensional (3D) volumetric reconstructions were generated using *Nrecon*® image analysis software. Images depict the degree of proximal and distal lung (left) branching in animals of different ages.

Figure 34. Analysis of ferret lung branching using nodal calculations.

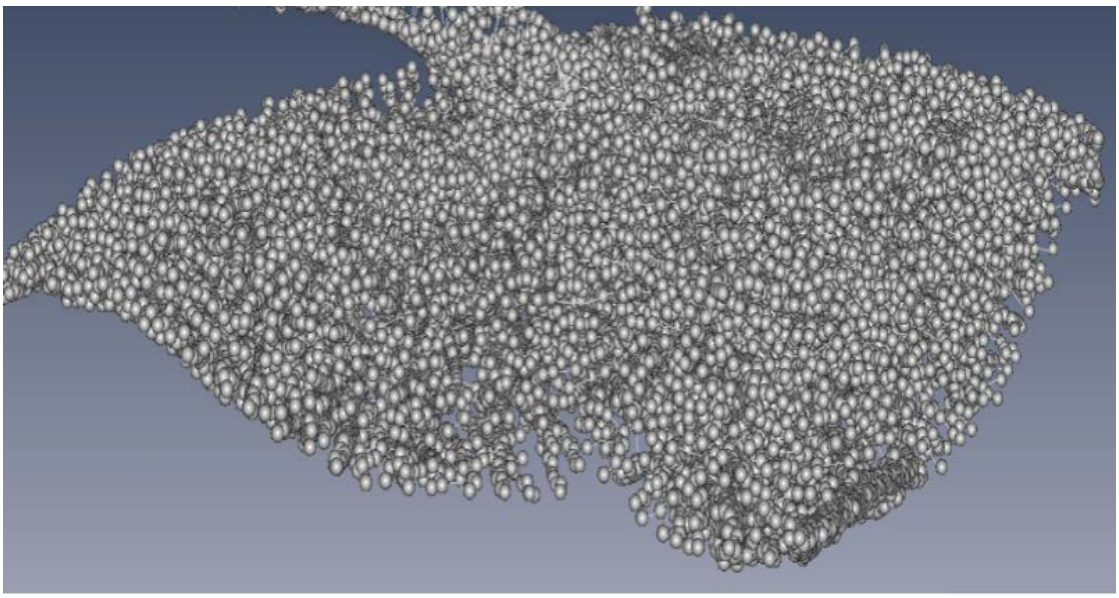

Figure 34 (cont'd)

Upon identifying regions of interest (ROI), the generated airway branching data sets are converted to node maps for analysis. Each node (point) represents locations where airways (conducting and respiratory) bifurcate. These regions are then quantified for right and left lungs and compared by age.

In summary, age is a predictor of clinical disease severity in ferrets infected with either the H1N1pdm or H3N2v influenza viruses. The presence of clinical disease in 6 month old ferrets was associated with more severe pathology and a more pro-inflammatory immune response mounted by older ferrets when compared to younger ferrets. These findings combined the extensive lung remodeling that occurs between 8 weeks and 6 months of age and more extensive branching and narrowing of distal airways likely account for more severe disease in older ferrets.

SUMMARY

-Young ferrets had mild clinical disease outcomes and less severe pathology than older ferrets despite evidence of virus replication in the URT and LRT.

-Neither sialic acids nor sialyltransferases in the lungs differed significantly between ferrets of different ages.

-6 month old ferrets tended to mount a pro-inflammatory immune (cytokine) response while 8 week old ferrets mounted a more anti-viral focused immune response.

-Micro-CT analysis and lung morphometrics indicate that significant remodeling occurs between 8 weeks and 6 months of age in ferrets.

DISCUSSION

Independent of the inoculum volume administered, age was a predictor of clinical disease severity in influenza virus infection in ferrets. Young ferrets failed to develop clinical signs of influenza infection. Age-related differences in the level of airway branching and arborization may contribute significantly to the extent of virus replication in the lung and and narrow distal airways could be more easily occluded by inflammatory infiltrates leading to increased severity of clinical disease.

Variability in clinical signs by age has been noted previously but the basis has not been investigated systematically. Stark et al (Stark et al., 2013) showed that when comparing the clinical profiles of ferrets infected with HPAI (H5N1), seasonal (H3N2 or H1N1) and swine (H1N1pdm) influenza viruses, animals infected with the H1N1pdm virus showed very mild clinical disease and steadily gained weight over the course of infection despite virus titers in the URT that were comparable to virus titers seen in ferrets infected with the HPAI H5N1 virus. Animals ranged from 8-15 weeks of age and were randomized into study groups according to starting body weights. Many of the animals with lower body weights, that were presumably younger animals, were randomly assigned to be infected with the H1N1pdm influenza virus. These animals gained the most weight over the 14-day course of the study. van Den Brand et al (van den Brand, Stittelaar, van Amerongen, et al., 2012) reported considerable clinical disease and pathology with both the seasonal H3N2 and H1N1pdm influenza viruses in 11 month old ferrets. However, Huang et al (Huang et al., 2012) showed that newly-weaned (5-8 week old) ferrets had significantly milder disease than 4-6 month old ferrets infected with the H1N1pdm influenza virus.

In my evaluation of the H3N2v virus study, efficient virus replication was noted in both the URT and LRT of ferrets, irrespective of age. However, 8 week old ferrets exhibited very mild clinical disease despite having high titer viral replication and pathology in the URT and LRT, while 6 month old ferrets showed clinical signs of infection with elevated temperature, weight loss and nasal discharge. In contrast to my findings, Pearce et al (Pearce et al., 2012) found that the A/MN/11/2010 (H3N2v) virus replicated efficiently in the URT (~5.5-7.3 $\log_{10}$ pfu/ml) but was undetectable in the LRT of ferrets. In this study the authors evaluated the pathogenicity of 4 different H3N2v influenza viruses (human isolates from 2009, 2010 and 2011) in ferrets, two of which were propagated in MDCK cells (A/Indiana/08/2011 and A/Minnesota/11/2010) and were not detected in the LRT and two that were propagated in eggs (A/Pennsylvania/14/2010 and A/Kansas/13/2009) and were detected in the LRT of experimentally infected ferrets. It is possible that the differences in the levels of the MN/10 (H3N2v) virus replication between Pearce et al and the current study are due to mutations acquired from growth of virus in MCDK cells in the Pearce study versus and egg-derived MN/10 virus in my study. Amplification of influenza viruses in embryonated eggs and MDCK cells is known to select for specific mutations in the hemagglutinin gene, that can be associated with differences in virulence (Katz, Wang, & Webster, 1990).

Suguitan et al found that 8-10 week old ferrets administered a dose of 10^6 $TCID_{50}$ of a highly pathogenic avian influenza (HPAI) H5N1virus had very mild clinical disease. However, when a similar dose of virus was administered to 6 month old ferrets, animals developed severe disease with weight loss and neurological signs including ataxia and hind limb paralysis (unpublished data and (Suguitan et al., 2012)). Thus, the association of age of ferret and clinical disease severity was observed even with well-characterized lethal avian influenza viruses.

There are a number of other possible explanations for the observed association between the age of the animal and the development of clinical illness. These include anatomical and/or developmental changes and differences in the inflammatory or innate immune responses between the two age groups. With the H1N1pdm virus, 6 month old ferrets had more severe pathology in the URT (see Fig. 22B) and LRT (see Fig. 23B) than young ferrets. Within the LRT, virus replication and inflammation were slightly delayed in the younger ferrets (Fig. 23A). In both age groups, the inflammation was centered on small airways (bronchioles) in the early stages, often characterized by airway lumina being completely filled with inflammatory cells and sloughed debris (see Figs. 23A and 23B). Later, on d6 p.i., older ferrets had severe inflammation largely centered on the submucosal glands (SMGs) adjacent the large airways but these changes were seldom observed in the younger animals. These findings were consistent with histochemical analysis of sialic acid distribution in the ferret lung. Strong positive staining with lectins specific for α2,6-linked sialic acids (SNA) that preferentially bind mammalian influenza viruses was observed in the bronchioles and the glandular epithelium lining the SMGs, while regions of bronchiolar epithelium and SMG did not stain with lectins specific for α2,3-linked sialic acids (MAAII) that preferentially bind avian influenza viruses (see Figs. 26A and 26B). Although the distribution of lectins was similar in animals of both ages, the lack of SMG inflammation in younger animals may play a role in the absence of disease.

The mRNA transcripts for a number of cytokines and chemokines were quantified following infection. With the H1N1pdm virus, significantly elevated levels of interleukin-6 (IL-6) ($p=0.003$ (d3); $p=0.0029$ (d6)) and CXCL10 (IP 10) ($p=0.0066$ (d3)) were found in older ferrets. Increased levels of IL-6 have been associated with elevations in body temperature (fever) following influenza infection in humans (Kaiser, Fritz, Straus, Gubareva, & Hayden,

2001) and IL-6 has been implicated as a major contributor to early symptoms of influenza (Hayden et al., 1998; Skoner, Gentile, Patel, & Doyle, 1999; Van Reeth, 2000). All the 6 month old ferrets had elevated body temperatures throughout the course of the study (Fig. 12B). IL-6 is also a principal mediator of acute inflammation (Wolf, Rose-John, & Garbers, 2014) and lung pathology was more severe in older ferrets and was characterized by an abundant and predominantly neutrophilic cellular infiltrate. Huang et al (Huang et al., 2012) reported similar findings with significant elevations in the neutrophil-derived myeloperoxidase (MPO) protein levels in older ferrets infected with the H1N1pdm virus, compared to newly-weaned ferrets. IP-10 (CXCL10) has also been implicated in increased severity of influenza disease (Cameron et al., 2008) and enhanced neutrophil-mediated lung injury (Ichikawa et al., 2013) and specifically with the course of H1N1pdm influenza disease in ferrets (Rowe et al., 2010).

There were no significant differences noted in the cytokine profiles of ferrets infected with the H3N2v influenza virus; however, both TNFα ($p=0.015$) and IFNγ ($p=0.012$) were of borderline significance and were higher in young ferrets compared to the older animals. TNFα is a pro-inflammatory cytokine with potent anti-influenza viral effects in vitro (Seo & Webster, 2002). Although clinical disease was mild in young ferrets, a mild to moderate, predominantly neutrophilic inflammatory infiltrate was present in the lungs. IFNγ is a well-characterized anti-viral protein that plays an important role in reducing the spread of virus in early infection (Kaiser et al., 2001). It is produced by a number of immune cells including (CD4, CD8, NK cells) in viral infections and is a modulator of the adaptive immune response (Lawrence, Reid, & Whalen, 2013). The adaptive immune response could not be assessed because of the relatively short duration (6 days post infection) of the study. IFNγ has been shown to protect influenza virus-infected mice from severe disease and death when administered in the early stages of infection,

resulting in reduced viral loads (Weiss et al., 2010). In the H3N2v-infected ferrets, there was a 100-fold higher titer of virus in the LRT of older ferrets (1.0 ml) compared to younger ferrets (see Figs. 20A and 20B). This difference in viral replication may reflect early and stronger activation of the innate immune response in younger animals.

Cytokine profiles in older and younger ferrets differed between the virus subtypes administered; the elevated pro-inflammatory mediators identified in the H1N1pdm infected ferrets were statistically significant (see Figs. 28 A and 28B) but the differences in the H3N2v-infected ferrets did not achieve statistical significance (see Figs. 29A and 29B). However, the statistical analysis combined data from all three inoculum volumes and at each timepoint. Both viruses were administered at the same dose, but the H3N2v virus achieved higher titers in the lungs of ferrets. Thus, there may be viral determinants of virulence that contribute to the differences observed.

After observing age-related differences in virus replication, pathology and immune response, I evaluated the anatomy and structural features of the flower respiratory tract in the two age groups. In humans, some reports indicate that the lung does not fully mature until after the second decade of life (Sharma & Goodwin, 2006). Micro-CT analysis of the ferret lungs revealed a striking extent of lung remodeling that occurred between 8 weeks and 6 months of age. Three independent observations were made related to lung remodeling; first, air bronchogram demonstrated increased branching in the distal regions of the lung of older ferrets. Second, 3D images reconstructed from the CT image data confirmed the differences in the distal airway branching between young and old ferrets and lastly, node analysis of the 3D image data showed increases in airway volume, airway length, and branching in older ferrets compared to younger ferrets. In particular, the increase in airway length with age was consistent with data

reported for rhesus monkeys (Van Winkle et al., 2004) and humans (Stick, 2000). A substantial decrease in the overall diameter or caliber of the airways was also observed in older ferrets. Consistent with reports of H1N1pdm-associated acute respiratory distress syndrome (ARDS) in humans (Takiyama et al., 2010), these likely contribute to impaired gas exchange and may explain severe disease in older ferrets.

Coates et al (Coates, Husseini, Rushton, Sweet, & Smith, 1984) showed that PR8 influenza (H1N1) virus infection was lethal for newborn (1 day old) ferrets following intranasal inoculation while suckling (15 day old) and adult ferrets appeared resistant to infection. Moreover, they reported that the death of newborn ferrets was likely the result of higher virus titers in the lower respiratory tract that was likely attributable to greater proportions of ciliated cells and alveolar cells which were 2-fold and 4-fold greater in number in newborn than in suckling and adult ferrets, respectively. It is plausible that newborn ferrets have a greater number of ciliated epithelial cells in the LRT and the airways continue to remodel and lengthen with age while the resident epithelial cell numbers appear to remain relatively stable (Stick, 2000). The authors conclude that occlusion of airways of the respiratory tract by exudate and desquamated epithelial cells was an overarching contributor to severe disease and death following infection. However, I observed more severe disease in older animals and an absence of clinical disease in younger animals. It is possible that the severe clinical findings reported by Coates et al in newborn ferrets were the result of an immature lung and immune response. In humans, it has been suggested that very young children are at greatest risk for severe lung disease because of the very small size of the respiratory tract, small energy reserves that are easily exhausted during infection (particularly if dyspnea or tachypnea are associated) and immunological immaturity (Tregoning & Schwarze, 2010). Furthermore, it is plausible that

newborn ferrets have a greater number of ciliated epithelial cells in LRT and the airways continue to remodel and lengthen with age while the resident epithelial cell numbers appears to remain relatively stable. The computational measurement of ferret lung airways was based on analysis of two animals. However, (see Fig. 31C), the μCT images from additional animals demonstrate the increased branching in older ferrets, compared to young animals.

In summary, ferret age is an important determinant of the severity of clinical disease with multiple influenza virus subtypes (H1N1pdm, H3N2v, and H5N1). Younger animals fail to develop clinical illness despite viral replication in the upper and lower respiratory tract. The lack of clinical disease in younger ferrets results from less airway branching and more anti-viral and less inflammatory immune responses. Therefore, ferrets ≥ 6 months of age should be used in experimental influenza infections, particularly when clinical disease outcomes are a desired study parameter.

CHAPTER 4: Summary and Implications

INTRODUCTION

The aim of this project was to elucidate the role of inoculum volume and age in the development and severity of clinical disease in ferrets following experimental infection with influenza A viruses. In the preceding chapters, I discuss a number of factors that can significantly affect the extent of virus infection and the degree to which clinical disease is manifested in ferrets. Ferrets are a valuable small model for the investigation of many aspects of influenza and general respiratory virus research including pathogenesis, transmission, and vaccine efficacy. Therefore efforts directed towards increasing reproducibility of data and standardization of approaches in using this model are of importance. In the following chapter, I will summarize the findings described in Chapters 2 (effect of inoculum volume) and Chapter 3 (effect of age) and speculate on the implications of these findings.

SUMMARY

In my investigation of the ferret model for influenza, I demonstrated the importance and influence of the volume of inoculum and the age of the animal used at the time of infection on the severity of clinical disease with the H1N1pdm, H3N2v, and H5N1 influenza virus subtypes. Through careful experimentation I have shown the individual contributions of these variables (inoculum volume and age) to the degree of clinical disease, viral replication in the lung, the severity of lower respiratory tract pathology, and the host response to the virus. I showed that the same dose of virus administered in different inoculum volumes resulted in significantly different virus titers in the lung. At the lowest inoculum volume (0.2 ml), virus replication in the lung and pathology were minimal or absent though high virus titers and severe pathology were observed in the upper respiratory tract. These findings reinforce the importance of assuring proper distribution and delivery of the virus to the appropriate organ in an animal model for the study of viral pathogenesis. In addition, and independent of inoculum volume, age is a determinant of clinical disease severity in ferrets. In younger ferrets, the lack of clinical disease resulted from a sub-mature stage of lung development, characterized by continued remodeling and arborization of the airways compared to adult ferret lungs. In addition, I showed that ferrets of different ages mount different types of innate immune responses following infection with the same dose and volume of influenza virus. There was a clear and consistent demonstration of clinical disease in 6 month old ferrets while younger animals that failed to develop clinical signs of influenza infection.

IMPLICATIONS

With experimental respiratory virus infections, the primary goal is to ensure that virus is delivered into the respiratory tract at a volume adequate to establish infection. I showed that viral replication in the lower respiratory tract was variable when influenza viruses were administered in a volume less than 1.0 ml . This was likely the result of a failure to adequately deliver virus inoculum to the lung. The differential susceptibility of hosts of different ages to pathogens raises intriguing questions about host-pathogen interactions. When the pathogenesis of a newly-emerged influenza virus is evaluated in ferrets, observations regarding viral replication and tropism could be misinterpreted if the pathogen is administered in a less than optimal volume and conclusions regarding clinical disease will be influenced by the age of the ferret. Importantly, the use of an outbred animal better reflects the spectrum of disease and immune responses that occur in an immunologically diverse human population and this is an advantage of the ferret model over inbred mice. These data and observations from my research provide a standardized approach for the use the ferret model to investigate different influenza viruses, particularly when clinical disease and pathology are the desired outcomes.

REFERENCES

REFERENCES

Ali, M. J., Teh, C. Z., Jennings, R., & Potter, C. W. (1982). Transmissibility of influenza viruses in hamsters. *Arch Virol, 72*(3), 187-197.

Baker, D. G. (1998). Natural pathogens of laboratory mice, rats, and rabbits and their effects on research. *Clin Microbiol Rev, 11*(2), 231-266.

Baric. (2006). Genomic and EST sequencing of the ferret (*Mustela putorius furo*).

Baskin, C. R., Garcia-Sastre, A., Tumpey, T. M., Bielefeldt-Ohmann, H., Carter, V. S., Nistal-Villan, E., & Katze, M. G. (2004). Integration of clinical data, pathology, and cDNA microarrays in influenza virus-infected pigtailed macaques (Macaca nemestrina). *J Virol, 78*(19), 10420-10432. doi: 10.1128/JVI.78.19.10420-10432.2004

Baum, L. G., & Paulson, J. C. (1990). Sialyloligosaccharides of the respiratory epithelium in the selection of human influenza virus receptor specificity. *Acta Histochem Suppl, 40*, 35-38.

Bellusci, S., Grindley, J., Emoto, H., Itoh, N., & Hogan, B. L. (1997). Fibroblast growth factor 10 (FGF10) and branching morphogenesis in the embryonic mouse lung. *Development, 124*(23), 4867-4878.

Belser, J. A., Gustin, K. M., Maines, T. R., Pantin-Jackwood, M. J., Katz, J. M., & Tumpey, T. M. (2012). Influenza virus respiratory infection and transmission following ocular inoculation in ferrets. *PLoS Pathog, 8*(3), e1002569. doi: 10.1371/journal.ppat.1002569

Bergmann, M., Garcia-Sastre, A., Carnero, E., Pehamberger, H., Wolff, K., Palese, P., & Muster, T. (2000). Influenza virus NS1 protein counteracts PKR-mediated inhibition of replication. *J Virol, 74*(13), 6203-6206.

Bissel, S. J., Wang, G., Carter, D. M., Crevar, C. J., Ross, T. M., & Wiley, C. A. (2014). H1N1, but not H3N2, influenza A virus infection protects ferrets from H5N1 encephalitis. *J Virol, 88*(6), 3077-3091. doi: 10.1128/JVI.01840-13

Bodewes, R., Morick, D., de Mutsert, G., Osinga, N., Bestebroer, T., van der Vliet, S., . . . Osterhaus, A. D. (2013). Recurring influenza B virus infections in seals. *Emerg Infect Dis, 19*(3), 511-512.

Boon, A. C., deBeauchamp, J., Hollmann, A., Luke, J., Kotb, M., Rowe, S., . . . Webby, R. J. (2009). Host genetic variation affects resistance to infection with a highly pathogenic H5N1 influenza A virus in mice. *J Virol, 83*(20), 10417-10426. doi: 10.1128/JVI.00514-09

Boon, A. C., Finkelstein, D., Zheng, M., Liao, G., Allard, J., Klumpp, K., . . . Webby, R. J. (2011). H5N1 influenza virus pathogenesis in genetically diverse mice is mediated at the level of viral load. *MBio, 2*(5). doi: 10.1128/mBio.00171-11

Bouvier, N. M., & Lowen, A. C. (2010). Animal Models for Influenza Virus Pathogenesis and Transmission. *Viruses, 2*(8), 1530-1563. doi: 10.3390/v20801530

Bridges, C. B., Kuehnert, M. J., & Hall, C. B. (2003). Transmission of influenza: implications for control in health care settings. *Clin Infect Dis, 37*(8), 1094-1101. doi: 10.1086/378292

Brown, E. G., Liu, H., Kit, L. C., Baird, S., & Nesrallah, M. (2001). Pattern of mutation in the genome of influenza A virus on adaptation to increased virulence in the mouse lung: identification of functional themes. *Proc Natl Acad Sci U S A, 98*(12), 6883-6888. doi: 10.1073/pnas.111165798

Burri, P. H. (2006). Structural aspects of postnatal lung development - alveolar formation and growth. *Biol Neonate, 89*(4), 313-322. doi: 10.1159/000092868

Cameron, C. M., Cameron, M. J., Bermejo-Martin, J. F., Ran, L., Xu, L., Turner, P. V., . . . Kelvin, D. J. (2008). Gene expression analysis of host innate immune responses during Lethal H5N1 infection in ferrets. *J Virol, 82*(22), 11308-11317. doi: 10.1128/JVI.00691-08

Carlson, B.M. (2014). *Human Embryology and Developmental Biology*.

CDC. (2013). The Flu Season. from http://www.cdc.gov/flu/about/season/flu-season.htm

CDC. (2014). Seasonal Influenza (flu). from http://www.cdc.gov/flu/about/disease/symptoms.htm

Cheng, X., Zengel, J. R., Suguitan, A. L., Jr., Xu, Q., Wang, W., Lin, J., & Jin, H. (2013). Evaluation of the humoral and cellular immune responses elicited by the live attenuated and inactivated influenza vaccines and their roles in heterologous protection in ferrets. *J Infect Dis, 208*(4), 594-602. doi: 10.1093/infdis/jit207

Coates, D. M., Husseini, R. H., Rushton, D. I., Sweet, C., & Smith, H. (1984). The role of lung development in the age-related susceptibility of ferrets to influenza virus. *Br J Exp Pathol, 65*(5), 543-547.

Colin, A. A., McEvoy, C., & Castile, R. G. (2010). Respiratory morbidity and lung function in preterm infants of 32 to 36 weeks' gestational age. *Pediatrics, 126*(1), 115-128. doi: 10.1542/peds.2009-1381

Compans, R. W., Bishop, D. H., & Meier-Ewert, H. (1977). Structural components of influenza C virions. *J Virol, 21*(2), 658-665.

Cook, P. M., Eglin, R. P., & Easton, A. J. (1998). Pathogenesis of pneumovirus infections in mice: detection of pneumonia virus of mice and human respiratory syncytial virus mRNA in lungs of infected mice by in situ hybridization. *J Gen Virol, 79 (Pt 10)*, 2411-2417.

Cox, N. J., & Subbarao, K. (2000). Global epidemiology of influenza: past and present. *Annu Rev Med, 51*, 407-421. doi: 10.1146/annurev.med.51.1.407

Danesh, A., Seneviratne, C., Cameron, C. M., Banner, D., Devries, M. E., Kelvin, A. A., . . . Kelvin, D. J. (2008). Cloning, expression and characterization of ferret CXCL10. *Mol Immunol, 45*(5), 1288-1297. doi: 10.1016/j.molimm.2007.09.018

Dawood, F. S., Iuliano, A. D., Reed, C., Meltzer, M. I., Shay, D. K., Cheng, P. Y., . . . Widdowson, M. A. (2012). Estimated global mortality associated with the first 12 months of 2009 pandemic influenza A H1N1 virus circulation: a modelling study. *Lancet Infect Dis, 12*(9), 687-695. doi: 10.1016/S1473-3099(12)70121-4

Doherty, P. C., Topham, D. J., Tripp, R. A., Cardin, R. D., Brooks, J. W., & Stevenson, P. G. (1997). Effector CD4+ and CD8+ T-cell mechanisms in the control of respiratory virus infections. *Immunol Rev, 159*, 105-117.

Dorrington, M. G., & Bowdish, D. M. (2013). Immunosenescence and novel vaccination strategies for the elderly. *Front Immunol, 4*, 171. doi: 10.3389/fimmu.2013.00171

Douglas, R. G., Jr. (1990). Prophylaxis and treatment of influenza. *N Engl J Med, 322*(7), 443-450. doi: 10.1056/NEJM199002153220706

Doyle, C., Roth, M. G., Sambrook, J., & Gething, M. J. (1985). Mutations in the cytoplasmic domain of the influenza virus hemagglutinin affect different stages of intracellular transport. *J Cell Biol, 100*(3), 704-714.

Duan, S., Boltz, D. A., Seiler, P., Li, J., Bragstad, K., Nielsen, L. P., . . . Govorkova, E. A. (2010). Oseltamivir-resistant pandemic H1N1/2009 influenza virus possesses lower transmissibility and fitness in ferrets. *PLoS Pathog, 6*(7), e1001022. doi: 10.1371/journal.ppat.1001022

Dubois, J., Terrier, O., & Rosa-Calatrava, M. (2014). Influenza viruses and mRNA splicing: doing more with less. *MBio, 5*(3), e00070-00014. doi: 10.1128/mBio.00070-14

Edwards, K. M., Davis, J. E., Browne, K. A., Sutton, V. R., & Trapani, J. A. (1999). Anti-viral strategies of cytotoxic T lymphocytes are manifested through a variety of granule-bound pathways of apoptosis induction. *Immunol Cell Biol, 77*(1), 76-89. doi: 10.1046/j.1440-1711.1999.00799.x

Eichelberger, M. C., Prince, G. A., & Ottolini, M. G. (2004). Influenza-induced tachypnea is prevented in immune cotton rats, but cannot be treated with an anti-inflammatory steroid or a neuraminidase inhibitor. *Virology, 322*(2), 300-307. doi: 10.1016/j.virol.2004.01.032

Fan, J., Liang, X., Horton, M. S., Perry, H. C., Citron, M. P., Heidecker, G. J., . . . Shiver, J. W. (2004). Preclinical study of influenza virus A M2 peptide conjugate vaccines in mice, ferrets, and rhesus monkeys. *Vaccine, 22*(23-24), 2993-3003. doi: 10.1016/j.vaccine.2004.02.021

Faulkner, O. B., Estevez, C., Yu, Q., & Suarez, D. L. (2013). Passive antibody transfer in chickens to model maternal antibody after avian influenza vaccination. *Vet Immunol Immunopathol, 152*(3-4), 341-347. doi: 10.1016/j.vetimm.2013.01.006

Fleischmann, W. R. (1996). Viral Genetics. In S. Baron (Ed.), *Medical Microbiology* (4th ed.). Galveston (TX).

Franca, M., Stallknecht, D. E., & Howerth, E. W. (2013). Expression and distribution of sialic acid influenza virus receptors in wild birds. *Avian Pathol, 42*(1), 60-71. doi: 10.1080/03079457.2012.759176

Furuya, Y. (2012). Return of inactivated whole-virus vaccine for superior efficacy. *Immunol Cell Biol, 90*(6), 571-578. doi: 10.1038/icb.2011.70

Garcia-Sastre, A. (2010). Influenza virus receptor specificity: disease and transmission. *Am J Pathol, 176*(4), 1584-1585. doi: 10.2353/ajpath.2010.100066

Garten, R. J., Davis, C. T., Russell, C. A., Shu, B., Lindstrom, S., Balish, A., . . . Cox, N. J. (2009). Antigenic and genetic characteristics of swine-origin 2009 A(H1N1) influenza viruses circulating in humans. *Science, 325*(5937), 197-201. doi: 10.1126/science.1176225

Goulet, M. L., Olagnier, D., Xu, Z., Paz, S., Belgnaoui, S. M., Lafferty, E. I., . . . Hiscott, J. (2013). Systems analysis of a RIG-I agonist inducing broad spectrum inhibition of virus infectivity. *PLoS Pathog, 9*(4), e1003298. doi: 10.1371/journal.ppat.1003298

Guarner, J., & Falcon-Escobedo, R. (2009). Comparison of the pathology caused by H1N1, H5N1, and H3N2 influenza viruses. *Arch Med Res, 40*(8), 655-661. doi: 10.1016/j.arcmed.2009.10.001

Haller, O., Kochs, G., & Weber, F. (2006). The interferon response circuit: induction and suppression by pathogenic viruses. *Virology, 344*(1), 119-130. doi: 10.1016/j.virol.2005.09.024

Hatta, M., & Kawaoka, Y. (2003). The NB protein of influenza B virus is not necessary for virus replication in vitro. *J Virol, 77*(10), 6050-6054.

Hayden, F. G., Fritz, R., Lobo, M. C., Alvord, W., Strober, W., & Straus, S. E. (1998). Local and systemic cytokine responses during experimental human influenza A virus infection. Relation to symptom formation and host defense. *J Clin Invest, 101*(3), 643-649. doi: 10.1172/JCI1355

Heldt, F. S., Frensing, T., & Reichl, U. (2012). Modeling the intracellular dynamics of influenza virus replication to understand the control of viral RNA synthesis. *J Virol, 86*(15), 7806-7817. doi: 10.1128/JVI.00080-12

Huang, S. S., Banner, D., Degousee, N., Leon, A. J., Xu, L., Paquette, S. G., . . . Kelvin, A. A. (2012). Differential pathological and immune responses in newly weaned ferrets are associated with a mild clinical outcome of pandemic 2009 H1N1 infection. *J Virol, 86*(24), 13187-13201. doi: 10.1128/JVI.01456-12

Huang, S. S., Banner, D., Fang, Y., Ng, D. C., Kanagasabai, T., Kelvin, D. J., & Kelvin, A. A. (2011). Comparative analyses of pandemic H1N1 and seasonal H1N1, H3N2, and influenza B infections depict distinct clinical pictures in ferrets. *PLoS One, 6*(11), e27512. doi: 10.1371/journal.pone.0027512

Ibricevic, A., Pekosz, A., Walter, M. J., Newby, C., Battaile, J. T., Brown, E. G., . . . Brody, S. L. (2006). Influenza virus receptor specificity and cell tropism in mouse and human airway epithelial cells. *J Virol, 80*(15), 7469-7480. doi: 10.1128/JVI.02677-05

Ichikawa, A., Kuba, K., Morita, M., Chida, S., Tezuka, H., Hara, H., . . . Imai, Y. (2013). CXCL10-CXCR3 enhances the development of neutrophil-mediated fulminant lung injury of viral and nonviral origin. *Am J Respir Crit Care Med, 187*(1), 65-77. doi: 10.1164/rccm.201203-0508OC

Ichinohe, T., Iwasaki, A., & Hasegawa, H. (2008). Innate sensors of influenza virus: clues to developing better intranasal vaccines. *Expert Rev Vaccines, 7*(9), 1435-1445. doi: 10.1586/14760584.7.9.1435

Ilyushina, N. A., Khalenkov, A. M., Seiler, J. P., Forrest, H. L., Bovin, N. V., Marjuki, H., . . . Webby, R. J. (2010). Adaptation of pandemic H1N1 influenza viruses in mice. *J Virol, 84*(17), 8607-8616. doi: 10.1128/JVI.00159-10

Imai, M., Kawasaki, K., & Odagiri, T. (2008). Cytoplasmic domain of influenza B virus BM2 protein plays critical roles in production of infectious virus. *J Virol, 82*(2), 728-739. doi: 10.1128/JVI.01752-07

Imai, M., Watanabe, S., Ninomiya, A., Obuchi, M., & Odagiri, T. (2004). Influenza B virus BM2 protein is a crucial component for incorporation of viral ribonucleoprotein complex into virions during virus assembly. *J Virol, 78*(20), 11007-11015. doi: 10.1128/JVI.78.20.11007-11015.2004

Iwasaki, A., & Medzhitov, R. (2010). Regulation of adaptive immunity by the innate immune system. *Science, 327*(5963), 291-295. doi: 10.1126/science.1183021

Iwasaki, A., & Pillai, P. S. (2014). Innate immunity to influenza virus infection. *Nat Rev Immunol, 14*(5), 315-328. doi: 10.1038/nri3665

Jackson, D., Hossain, M. J., Hickman, D., Perez, D. R., & Lamb, R. A. (2008). A new influenza virus virulence determinant: the NS1 protein four C-terminal residues modulate pathogenicity. *Proc Natl Acad Sci U S A, 105*(11), 4381-4386. doi: 10.1073/pnas.0800482105

Jegaskanda, S., Laurie, K. L., Amarasena, T. H., Winnall, W. R., Kramski, M., De Rose, R., . . . Kent, S. J. (2013). Age-associated cross-reactive antibody-dependent cellular cytotoxicity toward 2009 pandemic influenza A virus subtype H1N1. *J Infect Dis, 208*(7), 1051-1061. doi: 10.1093/infdis/jit294

Jhung, M. A., Swerdlow, D., Olsen, S. J., Jernigan, D., Biggerstaff, M., Kamimoto, L., . . . Finelli, L. (2011). Epidemiology of 2009 pandemic influenza A (H1N1) in the United States. *Clin Infect Dis, 52 Suppl 1*, S13-26. doi: 10.1093/cid/ciq008

Jia, N., Barclay, W. S., Roberts, K., Yen, H. L., Chan, R. W., Lam, A. K., . . . Haslam, S. M. (2014). Glycomic characterisation of respiratory tract tissues of ferrets: implications for its use in influenza virus infection studies. *J Biol Chem*. doi: 10.1074/jbc.M114.588541

Jin, H. K., Yamashita, T., Ochiai, K., Haller, O., & Watanabe, T. (1998). Characterization and expression of the Mx1 gene in wild mouse species. *Biochem Genet, 36*(9-10), 311-322.

Johansson, B. E., Bucher, D. J., & Kilbourne, E. D. (1989). Purified influenza virus hemagglutinin and neuraminidase are equivalent in stimulation of antibody response but induce contrasting types of immunity to infection. *J Virol, 63*(3), 1239-1246.

Johnson-Delaney, C. A., & Orosz, S. E. (2011). Ferret respiratory system: clinical anatomy, physiology, and disease. *Vet Clin North Am Exot Anim Pract, 14*(2), 357-367, vii. doi: 10.1016/j.cvex.2011.03.001

Kaiser, L., Fritz, R. S., Straus, S. E., Gubareva, L., & Hayden, F. G. (2001). Symptom pathogenesis during acute influenza: interleukin-6 and other cytokine responses. *J Med Virol, 64*(3), 262-268.

Katz, J. M., Wang, M., & Webster, R. G. (1990). Direct sequencing of the HA gene of influenza (H3N2) virus in original clinical samples reveals sequence identity with mammalian cell-grown virus. *J Virol, 64*(4), 1808-1811.

Katze, M. G., Tomita, J., Black, T., Krug, R. M., Safer, B., & Hovanessian, A. (1988). Influenza virus regulates protein synthesis during infection by repressing autophosphorylation and activity of the cellular 68,000-Mr protein kinase. *J Virol, 62*(10), 3710-3717.

Kimble, B., Nieto, G. R., & Perez, D. R. (2010). Characterization of influenza virus sialic acid receptors in minor poultry species. *Virol J, 7*, 365. doi: 10.1186/1743-422X-7-365

Kimura, H., Abiko, C., Peng, G., Muraki, Y., Sugawara, K., Hongo, S., . . . Nakamura, K. (1997). Interspecies transmission of influenza C virus between humans and pigs. *Virus Res, 48*(1), 71-79.

Kornfeld, R., & Kornfeld, S. (1985). Assembly of asparagine-linked oligosaccharides. *Annu Rev Biochem, 54*, 631-664. doi: 10.1146/annurev.bi.54.070185.003215

Kotecha, S. (2000). Lung growth: implications for the newborn infant. *Arch Dis Child Fetal Neonatal Ed, 82*(1), F69-74.

Lamb, R. A., Zebedee, S. L., & Richardson, C. D. (1985). Influenza virus M2 protein is an integral membrane protein expressed on the infected-cell surface. *Cell, 40*(3), 627-633.

Lawrence, S., Reid, J., & Whalen, M. (2013). Secretion of interferon gamma from human immune cells is altered by exposure to tributyltin and dibutyltin. *Environ Toxicol*. doi: 10.1002/tox.21932

Ljungberg, K., McBrayer, A., Camp, J. V., Chu, Y. K., Tapp, R., Noah, D. L., . . . Bruder, C. E. (2012). Host gene expression signatures discriminate between ferrets infected with genetically similar H1N1 strains. *PLoS One, 7*(7), e40743. doi: 10.1371/journal.pone.0040743

Lowen, A. C., Steel, J., Mubareka, S., Carnero, E., Garcia-Sastre, A., & Palese, P. (2009). Blocking interhost transmission of influenza virus by vaccination in the guinea pig model. *J Virol, 83*(7), 2803-2818. doi: 10.1128/JVI.02424-08

Lu, X., Tumpey, T. M., Morken, T., Zaki, S. R., Cox, N. J., & Katz, J. M. (1999). A mouse model for the evaluation of pathogenesis and immunity to influenza A (H5N1) viruses isolated from humans. *J Virol, 73*(7), 5903-5911.

Maines, T. R., Belser, J. A., Gustin, K. M., van Hoeven, N., Zeng, H., Svitek, N., . . . Tumpey, T. M. (2012). Local innate immune responses and influenza virus transmission and virulence in ferrets. *J Infect Dis, 205*(3), 474-485. doi: 10.1093/infdis/jir768

Maines, T. R., Jayaraman, A., Belser, J. A., Wadford, D. A., Pappas, C., Zeng, H., . . . Tumpey, T. M. (2009). Transmission and pathogenesis of swine-origin 2009 A(H1N1) influenza viruses in ferrets and mice. *Science, 325*(5939), 484-487. doi: 10.1126/science.1177238

Martinon, F., Burns, K., & Tschopp, J. (2002). The inflammasome: a molecular platform triggering activation of inflammatory caspases and processing of proIL-beta. *Mol Cell, 10*(2), 417-426.

Masson, F., Mount, A. M., Wilson, N. S., & Belz, G. T. (2008). Dendritic cells: driving the differentiation programme of T cells in viral infections. *Immunol Cell Biol, 86*(4), 333-342. doi: 10.1038/icb.2008.15

Matrosovich, M. N., Matrosovich, T. Y., Gray, T., Roberts, N. A., & Klenk, H. D. (2004). Human and avian influenza viruses target different cell types in cultures of human airway epithelium. *Proc Natl Acad Sci U S A, 101*(13), 4620-4624. doi: 10.1073/pnas.0308001101

Matsuoka, Y., Lamirande, E. W., & Subbarao, K. (2009). The ferret model for influenza. *Curr Protoc Microbiol, Chapter 15*, Unit 15G 12. doi: 10.1002/9780471729259.mc15g02s13

Matsuoka, Y., Suguitan, A., Jr., Orandle, M., Paskel, M., Boonnak, K., Gardner, D. J., . . . Subbarao, K. (2014). African green monkeys recapitulate the clinical experience with replication of live attenuated pandemic influenza virus vaccine candidates. *J Virol, 88*(14), 8139-8152. doi: 10.1128/JVI.00425-14

Matsuzaki, Y., Abiko, C., Mizuta, K., Sugawara, K., Takashita, E., Muraki, Y., . . . Nishimura, H. (2007). A nationwide epidemic of influenza C virus infection in Japan in 2004. *J Clin Microbiol, 45*(3), 783-788. doi: 10.1128/JCM.01555-06

McCown, M. F., & Pekosz, A. (2006). Distinct domains of the influenza a virus M2 protein cytoplasmic tail mediate binding to the M1 protein and facilitate infectious virus production. *J Virol, 80*(16), 8178-8189. doi: 10.1128/JVI.00627-06

McMichael, A. J., Gotch, F. M., Noble, G. R., & Beare, P. A. (1983). Cytotoxic T-cell immunity to influenza. *N Engl J Med, 309*(1), 13-17. doi: 10.1056/NEJM198307073090103

Miller, D. S., Kok, T., & Li, P. (2013). The virus inoculum volume influences outcome of influenza A infection in mice. *Lab Anim, 47*(1), 74-77. doi: 10.1258/la.2012.011157

Min, J. Y., Li, S., Sen, G. C., & Krug, R. M. (2007). A site on the influenza A virus NS1 protein mediates both inhibition of PKR activation and temporal regulation of viral RNA synthesis. *Virology, 363*(1), 236-243. doi: 10.1016/j.virol.2007.01.038

Moncla, L. H., Ross, T. M., Dinis, J. M., Weinfurter, J. T., Mortimer, T. D., Schultz-Darken, N., . . . Friedrich, T. C. (2013). A novel nonhuman primate model for influenza transmission. *PLoS One, 8*(11), e78750. doi: 10.1371/journal.pone.0078750

Moore, I. N., Lamirande, E. W., Paskel, M., Donahue, D., Qin, J., & Subbarao, K. (2014). Severity of clinical disease and pathology in ferrets experimentally infected with influenza viruses is influenced by inoculum volume. *J Virol*. doi: 10.1128/JVI.02341-14

Moore, K. A., Polte, T., Huang, S., Shi, B., Alsberg, E., Sunday, M. E., & Ingber, D. E. (2005). Control of basement membrane remodeling and epithelial branching morphogenesis in embryonic lung by Rho and cytoskeletal tension. *Dev Dyn, 232*(2), 268-281. doi: 10.1002/dvdy.20237

Morens, D. M., & Fauci, A. S. (2007). The 1918 influenza pandemic: insights for the 21st century. *J Infect Dis, 195*(7), 1018-1028. doi: 10.1086/511989

Mubareka, S., Lowen, A. C., Steel, J., Coates, A. L., Garcia-Sastre, A., & Palese, P. (2009). Transmission of influenza virus via aerosols and fomites in the guinea pig model. *J Infect Dis, 199*(6), 858-865.

Murphy, B. R., Sly, D. L., Hosier, N. T., London, W. T., & Chanock, R. M. (1980). Evaluation of three strains of influenza A virus in humans and in owl, cebus, and squirrel monkeys. *Infect Immun, 28*(3), 688-691.

Music, N., Reber, A. J., Lipatov, A. S., Kamal, R. P., Blanchfield, K., Wilson, J. R., . . . York, I. A. (2014). Influenza vaccination accelerates recovery of ferrets from lymphopenia. *PLoS One, 9*(6), e100926. doi: 10.1371/journal.pone.0100926

Neverov, A. D., Lezhnina, K. V., Kondrashov, A. S., & Bazykin, G. A. (2014). Intrasubtype reassortments cause adaptive amino acid replacements in H3N2 influenza genes. *PLoS Genet, 10*(1), e1004037. doi: 10.1371/journal.pgen.1004037

O'Donnell, C. D., & Subbarao, K. (2011). The contribution of animal models to the understanding of the host range and virulence of influenza A viruses. *Microbes Infect, 13*(5), 502-515. doi: 10.1016/j.micinf.2011.01.014

O'Donnell, C. D., Wright, A., Vogel, L., Boonnak, K., Treanor, J. J., & Subbarao, K. (2014). Humans and ferrets with prior H1N1 influenza virus infections do not exhibit evidence of original antigenic sin after infection or vaccination with the 2009 pandemic H1N1 influenza virus. *Clin Vaccine Immunol, 21*(5), 737-746. doi: 10.1128/CVI.00790-13

Pauli, E. K., Schmolke, M., Wolff, T., Viemann, D., Roth, J., Bode, J. G., & Ludwig, S. (2008). Influenza A virus inhibits type I IFN signaling via NF-kappaB-dependent induction of SOCS-3 expression. *PLoS Pathog, 4*(11), e1000196. doi: 10.1371/journal.ppat.1000196

Pearce, M. B., Jayaraman, A., Pappas, C., Belser, J. A., Zeng, H., Gustin, K. M., . . . Tumpey, T. M. (2012). Pathogenesis and transmission of swine origin A(H3N2)v influenza viruses in ferrets. *Proc Natl Acad Sci U S A, 109*(10), 3944-3949. doi: 10.1073/pnas.1119945109

Peiris, J. S., de Jong, M. D., & Guan, Y. (2007). Avian influenza virus (H5N1): a threat to human health. *Clin Microbiol Rev, 20*(2), 243-267. doi: 10.1128/CMR.00037-06

Pepicelli, C. V., Lewis, P. M., & McMahon, A. P. (1998). Sonic hedgehog regulates branching morphogenesis in the mammalian lung. *Curr Biol, 8*(19), 1083-1086.

Pichlmair, A., & Reis e Sousa, C. (2007). Innate recognition of viruses. *Immunity, 27*(3), 370-383. doi: 10.1016/j.immuni.2007.08.012

Polacino, P., Larsen, K., Galmin, L., Suschak, J., Kraft, Z., Stamatatos, L., . . . Hu, S. L. (2008). Differential pathogenicity of SHIV infection in pig-tailed and rhesus macaques. *J Med Primatol, 37 Suppl 2*, 13-23. doi: 10.1111/j.1600-0684.2008.00325.x

Ravi, M., Sundar, S. S., Kumar, K. K., Parvathi, D., & Paul, S. F. (2007). Hybridoma generation by in vitro immunization of murine splenocytes with cytosolic proteins of Chinese hamster ovary (CHO) mitotic cells. *Hybridoma (Larchmt), 26*(5), 311-315. doi: 10.1089/hyb.2007.0506

Reading, P. C., Miller, J. L., & Anders, E. M. (2000). Involvement of the mannose receptor in infection of macrophages by influenza virus. *J Virol, 74*(11), 5190-5197.

Reed. (1938). A Simple Mthod of Estimating Fifty Percent Endpoints. *American Journal of Epidemiology, 27*(3), 493-497.

Reuman, P. D., Keely, S., & Schiff, G. M. (1989). Assessment of signs of influenza illness in the ferret model. *J Virol Methods, 24*(1-2), 27-34.

Rock, F. L., Hardiman, G., Timans, J. C., Kastelein, R. A., & Bazan, J. F. (1998). A family of human receptors structurally related to Drosophila Toll. *Proc Natl Acad Sci U S A, 95*(2), 588-593.

Rosenthal, P. B., Zhang, X., Formanowski, F., Fitz, W., Wong, C. H., Meier-Ewert, H., . . . Wiley, D. C. (1998). Structure of the haemagglutinin-esterase-fusion glycoprotein of influenza C virus. *Nature, 396*(6706), 92-96. doi: 10.1038/23974

Rossman, J. S., & Lamb, R. A. (2011). Influenza virus assembly and budding. *Virology, 411*(2), 229-236. doi: 10.1016/j.virol.2010.12.003

Round, E. M., & Stebbing, N. (1981). Antiviral effects of single-stranded polynucleotide inhibitors of the influenza virion-associated transcriptase against influenza virus infection of hamsters and ferrets. *Antiviral Res, 1*(4), 237-248.

Rowe, T., Leon, A. J., Crevar, C. J., Carter, D. M., Xu, L., Ran, L., . . . Ross, T. M. (2010). Modeling host responses in ferrets during A/California/07/2009 influenza infection. *Virology, 401*(2), 257-265. doi: 10.1016/j.virol.2010.02.020

Rutigliano, J. A., Doherty, P. C., Franks, J., Morris, M. Y., Reynolds, C., & Thomas, P. G. (2008). Screening monoclonal antibodies for cross-reactivity in the ferret model of influenza infection. *J Immunol Methods, 336*(1), 71-77. doi: 10.1016/j.jim.2008.04.003

Sadler, J. E., Rearick, J. I., & Hill, R. L. (1979). Purification to homogeneity and enzymatic characterization of an alpha-N-acetylgalactosaminide alpha 2 leads to 6 sialyltransferase from porcine submaxillary glands. *J Biol Chem, 254*(13), 5934-5941.

Sadler, T.W. (2011). *Medical Embyology* (Vol. 12): Lippincott Williams and Wilkins.

Saslaw, S., Wilson, H. E., & et al. (1946). Reactions of monkeys to experimentally induced influenza virus A infection; an analysis of the relative roles of humoral and cellular immunity under conditions of optimal or deficient nutrition. *J Exp Med, 84*, 113-125.

Schrauwen, E. J., Herfst, S., Chutinimitkul, S., Bestebroer, T. M., Rimmelzwaan, G. F., Osterhaus, A. D., . . . Fouchier, R. A. (2011). Possible increased pathogenicity of pandemic (H1N1) 2009 influenza virus upon reassortment. *Emerg Infect Dis, 17*(2), 200-208. doi: 10.3201/eid1702.101268

Seo, S. H., & Webster, R. G. (2002). Tumor necrosis factor alpha exerts powerful anti-influenza virus effects in lung epithelial cells. *J Virol, 76*(3), 1071-1076.

Sharma, G., & Goodwin, J. (2006). Effect of aging on respiratory system physiology and immunology. *Clin Interv Aging, 1*(3), 253-260.

Shaw, Palese and. (2007). Orthomyxoviridae: The viruses and Their Replication. In M. David M. Knipe (Ed.), *Field's Virology, Fifth Edition* (Vol. 2, pp. 1647-1677). Phildelphia PA: Lippincott Williams & Wilkins.

Sheng, Z. M., Chertow, D. S., Ambroggio, X., McCall, S., Przygodzki, R. M., Cunningham, R. E., . . . Taubenberger, J. K. (2011). Autopsy series of 68 cases dying before and during the 1918 influenza pandemic peak. *Proc Natl Acad Sci U S A, 108*(39), 16416-16421. doi: 10.1073/pnas.1111179108

Shinya, K., Ebina, M., Yamada, S., Ono, M., Kasai, N., & Kawaoka, Y. (2006). Avian flu: influenza virus receptors in the human airway. *Nature, 440*(7083), 435-436. doi: 10.1038/440435a

Short, K. R., Brooks, A. G., Reading, P. C., & Londrigan, S. L. (2012). The fate of influenza A virus after infection of human macrophages and dendritic cells. *J Gen Virol, 93*(Pt 11), 2315-2325. doi: 10.1099/vir.0.045021-0

Simeckova-Rosenberg, J., Yun, Z., Wyde, P. R., & Atassi, M. Z. (1995). Protection of mice against lethal viral infection by synthetic peptides corresponding to B- and T-cell recognition sites of influenza A hemagglutinin. *Vaccine, 13*(10), 927-932.

Skoner, D. P., Gentile, D. A., Patel, A., & Doyle, W. J. (1999). Evidence for cytokine mediation of disease expression in adults experimentally infected with influenza A virus. *J Infect Dis, 180*(1), 10-14. doi: 10.1086/314823

Smith. (1936). Influenza Infections of man from the Ferret. *The Lancet, 228*(5890), 121-123.

Smith, G. J., Vijaykrishna, D., Bahl, J., Lycett, S. J., Worobey, M., Pybus, O. G., . . . Rambaut, A. (2009). Origins and evolutionary genomics of the 2009 swine-origin H1N1 influenza A epidemic. *Nature, 459*(7250), 1122-1125. doi: 10.1038/nature08182

Smith, J. H., Nagy, T., Driskell, E., Brooks, P., Tompkins, S. M., & Tripp, R. A. (2011). Comparative pathology in ferrets infected with H1N1 influenza A viruses isolated from different hosts. *J Virol, 85*(15), 7572-7581. doi: 10.1128/JVI.00512-11

Staeheli, P., Grob, R., Meier, E., Sutcliffe, J. G., & Haller, O. (1988). Influenza virus-susceptible mice carry Mx genes with a large deletion or a nonsense mutation. *Mol Cell Biol, 8*(10), 4518-4523.

Staeheli, P., & Sutcliffe, J. G. (1988). Identification of a second interferon-regulated murine Mx gene. *Mol Cell Biol, 8*(10), 4524-4528.

Stark, G. V., Long, J. P., Ortiz, D. I., Gainey, M., Carper, B. A., Feng, J., . . . Vela, E. M. (2013). Clinical profiles associated with influenza disease in the ferret model. *PLoS One, 8*(3), e58337. doi: 10.1371/journal.pone.0058337

Stegmann, T., Morselt, H. W., Scholma, J., & Wilschut, J. (1987). Fusion of influenza virus in an intracellular acidic compartment measured by fluorescence dequenching. *Biochim Biophys Acta, 904*(1), 165-170.

Stick, S. (2000). Pediatric origins of adult lung disease. 1. The contribution of airway development to paediatric and adult lung disease. *Thorax, 55*(7), 587-594.

Straight, T. M., Ottolini, M. G., Prince, G. A., & Eichelberger, M. C. (2008). Antibody contributes to heterosubtypic protection against influenza A-induced tachypnea in cotton rats. *Virol J, 5*, 44. doi: 10.1186/1743-422X-5-44

Subbarao, K., Murphy, B. R., & Fauci, A. S. (2006). Development of effective vaccines against pandemic influenza. *Immunity, 24*(1), 5-9. doi: 10.1016/j.immuni.2005.12.005

Suguitan, A. L., Jr., Matsuoka, Y., Lau, Y. F., Santos, C. P., Vogel, L., Cheng, L. I., . . . Subbarao, K. (2012). The multibasic cleavage site of the hemagglutinin of highly pathogenic A/Vietnam/1203/2004 (H5N1) avian influenza virus acts as a virulence factor in a host-specific manner in mammals. *J Virol, 86*(5), 2706-2714. doi: 10.1128/JVI.05546-11

Suzuki, Y., Ito, T., Suzuki, T., Holland, R. E., Jr., Chambers, T. M., Kiso, M., . . . Kawaoka, Y. (2000). Sialic acid species as a determinant of the host range of influenza A viruses. *J Virol, 74*(24), 11825-11831.

Svitek, N., & von Messling, V. (2007). Early cytokine mRNA expression profiles predict Morbillivirus disease outcome in ferrets. *Virology, 362*(2), 404-410. doi: 10.1016/j.virol.2007.01.002

Takiyama, A., Wang, L., Tanino, M., Kimura, T., Kawagishi, N., Kunieda, Y., . . . Tanaka, S. (2010). Sudden death of a patient with pandemic influenza (A/H1N1pdm) virus infection by acute respiratory distress syndrome. *Jpn J Infect Dis, 63*(1), 72-74.

Taubenberger, J. K., & Kash, J. C. (2010). Influenza virus evolution, host adaptation, and pandemic formation. *Cell Host Microbe, 7*(6), 440-451. doi: 10.1016/j.chom.2010.05.009

Taubenberger, J. K., & Kash, J. C. (2011). Insights on influenza pathogenesis from the grave. *Virus Res, 162*(1-2), 2-7. doi: 10.1016/j.virusres.2011.09.003

Taubenberger, J. K., & Morens, D. M. (2010). Influenza: the once and future pandemic. *Public Health Rep, 125 Suppl 3*, 16-26.

Terajima, M., Babon, J. A., Co, M. D., & Ennis, F. A. (2013). Cross-reactive human B cell and T cell epitopes between influenza A and B viruses. *Virol J, 10*, 244. doi: 10.1186/1743-422X-10-244

Thomas, P. G., Keating, R., Hulse-Post, D. J., & Doherty, P. C. (2006). Cell-mediated protection in influenza infection. *Emerg Infect Dis, 12*(1), 48-54. doi: 10.3201/eid1201.051237

Thompson, W. W., Shay, D. K., Weintraub, E., Brammer, L., Cox, N., Anderson, L. J., & Fukuda, K. (2003). Mortality associated with influenza and respiratory syncytial virus in the United States. *JAMA, 289*(2), 179-186.

Toennessen, R., Lauscher, A., & Rimstad, E. (2009). Comparative aspects of infectious salmon anemia virus, an orthomyxovirus of fish, to influenza viruses. *Indian J Microbiol, 49*(4), 308-314. doi: 10.1007/s12088-009-0055-4

Tong, S., Li, Y., Rivailler, P., Conrardy, C., Castillo, D. A., Chen, L. M., . . . Donis, R. O. (2012). A distinct lineage of influenza A virus from bats. *Proc Natl Acad Sci U S A, 109*(11), 4269-4274. doi: 10.1073/pnas.1116200109

Tong, S., Zhu, X., Li, Y., Shi, M., Zhang, J., Bourgeois, M., . . . Donis, R. O. (2013). New world bats harbor diverse influenza A viruses. *PLoS Pathog, 9*(10), e1003657. doi: 10.1371/journal.ppat.1003657

Trebbien, R., Larsen, L. E., & Viuff, B. M. (2011). Distribution of sialic acid receptors and influenza A virus of avian and swine origin in experimentally infected pigs. *Virol J, 8*, 434. doi: 10.1186/1743-422X-8-434

Tregoning, J. S., & Schwarze, J. (2010). Respiratory viral infections in infants: causes, clinical symptoms, virology, and immunology. *Clin Microbiol Rev, 23*(1), 74-98. doi: 10.1128/CMR.00032-09

Tumpey, T. M., Szretter, K. J., Van Hoeven, N., Katz, J. M., Kochs, G., Haller, O., . . . Staeheli, P. (2007). The Mx1 gene protects mice against the pandemic 1918 and highly lethal human H5N1 influenza viruses. *J Virol, 81*(19), 10818-10821. doi: 10.1128/JVI.01116-07

Uzri, D., & Gehrke, L. (2009). Nucleotide sequences and modifications that determine RIG-I/RNA binding and signaling activities. *J Virol, 83*(9), 4174-4184. doi: 10.1128/JVI.02449-08

Valleron, A. J., Cori, A., Valtat, S., Meurisse, S., Carrat, F., & Boelle, P. Y. (2010). Transmissibility and geographic spread of the 1889 influenza pandemic. *Proc Natl Acad Sci U S A, 107*(19), 8778-8781. doi: 10.1073/pnas.1000886107

van den Brand, J. M., Kreijtz, J. H., Bodewes, R., Stittelaar, K. J., van Amerongen, G., Kuiken, T., . . . Osterhaus, A. D. (2011). Efficacy of vaccination with different combinations of MF59-adjuvanted and nonadjuvanted seasonal and pandemic influenza vaccines against pandemic H1N1 (2009) influenza virus infection in ferrets. *J Virol, 85*(6), 2851-2858. doi: 10.1128/JVI.01939-10

van den Brand, J. M., Stittelaar, K. J., Leijten, L. M., van Amerongen, G., Simon, J. H., Osterhaus, A. D., & Kuiken, T. (2012). Modification of the ferret model for pneumonia from seasonal human influenza A virus infection. *Vet Pathol, 49*(3), 562-568. doi: 10.1177/0300985811429812

van den Brand, J. M., Stittelaar, K. J., van Amerongen, G., Reperant, L., de Waal, L., Osterhaus, A. D., & Kuiken, T. (2012). Comparison of temporal and spatial dynamics of seasonal H3N2, pandemic H1N1 and highly pathogenic avian influenza H5N1 virus infections in ferrets. *PLoS One, 7*(8), e42343. doi: 10.1371/journal.pone.0042343

Van Reeth, K. (2000). Cytokines in the pathogenesis of influenza. *Vet Microbiol, 74*(1-2), 109-116.

van Riel, D., Munster, V. J., de Wit, E., Rimmelzwaan, G. F., Fouchier, R. A., Osterhaus, A. D., & Kuiken, T. (2006). H5N1 Virus Attachment to Lower Respiratory Tract. *Science, 312*(5772), 399. doi: 10.1126/science.1125548

van Riel, D., Munster, V. J., de Wit, E., Rimmelzwaan, G. F., Fouchier, R. A., Osterhaus, A. D., & Kuiken, T. (2007). Human and avian influenza viruses target different cells in the lower respiratory tract of humans and other mammals. *Am J Pathol, 171*(4), 1215-1223. doi: 10.2353/ajpath.2007.070248

Van Winkle, L. S., Fanucchi, M. V., Miller, L. A., Baker, G. L., Gershwin, L. J., Schelegle, E. S., . . . Plopper, C. G. (2004). Epithelial cell distribution and abundance in rhesus monkey airways during postnatal lung growth and development. *J Appl Physiol (1985), 97*(6), 2355-2363; discussion 2354. doi: 10.1152/japplphysiol.00470.2004

Wang, M., Tscherne, D. M., McCullough, C., Caffrey, M., Garcia-Sastre, A., & Rong, L. (2012). Residue Y161 of influenza virus hemagglutinin is involved in viral recognition of sialylated complexes from different hosts. *J Virol, 86*(8), 4455-4462. doi: 10.1128/JVI.07187-11

Webster, R. G., & Berton, M. T. (1981). Analysis of antigenic drift in the haemagglutinin molecule of influenza B virus with monoclonal antibodies. *J Gen Virol, 54*(Pt 2), 243-251.

Weis, W., Brown, J. H., Cusack, S., Paulson, J. C., Skehel, J. J., & Wiley, D. C. (1988). Structure of the influenza virus haemagglutinin complexed with its receptor, sialic acid. *Nature, 333*(6172), 426-431. doi: 10.1038/333426a0

Weiss, I. D., Wald, O., Wald, H., Beider, K., Abraham, M., Galun, E., . . . Peled, A. (2010). IFN-gamma treatment at early stages of influenza virus infection protects mice from death in a NK cell-dependent manner. *J Interferon Cytokine Res, 30*(6), 439-449. doi: 10.1089/jir.2009.0084

Wolf, J., Rose-John, S., & Garbers, C. (2014). Interleukin-6 and its receptors: A highly regulated and dynamic system. *Cytokine*. doi: 10.1016/j.cyto.2014.05.024

Woodland, D. L., & Scott, I. (2005). T cell memory in the lung airways. *Proc Am Thorac Soc, 2*(2), 126-131. doi: 10.1513/pats.200501-003AW

Xu, L., Bao, L., Li, F., Lv, Q., Ma, Y., Zhou, J., . . . Qin, C. (2011). Adaption of seasonal H1N1 influenza virus in mice. *PLoS One, 6*(12), e28901. doi: 10.1371/journal.pone.0028901

Yao, L., Korteweg, C., Hsueh, W., & Gu, J. (2008). Avian influenza receptor expression in H5N1-infected and noninfected human tissues. *FASEB J, 22*(3), 733-740. doi: 10.1096/fj.06-7880com